MASTER´S THESIS
DIPLOMARBEIT

JOINING OF SPATIALLY CURVED SURFACES FROM THIN-WALLED PREFABRICATED ELEMENTS

Ausgeführt zum Zwecke der Erlangung des Akademischen Grades eines Diplom-Ingenieur unter der Leitung von

O.UNIV.PROF. DIPL.-ING. DR.TECHN.
JOHANN KOLLEGGER

und

DIPL.-ING.
SONJA DALLINGER

E212 – INSTITUT FÜR TRAGKONSTRUKTIONEN

Eingereicht an der Technische Universität Wien
Fakultät für Bauingenieurwesen

von

PATRICIA FERNÁNDEZ ALLOZA

Matr.:0727526
Instituto Obrero de Valencia, 19
46013 Valencia SPANIEN

Wien, am 11. Juli 2008 PATRICIA FERNÁNDEZ

Acknowledgements

This thesis constitutes the end of my degree in Civil Engineering. Many people have helped and guided me during both my formation and this final work and they deserve all my gratitude. Nevertheless I would like to do a special mention to two persons, my parents, Julián and Pilar. Thanks for your inconditional support and for all the confidence that you have always deposited in me.

I give my biggest acknowledgement to the Institut of Structural Engineering of the Vienna University of Technology. A special gratitude is dedicated to my thesis tutor O.Univ.Prof. Dipl.-Ing. Dr.Techn. Johann Kolleger and to Dipl.-Ing. Sonja Dallinger because of their support, their patience, their constructive explanations and their personal treatment. They have done possible that I have carried out this thesis and I have really increased my knowledge with them. I also would like to thank Herbert Pardatscher for all his help in the laboratory.

I also would like to show my gratitude to my spanish tutor Luis Pallarés and my spanish co-tutor María Carmen Castro because of their interest, encouragement and support.

Finally I thank all my classmates and friends who have helped me during my university years and who I have shared wonderful moments with.

Abstract

This thesis is part of a bigger research project which is being carried out at the Institute for Structural Engineering of the Vienna University of Technology, under the management and supervision of o.Univ.-Prof. Dr.-Ing. Johann Kollegger. The main aim of this work is the development of new construction techniques for shells which involve a simplification of the constructive procedures and a decrease of the economic costs.

The basis of this work is the creation and the analysis of a semispherical dome by joining independent flat elements with a pre-stressed cable system. The chosen material for this first model is wood, but afterwards, the same technique is expected to be used for concrete and ice shells taking into account the obtained results.

In the first chapter of this project, of more descriptive nature, the definition of these kind of structures is studied, expounding the different existing kinds, as well as its functional characteristics and its analysis methods. Later an overview about dome history is shown using examples of the more outstanding constructions.

The following section of this thesis constitutes a global vision of the existing techniques and the studies which are being developed for the construction of shells.

Then the structural behaviour of the semispherical dome, which is the object of the experiment, is studied in depth in order to facilitate the understanding of some concepts in connection with the creation of the model, the interpretation of the results and the establishing of conclusions.

The second chapter constitutes the experimental part of the study. This section includes all the aspects related to the definition, design, construction and tests of the built model. Conclusions and improvement proposals are obtained from this first structure.

In order to study the influence of the dimensions of the model and apply some of the suggested improvements, a bigger semispherical dome is built.

Computer models and analytical problems are developed in order to verify the validity of the obtained results and to study the feasibility of this new technique. Subsequently the results are compared and conclusions are made.

CHAPTER 1. SHELL STRUCTURES OVERVIEW

CHAPTER 2. CONSTRUCTION OF DOME MODELS FROM INDEPENDENT FLAT ELEMENS AND PRE-STRESSED CABLES

CHAPTER 3. ANALYSIS OF SEMISPHERICAL DOMES

Chapter content **.....** **79**

CHAPTER 1

SHELL STRUCTURES OVERVIEW

Chapter content

The first chapter of this project constitutes an introduction to the shell structures. The nature of it is mainly descriptive.

In the section *Basic concepts* the definition of a shell and the classification of this kind of structures is included. Then the comparison arch-dome and beam-barrel is established in connection with its structural behaviour. At the end, the principles of the thin shell analysis are briefly explained.

In the following section a general dome history overview is shown.

The third part of the chapter is about the existing shell construction techniques. It differentiates between the several kinds of domes and it includes the new constructive procedures which have been devoloped at the Vienna University of Technology during the last years.

In order to understand correctly the content of this project, the structural behaviour of a dome is explained in the last section of the chapter.

1. Basic concepts

1.1 Definition

A thin shell is a curved slab whose thickness h is small compared with its other dimensions and compared with its principal radii of curvature r_x and r_y. The surface that bisects the shell thickness is called the middle surface, and by specifying the form of this surface and the thickness h at every point, we completely define the geometry of the shell [1].

1.2 Classification of shell systems

The mechanical properties of a shell element describe its resistance to deformation in terms of separable stretching and bending effects. Loads applied to the shell are carried in general through a combination of bending and stretching actions, which generally vary from point to point. One of the major difficulties in the theory of shells is to find a relatively simple way of describing the interaction between the two effects [2].

As in the case of plates, one can classify shell mathematical models in terms of the ratio of the thickness to a characteristic dimension. According to this ratio, it is possible to define the importance of stretching, bending and transverse shear effects:

- Very thick: 3D effects
- Thick: stretching, bending and higher order transverse shear
- Moderately thick: streching, bending and first order transverse shear
- Thin shells: stretching and bending energy considered but transverse shear neglected
- Very thin shells: dominated by stretching effects. Also called membranes.

The main difference from flat plates is that the determination of characteristic dimensions is more complex.

Thin shells are the object of this project. Following the two possible classifications of this kind of shells structures is shown [1].

Possitive – Negative gaussian curvature

The most general classification of thin shells is by gaussian curvature. The gaussian curvature can be positive, zero or negative.

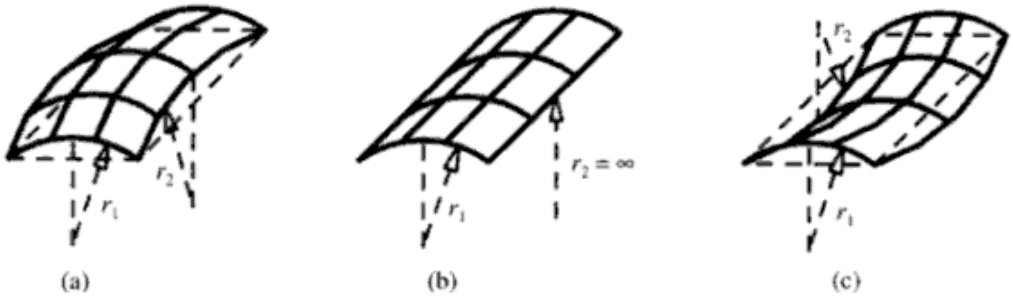

Figure 1: Gaussian curvature of surfaces: (a) positve; (b) zero; (c) negative

Mathematically the gaussian curvature of a surface is defined as the product of the principal curvatures:

$$K = \frac{1}{r_1}\frac{1}{r_2}$$

Shells of **positive gaussian curvature**, sometimes called synclastic shells, are formed by two families of curves both with the same direction. Spherical domes and elliptic paraboloids are examples.

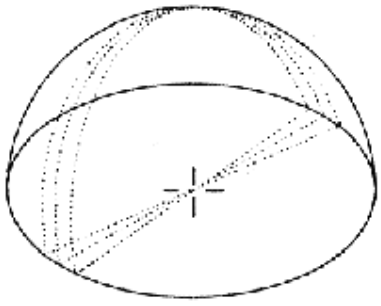

Figure 2: Semi spherical dome

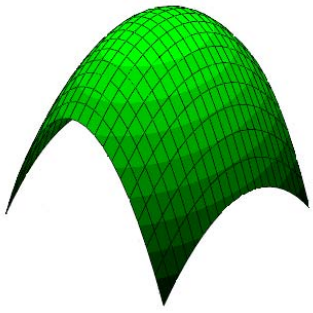

Figure 3: elliptic paraboloid

Shells of **zero gaussian curvature** or singly curved shells are formed by one family of curves only; some examples are cylinders and cones.

Figure 4: Barrel

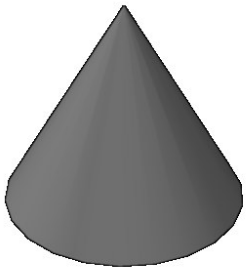

Figure 5: cone

Shells of **negative gaussian curvature**, sometimes called anticlastic, are formed by two families of curves each in opposite directions. Hyperbolic paraboloids and hyperbolas of revolution are examples.

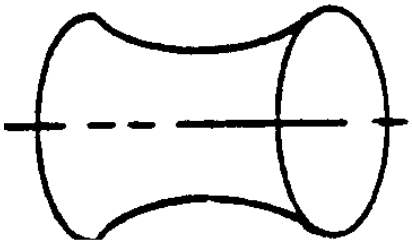

Figure 6: Hyperbola of revolution

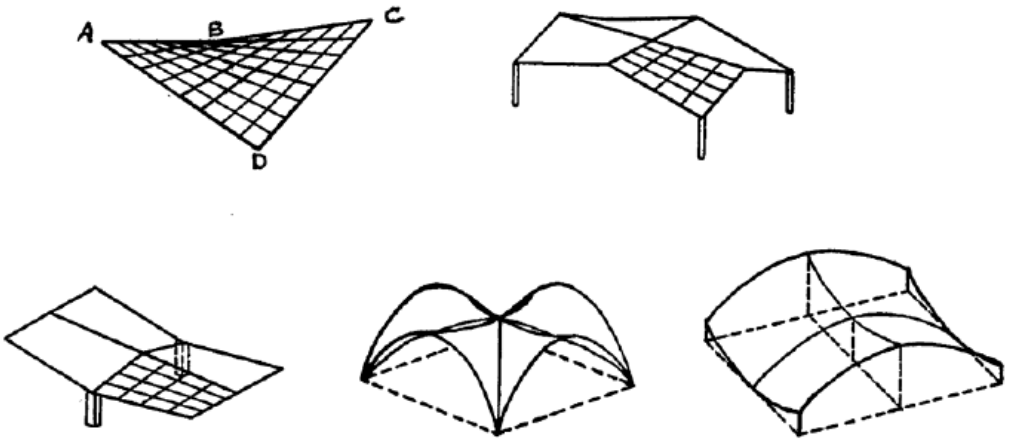

Figure 7: Varios hiperbolic paraboloid configurations

One important characteristic difference among these shell types is the propagation of edge effects into the shell.

For shells of positive curvature the edge effects tend to damp rapidly and are ususally confined to a narrow zone at the edge. Thus in these shells the memebrane theory will often be valid throughout the entire shell except just at the boundary. This rapid damping has been clearly demonstrated for spherical domes.

For shells of zero curvature the edge effects are damped but tend to extend further into the shell than in shells of positive curvature.

Finally, for shells of negative curvature the damping is less than for the othters. Thus the boundary effects tend to become significant over large portions of the shell.

Rotational – Translational

Another useful classification divides shells into rotational and translational systems. Domes and tanks are normally surfaces of rotation, whereas cylindrical barrels, elliptic paraboloid, and hyperbolic paraboloids are sufarces of translation. This classification is helpful in visualizing the analysis and the construction, but it has little general merit wiht regard to structural action. For example, the behaviour of the shallow spherical domes normally used for roofs is about the same as that of shallow elliptic paraboloids. In fact, it has been pointed out that for commonly used roof dimensions the maximum difference between the surfaces of rotation and of translation will be cosinderably less than the thickness of the shell itself. Furthermore, a small constructional deviation in shell form can result in large differences in geometry between the designed and the constructed shell.

1.3 Comparison with planar systems

The two most well-defined systems of thin shells commonly used in reinforced concrecte construction are the dome and the segment of a cylinder. In each case some insight into the structural action can be obtained by comparing and contrasting these systems with similar planar ones [1].

Arch versus dome

Both structures are going to be considered. First the loads acting on the arch are studied. The uniform load on a parabolic arch produces practically no bending if the boundary conditions do not permit horizontal displacement. However, once the load is changed to a partial load, substantial bending develops in the arch. In the case of the dome the uniform load is carried by forces in the plane of the shell that are similar to the forces which carry the uniform load in the arch. However, in the dome additional forces (called hoop forces) are set up at right angles to these arching or meridional forces.

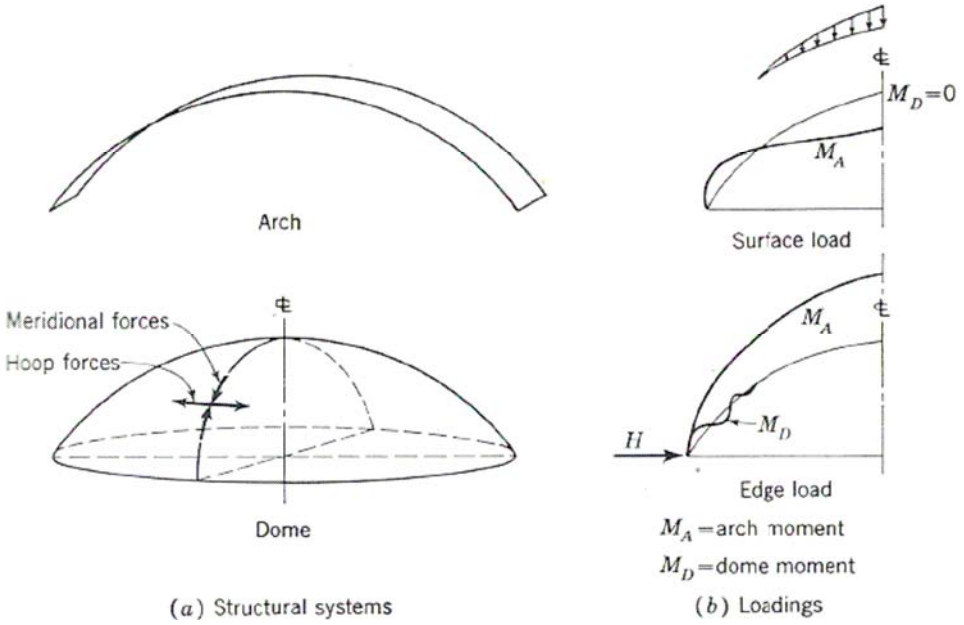

Figure 8: Arch and dome comparison

The existence of two sets of forces in two separate directions within the shell makes this structural system similar to plate structures. The hoop forces, however, do not enter into the equations of vertical equilibrium. Therefore the entire vertical load must be transmitted by the meridional forces.

Now the case of the dome with a partial load is going to be considered. As long as this load has a smooth variation, that is to say as long as there is no strong discontinuity at the point where the load goes to zero, we will observe that the shell is able to carry this load almost entirely by the same arching forces as before. This action is quite unlike the action of the arch, and the reason for the difference is the existence of the hoop forces. Physically one may say that as an arch segment of the dome attempts to bend under the partial load in the same way that the arch bends, the hoop forces restrain it just as if stiff fings were wrapped around the structure. Thus whereas the arch is best suited to only one type of loading, the dome is well suited to almost any type of loading within certain restrictions.

The effect of boundary conditions, or edge restraints, on both the arch and the dome structures must be taken into account. If the arch is given a horizontal push at one side, this force must be held in equilibrium by an equal and opposite force acting at the other support. The only way that the force can be transmitted through the system is up through the arch, over the crown, and down the other side. The effect clearly is to produce high bending moments throughout the entire arch system, with a maximum moment at the crown. We see, therefore, that the arch is not only restricted in its most efficient form by the nature of the loading but it is also very sensitive to foundation displacements or edge forces.

The same corresponding horizontal force can be also given to the dome. Such a force may be considered as a uniform horizontal thrust applied all around the circular edge of the dome. In cross section it would appear that this horizontal force would create bending moments throughout the dome similar to those created in the arch. This is, however, not the case. As the horizontal force tends to bend the shell, and thus to be carried up a meridian, the hoop forces again come into play and cause a rapid damping of the bending so that at a relatively short distance from the edge the bending effect is no longer observable. Thus edge forces in equilibrium applied to an arch propagate throughout the entire structural system and create large bending moments in a very narrow region near the edge and have generally no effect throughout a large portion of the structure.

Beam versus barrel

Just as arches are limited by functional requirements and do not find as wide application as beams, domes are also limited and do not find as wide application as barrels. The following pictures illustrates beam and barrel systems, both of which are used in the framing of rectangular plan areas.

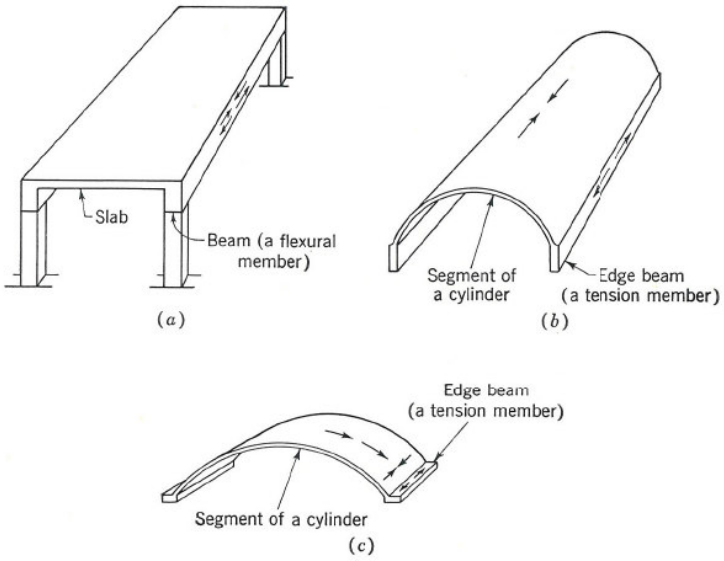

Figure 9: Beam and barrel systems

To make a close comparison, the shown framing plan is going to be considered, in which the loads are essentially carried transversely by the slab and longitudinally by the beams. We may improve this system by building the slab and the beam monolithically, thus obtaining some T-beam action and thereby increasing considerably the stiffness of the beams. Since the beam is relatively shallow compared to its span, it is known that the simple flexural theory is valid and that the magnitudes of the stresses are directly proportional to the depth and vary as a straight line form top to bottom. Even in the slab the loads are essentially carried by bending moments, the sizes of which are functions of the transverse span.

If now the slab is given a curvature and the longitudinal beams are reduced in cross section, a typical simply supported barrel shell spanning the same distance as the beams is obtained. The structural action, however, is significantly different.

Considering the transverse slab, which is now curved, it is logical to think that this would act as an arch, but it does not because the slender edge beam is unable to sustain horizontal forces. Therefore, although the curved slab will try to act as an arch, the thrust contained at the springing lines will be very small. The principal structural action of this system is found to be longitudinal. In the previous case the beam had to carry the entire load with perhaps some additional flange help from the slab, but in this case the entire system acts as a beam with curved cross section to carry the load.

The principal action, therefore, of the barrel shell with small flexible edge beams is longitudinal bending, but the bending stresses are within the plane of the shell itself. Thus the entire shell-and-edge-beam system can be like a beam with the compression stresses near the crown and with the tension stresses concentrated in the edge beam on either side. In fact one approximation for a certain class of barrel shells which makes use of the simple flexural theory is based entirely upon this physical picture of the system.

However, the simple flexural theory, which leads to a straight-line stress distribution, requires that all points within the cross section of a member deflect exactly the same amount, which is the case in a solid rectangular beam. In a T beam with wide flanges the extremities of the flanges may not deflect the same as the web. In a barrel shell the cross section may undergo substantial lateral distortion, and it is principally this distortion which causes the longitudinal stresses to depart from the straight-line distribution of the beam theory.

It is roughly true that the longer the span in comparison with the transverse-chord width, the more the entire cross section behaves as a beam. The shorter span compared with the chord width, the more the structure behaves as an arch with a supporting sloped deep beam near the edge.

1.4 Analysis of thin shells

There are several methods to analyze thin shell structures based on static analysis, graphical analysis and numerical finite element methods. Some of them will be briefly explained in the third chapter of this project, where the analysis of the designed model is carried out using analytical and finite element computer programs. In this section the method applied in the general theory of thin shells is going to be shown [1].

This method of thin shells analysis consists first of establishing equilibrium of a differential element cut from the shell and second of achieving strain compatibility so that each element remains continiuous with each adjacent element after deformation.

Stress resultants and stress couples, defined as the total forces and moments acting per unit length of middle surface (Fig. 10), are integrals of stress over the shell thickness (Fig. 11).

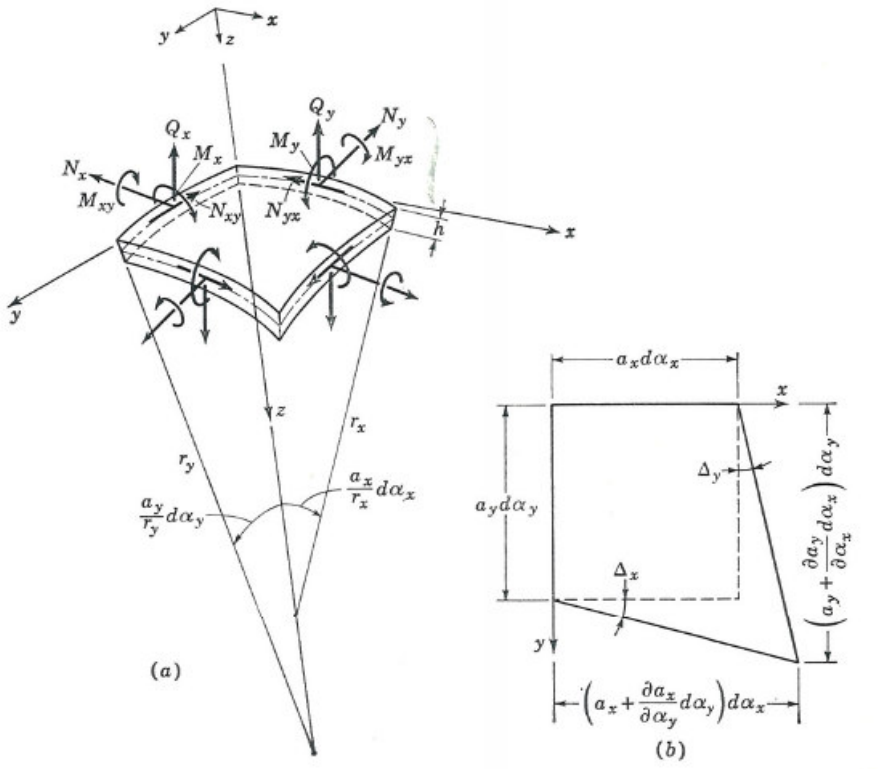

Figure 10: Stress resultants and stress couples

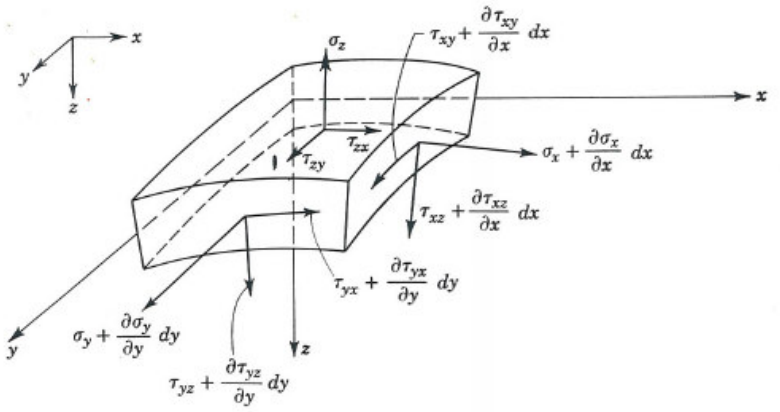

Figure 11: Stresses

The stresses σ_z, τ_{zx}, and τ_{zy} are neglected because of the small shell thickness; thus the twisting moments about the z axis are normally taken as zero.

Small-deflection theory, which is normally the basis for analysis of thin shells, implies that the deflections under load are small enough so that changes in geometry of the shell will not alter the static equilibrium of the system. This assumption is used in frame analysis to justify superposition.

Linear elastic behaviour, also generally used in analysis of thin shells, provides a direct relation ship between stress and strain by which the equilibrium of the stress resultants and stress couples is related to the strain compatibility equations.

In addition, some assumptions can be made:

- Points on lines normal to the middle surface before deformation remain on lines normal to the middle surface after deformation.

- Deformations of the shell due to radial shears (Q_x and Q_y) are neglected.

Both of these assumptions have been used in elementary beam theory as plane sections remain plane after bending, and deformations due to shear are neglected.

Based of the above definitions and assumptions, the general shell theory can be formulated in five steps by:

1. Determining the equilibrium forces on the differential element (five equations with eight unknows).
2. Establishing strain-displacement relationships (six equations with three unknows)
3. Establishing stress-strain relationships into force-displacement equations (six equations with three unknows).
4. Transforming the force-strain relationships into force-displacement equations (still six equations with three unknows).
5. Obtaining a complete formulation by combining the force-displacement equations with the equilibrium equations (11 equations with 11 unknows)

1.5 Application

Architecture and building. The development of masonry domes and vaults in the Middle Ages made possible the construction of more spatious buildings. In more recent times the availability of reinforced concrete has stimulated interest in the use of shells for roofing pruposes [2].

Power and chemical engineering. The development of steam power during the Industrial Revolution depended to some extent on the construction of suitable boilers. These thin shells were constructed from plates suitable formed and joined by riveting. More recently the use of welding in pressure vessel construction has led to more efficient designs. Pressure vessels and associated pipework are key components in thermal and nuclear power plants, and in all branches of the chemical and petroleum industries.

Structural engineering. An important problem in the early development of steel for structural pruposes was to design compression members against buckling. A striking adavance was the use of tubular members in the construction of the Forth railway bridge in 1889: steel plates were riveted together to form reinforced tubes as large as 12 feet in diameter, and having a radius/thickness ratio of between 60 and 180.

Vehicle body structures. The construction of vehicle bodies in the early days of road transport involved a system of structural ribs and non-structural paneling or sheeting. The modern form of vehicle construction in which the skin plays an important structural part followed the introduction of sheet-metal components, preformed into doubly curved shells by large power presses, and firmly connected to each other by welds along the boundaries. The use of the curved skin of vehicles as a load bearing member has similarly revolutionized the construction of railway carriages and aircrafts. In the construction of all kind of spacecraft the idea of a thin but strong skin has been used from the beginning.

Composite construction. The introduction of fiberglass and similar lightweight composite materialas has impacted the construction of vehicles ranging from boats, racing cars, fighter and stealth aircraft, and so on. The exterior skin can be used as a strong structural shell.

Miscellaneous Examples. Other examples of the impact of shell structures include cooling towers for power stations, grain silos, armour, arch dams, tunnels, submarines, and so forth.

2. Domes history overview

The first and oldest example of thin and double curved structures can be found in the nature. Eggshells, conches, nutshell or orange peel can be named as examples. In this examples is the shell simlutaneosly a protective cover against bad enviromental influence and a static and active support structure.

Humans have also used this kind of structures as an architectural form throughout history. Despite the fact that they are thin, domes are the strongest architectural element, thanks to compressive and frictional forces they create [3].

Although the first examples of wooden spherical structures appear as soon as 6000 BC in Cyprus, they are not big enough to be considered true domes. The first stone domes are built for tombs such as the tholos of the **Treasure of Atreus** (Mycenae, 13th century BC) and the **Stupa in Sanchi** (India, 3rd century BC). These structure are not high since they lie directly on the ground, being the dome subterraneous.

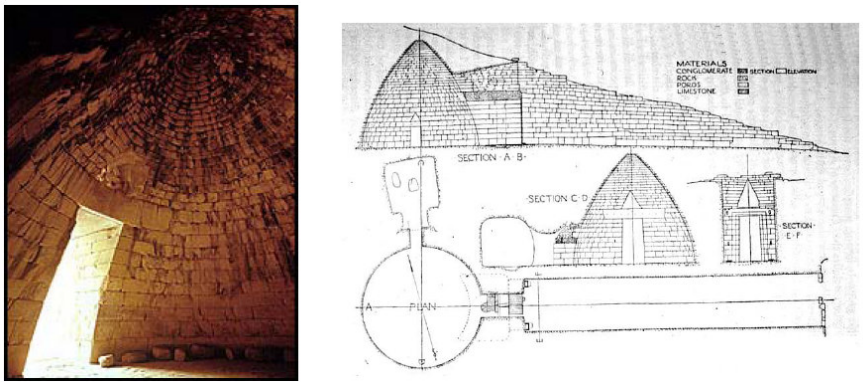

Figure 12: Corbel dome of the Treasury of Atreus in Myceane [4]

It was the Roman civilisation the first to construct buildings with semispheric domes. Examples are known since times of Nero, achieving the culminating point with the **Pantheon of Hadrianus**, built in 125 A.D, and still standing. The Pantheon is the best-preserved example of an Ancient Roman monumental building and it has been enormously influential in Western Architecture from at least the Renaissance on [5].

The 4.535 metric ton weight of the concrete dome is concentrated on a ring of voussoirs 9.1 metres in diameter which form the oculus while the downward thrust of the dome is carried by eight barrel vaults in the 6.4 metres at the base of the dome to 1.2 metres around the oculus. The height to the oculus and the diameter of the interior circle are the

same, 43.3 metres, so the whole interior could house a sphere 43.3 metres in diameter [6].

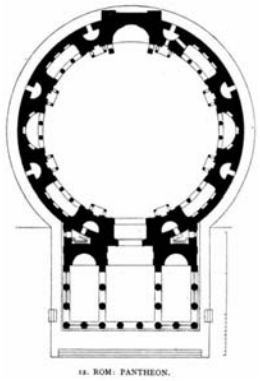

Figure 13: Floor Plan of the Pantheon [7]

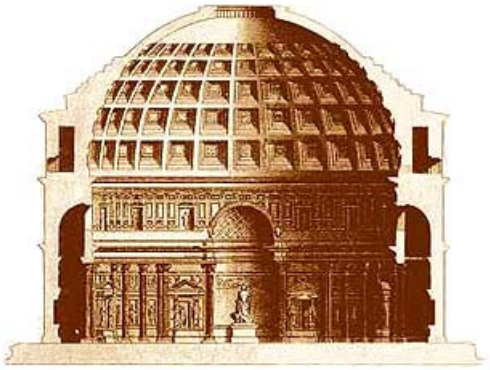

Figure 14: Cross Section of the Pantheon

The Romans had a ingenious way of dealing with the tension and compression forces. To deal with the massive tension forces at the lower part of the dome, the Roman architects poured several layers of concrete around the base of it. These layers are called step rings, and they provide a normal force to push inward against the tension forces that push out. The rings also help to redirect the tension forces down into the walls bellow. Right where the compression forces are the greatest on the dome (the top), the Roman architects chose to have nothing but air. The occulus is made up of bricks. Compressive forces are redirected along the ring´s body. The compression forces come from all directions. These forces wedge the ring stones tightly together. The compression forces cancel each other out and the top of the dome is left in a state of horizontal equilibrium [8].

The exact composition of the Roman concrete used in the dome remains a mystery. An unreinforced dome in these proportions made of modern concrete would hardly stand the load of its own weight. The high tensile strength appears to come from the way the concrete was applied in very small amounts and then was tamped down after every application to remove excess water and trapped air bubbles [6].

Paralelly, in Persia appeared the first domes in which pendentives were used from the beginning. This new element provided a strong support to domes, allowing them to become higher and the walls to become progressively thinner. First examples are found in the Sassanid **palaces of Firuzabad and Fars**, erected around 240 and 430, respectively. The technique spread to other areas of Central Asia, being most important the **mausoleums of Bokhara** (943) **and Tim** (978), but it did not evolve dramatically [5].

Byzantine architecture gave us the pendentive domes and it provided the unique way of adjusting the circular form of a dome roof to a square or polygonal plan. This type of dome was invented by the romans but was seldom used by them. The pendentive dome is derived by trimming the sides of a regular dome over a square plan as shown in A. The pendentive dome enables the transfer the total load of the dome to the four corneres of a building, meaning that only the four of the corners need to be reinforced (Fig. 15).

This allows the dome roof to be adapted for a square building as shown in B. Additionally, the top of the pendentive dome can be trimmed to introduce another dome on top of it as shown in C. The additional dome can further be raised to introduce a cylinder between the pendentive dome and the additional dome as in D. Windows can then be introduced in the cylinder enabling architects to creating dazzling interior light effects.

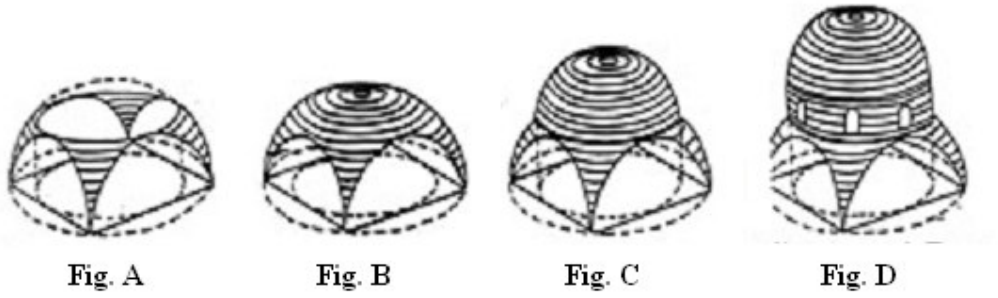

Figure 15: Pendentives and Dome on Pendentive

The maximun achievement of the technique was **Hagia Sofia** in Constantinople (532), a true architectural wonder of the era.

Hagia Sophia was the greatest vaulted space without intermediate supports that has ever been built. Its architects were Isidore of Miletus and Anthemius of Tralles. The church provides an expert solution to the problem of how to place a dome on a square base by using pendentives. Hagia Sophia is covered by a central dome 31 m across, slightly smaller than the Panthen´s. The dome seems rendered weightless by the unbroken arcade of arched windows under it, which help flood the colorfull interior with light. The dome is carried on pendentives. The weight of the dome passes through the pendentives to four massive piers at the corners. Between them the dome seems to float upon four great arches.

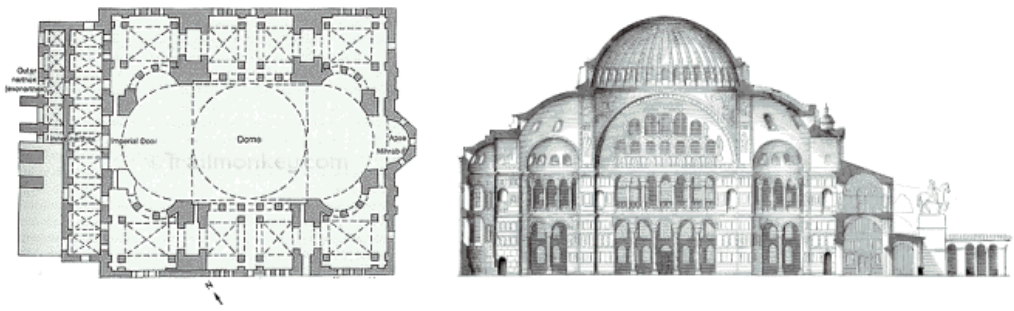

Figure 16: Floor plan and section of Hagia Sophia

The church form is a combination of a centralized and a longitudinal structure. Longitudinal direction is defined by domes to the east and west. At Hagia Sophia, two opposing arches

on the central square open into semi-domes, each pierced by 3 smaller radial semi-domes. At the west and east ends, the arched openings are extended and by great half domes carried on smaller semi-domed exedras. Thus a hierarchy of dome-headed elements build up to create a vast oblong interior crowned by the main dome, a sequence never seen before in antiquity.

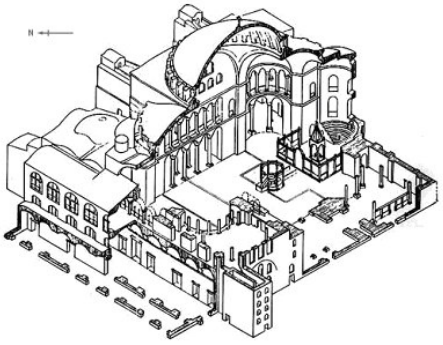

Figure 17: Axonometrical View of Hagia Sophia

Figure 18: Exterior view of Hagia Sophia

Hagia sophia dominated church architecture after the 6th century. Many cities built Byzantine churches that were reflective of regional practices. Some of the most prominent ones are **Santa Sophia Kiev** (1037), **Saint Basils Moscow** (1551), **Monastry of Hosios Loukas** (1020), and **St. Markus Venice** (1073) [9].

It was also Byzantine engineers who designed the **Mosque of the Rock** (691) in Jerusalem and the **Great Mosque of Damascus** (715). Soon the Islamic style adopted bulbous or pointed domes, which were widely used in its architecture. The design spread to Russia in the XIII century, where it gained great popularity in the form of the onion dome, a pointed, domelike roof structure.

Meanwhile, in Western Europe, domes disappeared from architecture after the fall of the Roman Empire. There were several good attempts, such as half domes (apses), rib vaults or tronconic domes such as the one in the **Baptistry of Pisa**, finished in 1363 (the current one is more recent, though), but the technique of the semispheric dome had disappeared.

Then, Brunelleschi reinvented it with much style. He built the great dome of **Santa Maria del Fiori** in Florence (1418). He took inspiration from the circular dome in the Pantheon and gave ingenious and unprecedented solutions: the distinctive octagonal design of the double-walled dome, resting on a drum and not on the roof itself, allowed for the entire dome to be built without the need for scaffolding from the ground. But, because the dome rested on a drum with no external butresses supporting it, there could be no lateral thrusts at the base of the dome. To ensure this, Brunelleschi used horizontal tension chains of wood and iron set at the base of the dome [5].

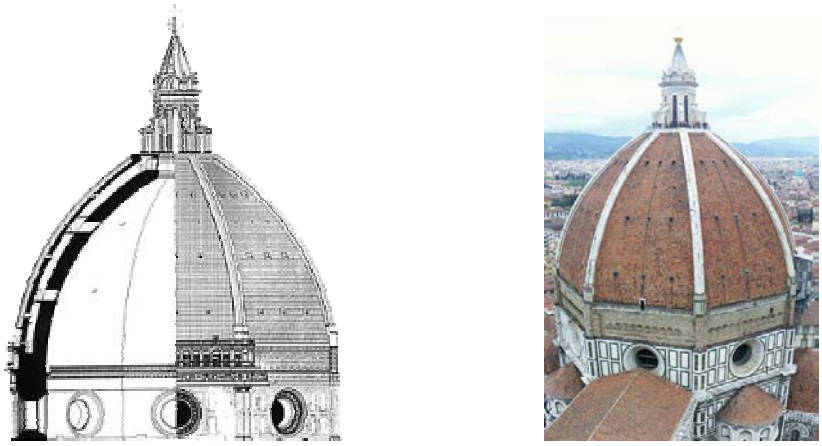

Figure 19: Section and exterior of Santa Maria del Fiori, Florence

In this manner he built the highest dome at the time, and a true architectonic model, since it was copied in Saint Peter of Rome by Giacomo della Porta in 1953. The later domes of **Saint Paul** in London (1708) and **the Capitol** in Washington (1850) use the same technique.

In the quest for height, engineers came up with a few tricks. The U.S. Capitol gets its height from this sleight of hand. The larger outer dome is a thin shell, held up by a ring of curved iron ribs. Underneath it all is a smaller, self-supporting dome, visible only from the inside. The Capitol in Washington is also one of the earliest domes made of pre-fabricated cast-iron ribs. The switch from heavy masonery to lightwight metal ribs in the late 18th century greatly reduced the weight of domes being built around the world [10].

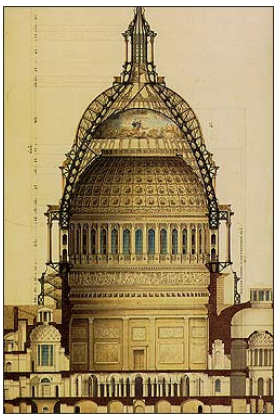

Figure 20: U.S. Capitol, Washington

Still paralelly to these constructions, in Persia, the dome of the **Oljeitu Mausoleum** (Soltaniyeh, 1312) was built. This was, in fact, the first double-shell dome, and was additionaly reinforced with arches between both shells, wich was an architectural revolution in the Muslim world, comparable to that of Brunelleschi. It started and architectural trend that designed domes as big as the **Mausoleum of Khoja Ahmed Yasavi** (Kazakhstan, 1405) and the **Taj Mahal** (India, 1653).

The marble dome of the Taj Mahal has a height of about the same size as the base of the building, about 35 meters, and is accentuated as it sits on a cylindrical "drum" of about 7 metres high. This dome is a clear example of the so called onion-dome.

Figure 21: Oljeitu Mausoleum, Soltaniyeh

Figure 22: Taj Mahal, India

One of the most characteristic elementes of the Baroc architecture was the oval dome, invented by Giacomo da Vignola (Chapel of Saint Andreas, Rome, 1553) and especially developed in the churches of Bernini and Borromini. This kind of dome gave a dramatic dynamism to Baroc churches. The biggest of this kind was built by Francesco Gallo in the **Basilica of Vicoforte** (Italia, 1773).

In the following centuries different techniques and construction procedures of domes have been developed, as well as new materials have been introduced.

Through the XIX century some domes made out of glass and iron have been built. Walter Benjamin was the first who wrote about iron and glass construction in his work “Paris, capital of the 19th century”. Then Günther Bantmann has designed the **Galleria Vittorio Emanuele** and since then several projects and constructions have been carried out by using this materials [11].

Modern thin concrete shells, which began to appear in the 1920s, are made from thin steel reinforced concrete, and in many cases lack any ribs or additional reinforcing structures, relying wholly on the shell structure itself.

Shells may be cast in place, or pre-cast off site and moved into place and assembled. The strongest form of shell is the monolithic shell, which is cast as a single unit. The most common monolithic form is the dome, but ellipsoids and cylinders are also possible using similar construction methods.

Monolithic domes are cast in one piece out of reinforced concrete, and date back to the 1960s. Advocates of these domes consider them to be cost-effective and durable structures, especially suitable for areas prone to natural disasters. They also point out the ease of maintenance of these buildings. Monolithic domes can be built as homes, office buildings, or for other purposes [12].

The **Seatle Kingdome** was the world's first (and only) concrete-domed multi-purpose stadium. It was completed in 1976 and demolished in 2000. The Kingdome was constructed of triangular segments of reinforced concret that were cast in place. Thick ribs provided additional support.

Domes made from iron bars continued its development. The more simple ones were the ringnets. But at the beginning of the 20th-century a radical new design – the geodesic dome - would change dome engineering forever [13]. A geodesic dome is an almost spherical structure based on a network of great circles (geodesics) lying approximately on the surface of a sphere. The geodesics intersect to form triangular elements that have local triangular rigidity and yet also distribute the stress across the entire structure. Geodesic domes are far stronger as complete units than the individual struts would suggest.

The first dome that could be called “geodesic” was designed just after the World War I by Walther Bauersfeld for a planetarium. The dome was patented and it was constructed on the roof of the Zeiss plant in Jena, Germany 1922. Some thirty years later R.Buckminster Fuller further investigated this concept and named the dome “geodesic” from field experiments. The geodesic dome appealed to Fuller because it was extremely strong for its weight, its “omnitriangulated” surface provided an inherently stable structure, and because a sphere encloses the greatest volume for the least surface area.

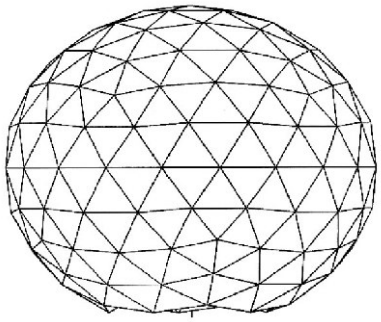

Figure 23: Geodesic dome

Today, geodesic domes come in an almost endless variety of shapes and styles. The dome was successfully adopted for specialized industrial use, such as the 1958 Union Tank Car Company dome near Baton Rouge, Lousiana and specialty buildings like the Henry Kaiser dome, auditoriums, weather observatories, and storage facilities.

Another dome from Expo 67 in Montreal was built as part of the American Pavilion. The structure's covering later burned, but the structure itself still stands and, under the name Biosphère, currently houses an interpretive museum.

In the 1970s the Cinesphere dome was built at the Ontario Place amusement park in Toronto, Canada. In 1975, a dome was constructed at the South Pole, where its resistance to snow and wind loads is important.

Possibly one of the most famous domes in the world, the **Epcot Center** in Orlando, Florida, is also a geodesic dome. The EPCOT dome is a complete geodesic sphere which stands 180 feet tall, is supported on 6 steel legs 15 feet off the ground, and is constructed of a steel frame dressed with aluminum panels. The sphere diameter of 165 feet encloses 22 million cubic feet of airspace.

Figure 24: Montreal Biosphère

Figure 25: Epcot Center in Orlando, Florida

A new generation of domes equipped with retractable roofs, like the **Toronto SkyDome**, has become a popular choice for sports stadiums throughout the world.

3. Dome construction techniques

There are different dome construction techniques depending on the kind of shell and the materialas which are used to build them. The most common and used techniques are following explained, as well as some new techniques which has been recently developed in the Institute for Structural Engineering of the Vienna University of Technology.

3.1 Geodesic domes

Hub and strub dome

Wooden domes have a hole drilled in the width of a strut. A stainless steel band locks the strut's hole to a steel pipe. With this method, the struts may be cut to the exact length needed. Triangles of exterior plywood are then nailed to the struts. The dome is wrapped from the bottom to the top with several stapled layers of tar paper, in order to shed water, and finished with shingles. This type of dome is often called a hub-and-strut dome because of the use of steel hubs to tie the struts together.

Panelized timber frame

Panelized domes are constructed of separately-framed timbers covered in plywood. The three members comprising the triangular frame are often cut at compound angles in order to provide for a flat fitting of the various triangles. Holes are drilled through the members at precise locations and steel bolts then connect the triangles to form the dome. These members are often 2x4's or 2x6's, which allow for more insulation to fit within the triangle. The panelized technique allows the builder to attach the plywood skin to the triangles while safely working on the ground or in a comfortable shop out of the weather. This method does not require expensive steel hubs.

Concret and foam plastic domes

Concrete and foam plastic domes generally start with a steel framework dome, wrapped with chicken wire and wire screen for reinforcement. The chicken wire and screen is tied to the framework with wire ties. A coat of material is then sprayed or molded onto

the frame. Tests should be performed with small squares to achieve the correct consistency of concrete or plastic. Generally, several coats are necessary on the inside and outside. The last step is to saturate concrete or polyester domes with a thin layer of epoxy compound to shed water.

Some concrete domes have been constructed from prefabricated, prestressed, steel-reinforced concrete panels that can be bolted into place. The bolts are within raised receptacles covered with little concrete caps to shed water. The triangles overlap to shed water. The triangles in this method can be molded in forms patterned in sand with wooden patterns, but the concrete triangles are usually so heavy that they must be placed with a crane. This construction is well-suited to domes because there is no place for water to pool on the concrete and leak through. The metal fasteners, joints and internal steel frames remain dry, preventing frost and corrosion damage. The concrete resists sun and weathering. Some form of internal flashing or caulking must be placed over the joints to prevent drafts [13].

3.2 Thin concrete shells

Shells may be cast in place, or pre-cast off site and moved into placed and assembled. In this section are shown some techniques to build thin concrete shells.

Framework system

The concrete can be cast in place by using frameworks. This is the traditional system to build with concrete and it has been employed in all kind of structures. A formwork, usually made of wood, is use to create the required shape. Then the concrete is poured on it to adopt the final shape.

Nowadays, this method is the most used in the construction of concrete structures. It allows to obtain complex shapes and the final quality which is reached by the material is suitable. Nevertheless, creating such formwork increases the construction time and consumes additional material which is useless after the shell has been finished. Since additional resources (time and material) are consumed, this production method significantly raises the costs [14].

In order to achieve more economic production of shell structures many new production methods have been developed. For example, Heinz Insler [15] tries to use one formwork structure for more than one concreting step.

Monolithic domes

As an alternative to the conventional wooden formwork, inflated membranes can be used. Monolithic shells are usullay built using this system.

Monolithic shells are cast in one piece out of reinforced concrete. One possibility to construct these domes can be divided in the following steps [16]:

- A rebar-reinforced concrete foundation is poured, defining the shape of the base of the structure.

- The fabric form, or airform membrane, usually made from PVC, is attached to the foundation and inflated with an air blower. The airform contains an airlock to allow workers to enter the form while it is inflated.

- A thin layer of polyurethane foam with a thickness of approximately 100 mm is sprayed inside the form. The foam serves several purposes; it will hold the rebar in place, provide support for spraying in the concrete mixture and it will insulate the final structure.

- Rebar is attached to the inside foam, using clips that are attached to the foam.

- Several centimeters of concrete are sprayed over the rebar frame. The concrete may be thicker at the bottom than the top of the structure.

- After the concrete has set, the blower is turned off. The airform remains in place as an outer covering protecting the foam.

- The exposed surface of the airform may be covered with a surface treatment. Some type of covering is desirable to protect the airform from long-term degradation.

- A non-insulated version of the monolithic dome is available in which the airform can be removed after the completion and re-used to build additional domes.

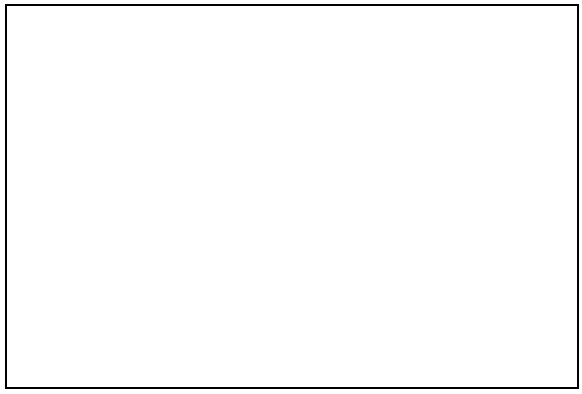

Figure 26: Monolithic dome section

Another process to build this kind of shells consists in inflating a membrane covered with freshly mixed concrete.

"Hanging type" shells

Another construction method can be applied for shells which are of the pure "hanging type". On a frame of steel beams a cable net can be constructed which consists of the reinforcement of the shell. Then a thin wire mesh is attached at the bottom side of the cable net which serves as lost formwork for the concrete. After hardening of the concrete a reinforced concrete shell is obtained which is upside down with respect to its final position and therefore it has to be turned [17].

3.3 New techniques in the Vienna University of Technology

In the Vienna University of Technology other experiments in the construction of concrete and ice shells has been already carried out [18, 19].

The constructive procedure is for all of them the same: a flat plate is forced into a double curvature shell. This procedure requires large strains in the middle plane of the flat shape which cannot be achieved with conventional construction materials. However, if an orthotropic material was available which would permit large strains at low stresses in one direction and which had much better strength properties in the perpendicular direction, the transformation of a flat plate into a dobule curved shell could be accomplished. Keeping this in mind a construction precedure was developed in which a flat plate was made by using a strong material (e.g. ice or concrete) and a soft component (e.g. styrofoam) which could then be deformed into a double curved shell.

The first experiments which were done was the construction of an ice and a reinforced concrete shells with a diameter of five meters in a room of the laboratory of the Institute for Structural Engineering. Afterwards, more shells with bigger diameters have been built in order to check the validity of the new construction technique.

The soft component placed between segments enables the plate to be deformed. Along the edge of the plate a tendom is placed. The erection becomes possible by stressing of the tendom so that the circular plate slowly lifts up. Moreover, the raising of the structure was done by placing a pneumatic formwork underneath the plate. When the air enters the pneumatic formwork, the structure is raised.

The following pictures show the design of the structures in the initial and in the final shape and help to understand the previously explained concepts. Also some pictures which were taken during the construction procedure of these shells are included.

Ice shells

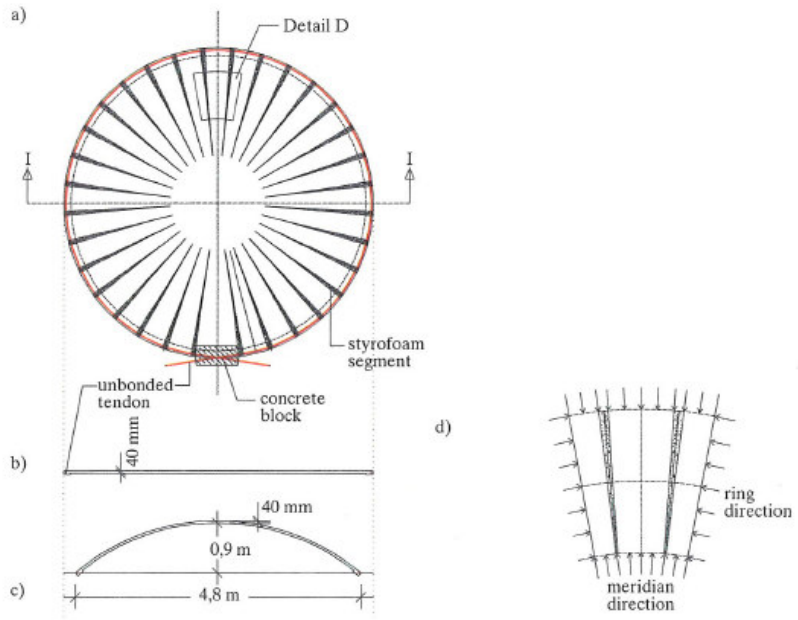

Figure 27: (a) Plan view of ice plate, (b) Section of ice plate, (c) Section of ice shell, (d) Detail D showing forces

The previous pictures show several views of the design of the ice shell. As it is shown, styrofoam segments where placed between the ice segments. All the shell was surrounded with an unbonded tendom. This experiment was carried out in the laboratoy of the Institute for Structural Engineering after its suitable fitting out.

The following pictures show the transforming process of this ice plate into an ice shell.

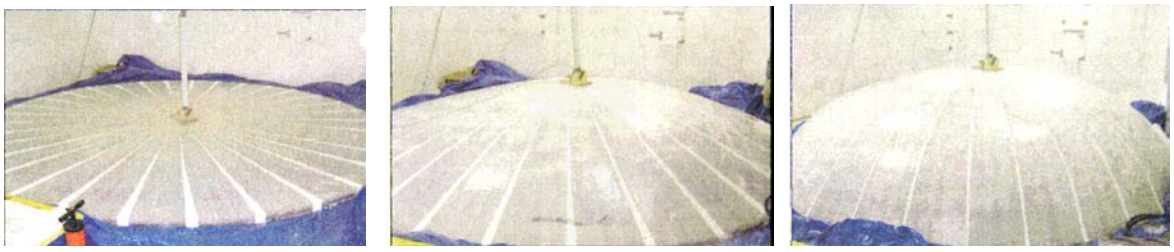

Figure 28: Tranforming an ice plate into an ice shell

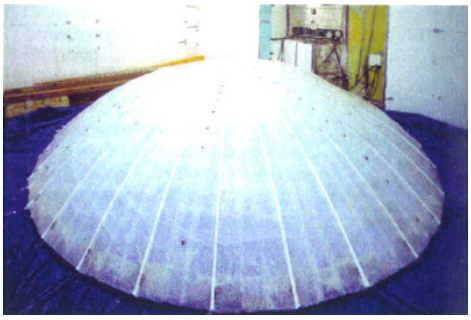

Figure 29: Final ice shell

After the raising process the final shape is reached. The span of it is 4,8 m and the height 0,9 m as the figures show.

In the final position the ice dome is a very stable structure. Without reducing the safety of the structure, large portions of the shell can be cut out. Experiments with various shapes of shells were carried out.

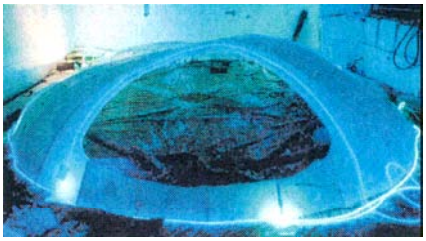

Figure 30: Ice shell with fibre optic cables

Concrete shells

The design of this shells is quite similar to the ice shell one. Several shells with different diameters have been built. The first one had a flat diameter of 5 m. The biggest one a diameter of 13 m. The following pictures show the transforming process of one of them.

Figure 31: Transforming a plate into a shell

4. Structural behaviour of domes

In order to understand the contents of this project it is considered fundamental to know the structural behaviour of a dome, specifically of semispherical domes. Although in the first part of this project the comparison between an arch and a dome structure has been explained, at this point the most important aspects in connection with the effects that are caused in this kind of structure under the acting of a fixed load or just its self-weight are going to be summarized.

Dome structures must provide strength, stiffness and stability. They must be capable of supporting applied loads and self weight without excessive deflection or displacements. Similar to an arch, a dome develops internal meridional forces that transfer loads to a support structure at its base. These forces are compressive and increase in magnitude from crown to the base for any dome loaded axisymmetrically by self weight [20].

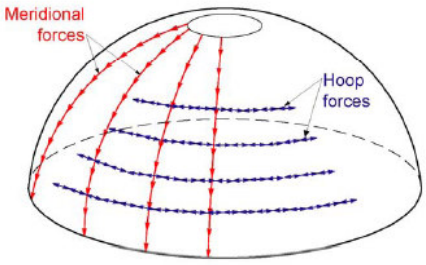

Figure 32: Meridional and hoop forces in a dome

Unlike an arch, a dome can resist out-of-plane bending of the meridian by developing internal hoop forces that act in the latitudinal direction as parallel rings. Hoop forces allow ring-by-ring construction of a dome without centering, an unfeasible task for an arch. As a result, though an arch is unstable without its keystone, a dome with an oculus is perfectly stable, as evidenced by the “incomplete” domes around the world.

When a symetric load acts, the upper part of the segments descend and lap their edges with the decrease of the curvature. The lower parts move outwards and open with the increasing curvature [21].

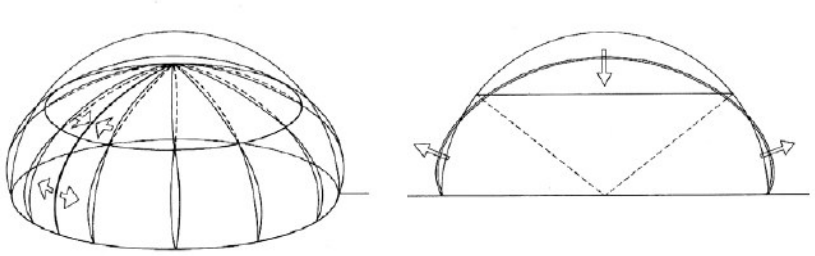

Figure 33: Segments deformation

The ability of the dome to generate ring forces avoids the deformation. The upper part acts like a sequence of compressed rings and the inferior part like tensile rings.

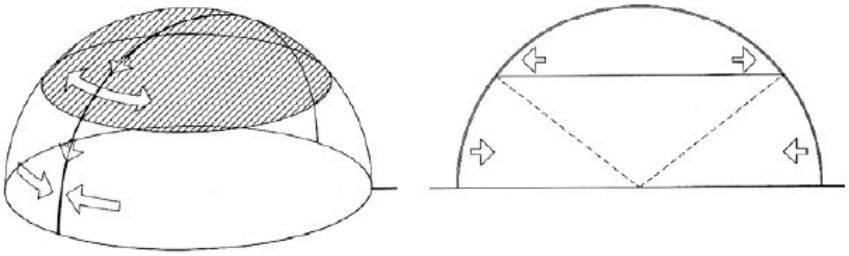

Figure 34: Effect of the ring forces

For a hemispherical dome loaded axisymmetrically, the transition between compressive hoop forces near the crown and tensile hoop forces near the base occurs at 51°49´ from the axis of rotation.

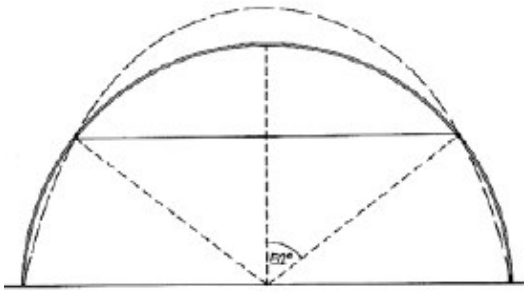

Figure 35: Angle where occurs the transition between compressive and tensile hoop forces

At the base of the dome, the support structure must resist the inclined loads from the dome with equal and opposite reactions. The support structure typically resists the vertical component of the inclined force with ease. However, the dome and support structure must also resist the horizontal component, the outward thrust, particulary near the base of the dome where the total thrust is greatest. External means of resistance may be employed , such as massive support structure walls or a metal tension ring around the dome´s base.

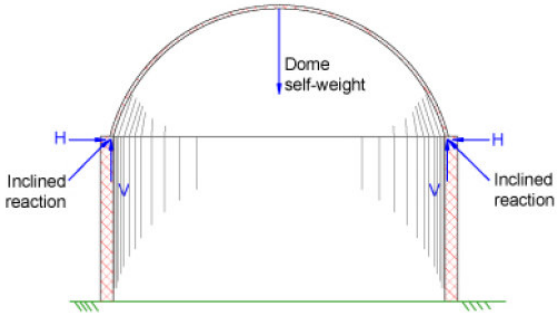

Figure 36: Inclined reaction at the base of the dome

If the only desired stresses in the dome are the ones typical from membranes, the edges of the structure must be able to have free horizontal displacement on its restrains. If the shell was encased, it would develope bounding effects in the springings that the dome would absorb quickly.

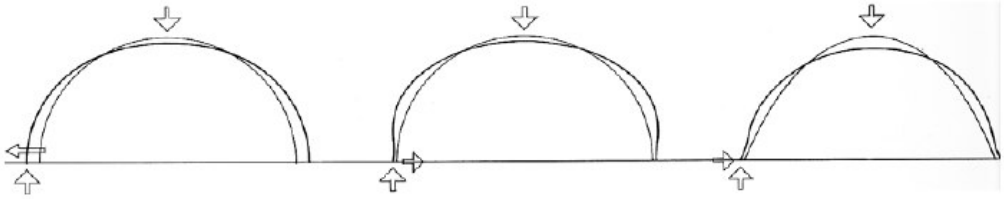

Figure 37: Bounding effects

It is useful for later chapters of this thesis to clarify that a semispherical dome acted upon its self weight or a symetric distributed gravitacional load will only generate compression and tensile stresses. No bending moments will appear.

Local or comprehensive failure of masonry´s domes may result from the inability of the material to resist tensile or bending forces that develop due to unanticipated load on the dome. A typical failure or collapse mechanism consits of: first, the formation of radial cracks along its meridians that divide the dome into lunes, or pie-shaped arches. Second, two hinge circles form in the dome mid-section, with a third hinge circle formation at or near the base. The cap of the dome will fall straight down, while the base of the lunes, as defined by the radial cracks, will rotate outward.

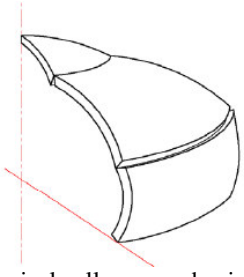

Figure 38: Typical collapse mechanism for a dome

CHAPTER 2

CONSTRUCTION OF DOME MODELS BY INDEPENDENT FLAT ELEMENTS AND PRE-STRESSING CABLES

Chapter content

The Institut for Structural Engineering of the Vienna University of Technology is carrying out several research works in order to develope new construction techniques and procedures of thin-walled shells without formworks.

The new technique which is being developed in this thesis consits in the lifting of a flat plate formed by independent flat elements in order to create a semispherical dome.

Two different models have been built in order to analyze the requirements and the feasibility of this new construction procedure.

In the first part of this chapter it is going to be described the design, the constrution, the erection and the reuslts of the load test corresponding to the first experiment which has been carried out. The diameter of the initial plate of this wooden dome is approximately 2 m and its final spatial radius is 0,64 m.

Taking into account the results of this first model, a bigger dome is built. The diameter of the initial plate of this shell is approximately 4 m. The second part of the chapter is about its design, construction and erection. The improvements which have been done in this bigger model are also shown.

1. CONSTRUCTION OF THE FIRST DOME (PLATE DIAMETER = 2 m)

1.1 Introduction

The aim of this experiment is the construction of a semispherical wood shell by independent flat elements. The different pieces are joined by a system of pre-stressing cables in both meridional and latitudinal directions.

To build this dome a diameter of 2 m has been chosen. The dimensions of the structure itself and its different parts, as well as the materials which are used are shown in the following sections. Wood has been chosen to build the shell because it is easy workable and more cost-effective for a first approximation and feasibility study of this new technique. Later on and attending to the obtained results, concrete and ice shells are expected to be built using the same method.

The first step of the construction procedure consists of the correct placing of the flat elements and its assembly by the pre-stressed vertical cables. The raising of the plate is performed by a pneumatic formwork placed underneath the plate. The horizontal cables are gradually adjusted during the lifting process until the final position is reached.

Several attempts with successive improvements have been required to reach a suitable final position. Each of them are later described and explained.

In order to analyze the structural behaviour a load test has been carried out and the displacements of some points of the shell when a fixed load acts on it have been obtained.

Taking into account these results, conclusions are made and some possible improvements are suggested.

1.2 Materials

The following materials and elements have been used to build the shell model:

- Medium density fiberboard (MDF)
- Hardboard (HB)
- U-profile
- Multiple screw terminal
- Wires

Medium density fiberboard

MDF panel of thickness 12 mm is used for the upper layer of the three ones that constitute each independent element.

MDF is an engineered wood product formed by breaking down softwood into wood fibers, combining it with wax and a resin binder, and forming panels by applying high temperature and pressure. It is a building material similar in application to plywood but made up of separated fibers, not wood veneers. It is denser than normal particle board.

This material is characterized by its isotropy and homogeny which avoid the tendency to split and by its flexibility, which makes it possible to use it for curved walls or surfaces. Its high structural strength has been decisive to the use of this material in the experiment. Some variants are also cheaper than other natural woods.

Hardboard

Panels with different thickness of HB have been used in the other two layers of each element.

In the middle layer HB panels with a thickness of 3 mm are utilized in order to create the ducts through which the wires of 2 mm of diameter are passed later. The use of this material is not important in this layer.

In the lower layer the thicknes of the panel is 5 mm.

Hardboard is a type of fiberboard, which is an engineered wood product. It is similar to particleboard and medium-density fiberboard, but is denser and much stronger and harder because it is made out of exploded wood fibers that have been highly compressed. It has significant structural strength and will not split or crack.

U-profile

An U-profile with an inner separation of 20 mm has been chosen in order to fit the outer edges of the central elements inside of it.
This profile has been cut and fit in the sixteen upper parts of the central. Between the pieces and this metallic element has been left a duct to install the central horizontal cable.

Wires and multiple screw terminal

The wires of 2 mm have been used to simulated the pre-stressed cables. They cables in meridional direction have been installed through each element and the ones in the latitudinal direction outside them.

The metallic part of the multiple screw terminal has been seperated of the plastic part and used as anchorage for the wires. By using these elements the simple and correct adjustment of the wires which join the different elements of the structure has been possible.

1.3 Design of the model

For the construction of this first shell a diameter of approximately 2 m for the circle in the plan has been chosen. After the lifting of this flat structure a semispherical dome with a span of 1,28 m and a camber hight of 0,64 m will be obtained.

In order to achieve a perfect curved shape and fitting in the final position between the independent elements which compose the shell, these need to be double curved. Geometry has been calculated in this case.

Nevertheless, in the practical work of the construction of this shell, flat elements have been used due to its simple making. The initial geometry which was obtained for the double curved ones, has been slightly modified and some measures have been introduced to guarantee the correct final fitting.

After this geometrical simplification, the possibility of the shells construction from flat elements without introducing significant changes as for shape or structural behaviour has been studied and developed in a next section of this project. The number of elements which compose the shell are established according to the shell size.

Next dimensioning calculations and geometry for shells formed by curved and flat elements are shown, as well as the explanation of the simplifications which have been done in the building of the structure.

1.3.1 Shell formed by double curved elements

The use of double curved elements allows to achieve a perfect final shape and fitting of the independent elements, although its making as prefabricated thin-walled elements is more laborious and costly. In this section only a theorical model has been analyzed.

In this first experiment the flat structure is composed by 16 longitudinal segments with 16 air spaces between them. Each of the longitudinal segments are formed by 6 pieces. There are 96 elements altogether. This division has been chosen taking into account the size of our model and in order to reach a suitable final shape.

The calculation basis starts from the desidered diameter in the flat initial position (Dp) and the diameter of the semispherical final shape (Ds).

Radius of the semispherical shell

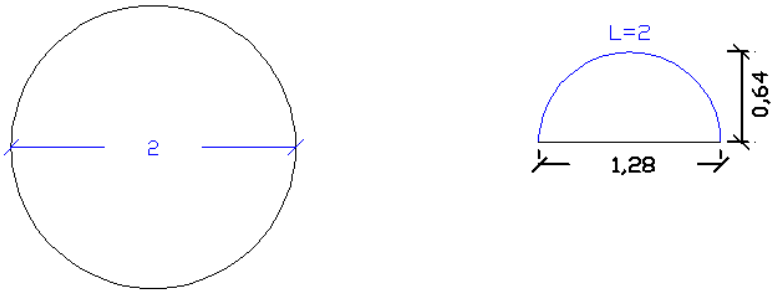

Figure 39: Sketches of the flat structure floor plan and the elevation of the final semispherical structure.

$$L = \frac{2 \times \pi \times r}{2} \qquad r = \frac{L \times 2}{\pi \times 2} = \frac{2}{\pi} = 0.64m$$

$$h = 0.64m$$
$$Ds = 1.28m$$

Air separation and length of the outer piece border

This process is based on the comparison of a concrete ring diameter formed by pieces and air spaces in the flat structure and the diameter of this same ring in the spacial position without any air spaces.

Outer plane perimeter: $Up = 2 \times \pi \times rp = 2 \times \pi \times 1 = 6.283m$
Outer spatial perimeter: $Us = 2 \times \pi \times rs = 2 \times \pi \times 0.64 = 4.021m$

$\Delta U = Up - Us = 2.262m$

Air separation: $s = \frac{\Delta U}{16} = 0.141m$

Lenght outer border: $l = \frac{Us}{16} = 0.251m$

Air separation and length along the radius of the structure

The previous process is repeated for several points along the radius of the structure in order to obtain the approximated dimensions of each piece and the air separation between them. The edge of each piece has been defined by straight lines connecting the calculated points.

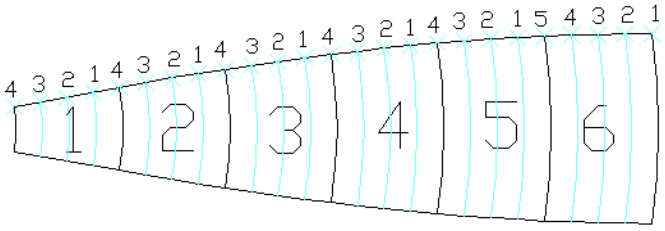

Figure 40: Numbering of the pieces and location of the points.

Piece	Point	Plane Perimeter (m)	Spatial Diameter (m)	Vertical section perimeter (m)	Air separation (cm)	Arch length (cm)
6	1	6,283	1,280	4,021	14,14	0,25
	2	6,061	1,271	3,994	12,92	0,25
	3	5,838	1,265	3,975	11,64	0,25
	4	5,616	1,255	3,944	10,45	0,25
	5	5,393	1,242	3,901	9,33	0,24
5	1	5,171	1,224	3,846	8,28	0,24
	2	4,949	1,203	3,778	7,32	0,24
	3	4,726	1,178	3,700	6,42	0,23
	4	4,504	1,149	3,609	5,59	0,23
4	1	4,281	1,116	3,507	4,84	0,22
	2	4,059	1,081	3,395	4,15	0,21
	3	3,837	1,041	3,272	3,53	0,20
	4	3,614	0,999	3,138	2,97	0,20
3	1	3,392	0,953	2,995	2,48	0,19
	2	3,169	0,905	2,843	2,04	0,18
	3	2,947	0,854	2,682	1,65	0,17
	4	2,724	0,800	2,513	1,32	0,16
2	1	2,502	0,743	2,335	1,04	0,15
	2	2,280	0,685	2,151	0,81	0,13
	3	2,057	0,624	1,960	0,61	0,12
	4	1,835	0,561	1,762	0,45	0,11
1	1	1,612	0,497	1,560	0,33	0,10
	2	1,390	0,431	1,353	0,23	0,08
	3	1,167	0,363	1,142	0,16	0,07
	4	0,945	0,295	0,927	0,11	0,06

Table 1: Pieces size calculation

The longitudinal length of each piece is 14.23 cm. Specifying the dimensions of each piece is not considered important since a model formed by curved independent elements is not going to be built. This is just the basis for later calculations.

Curvature of the pieces

The longitudinal curvature of the pieces has been calculated in accordance with the semispherical shape.

$$c = \frac{1}{r} = 1.562$$

Technical drawings of the structure

The complete drawings of the design and of the flat elements structure, are included in one of the attached documents of this project. The following pictures are only used to facilitate the understanding of the initial and final shapes, and the distribution of the pieces which make up the shell.

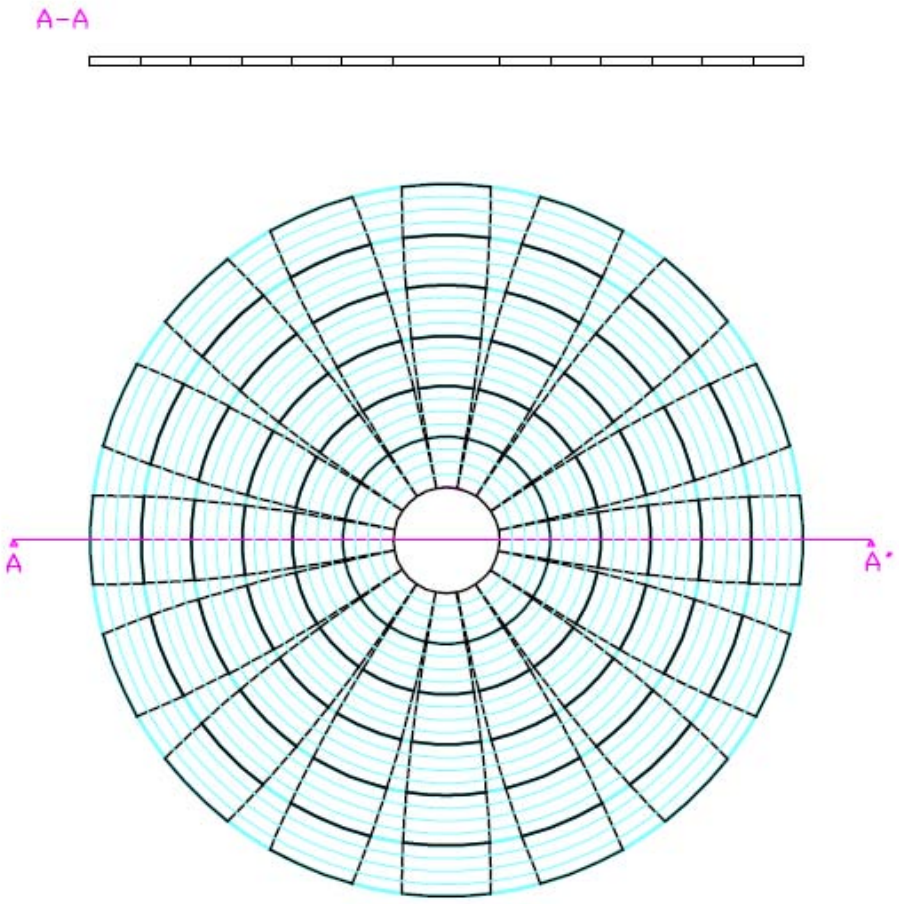

Figure 41: Floor plan and cross section of the flat structure

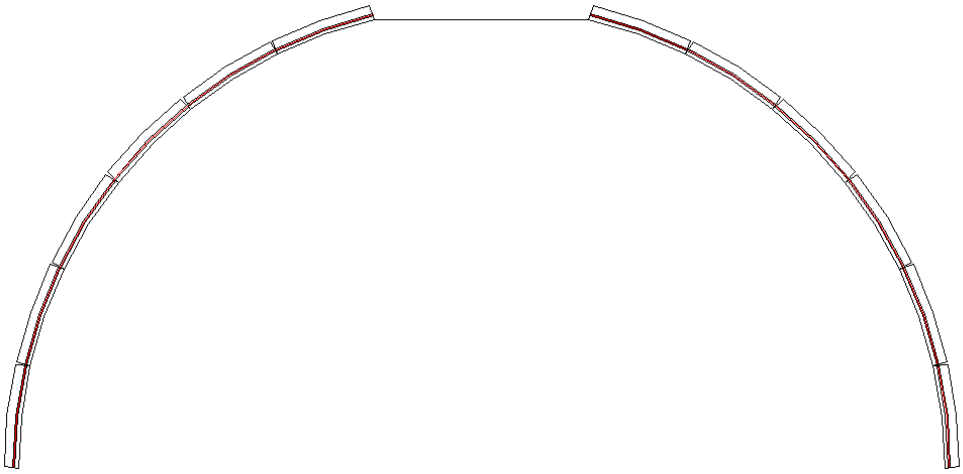

Figure 42: Cross section in the final position after the elevation

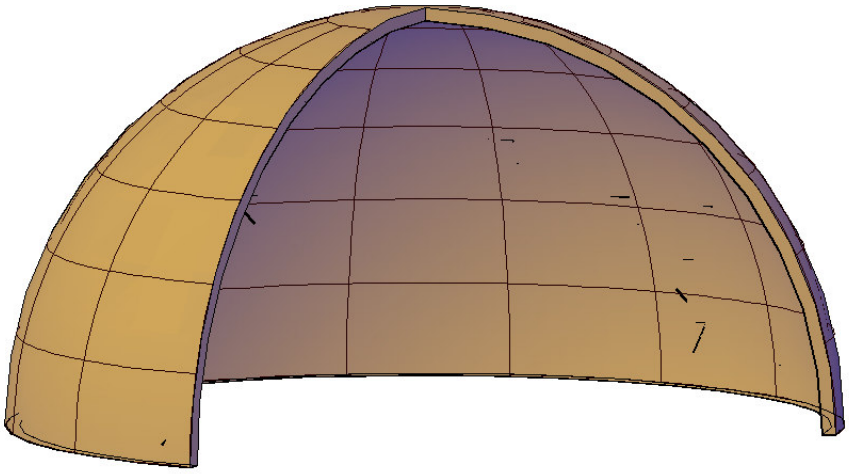

Figure 43: 3D Model of the final position

1.3.2 Shell formed by flat elements

The dome which has been constructed in the laboratory is formed by independent flat elements which are joined by pre-stressing cables. In this section the size and the shape of the differents pieces are going to be deteremined on the basis of the previous calculations.

The first thing to take into account is that all the edges of the pieces have to be straight. In this way each element is able to transfer the generated stresses to the other ones through a contact line. If the edges were curved, there would be only 4 points of contact among the pieces, so that the stresses on them would be really high and the areas next to them could be problematic.

Flat surfaces and straight edges are the difference between the two models. The geometry has been adjusted to this two requirements.

To facilitate the order of the wood and work in the centimeters magnitude the dimensions of each piece have been modified. The length of the pieces has been changed to 14 cm and the radius of the central circle has been kept 16 cm. The diameter of the flat structure is also 2 m. The air spaces between elements have been calculated again using the same analogy between the flat structure and the final curved structure. Nevertheless, no intermedate points have been used due to the fact that all the edges are now straight lines.

Piece	Edge	Plant Perimeter	Diameter vertical section	Vertical section perimeter	Air separation (cm)	Arch length (cm)	Edge length (cm)
1	1	6,283	1,280	4,021	14,137	0,251	25,0
	2	5,404	1,249	3,925	9,240	0,245	24,4
2	1	5,404	1,249	3,925	9,240	0,245	24,4
	2	4,524	1,159	3,641	5,517	0,228	22,7
3	1	4,524	1,159	3,641	5,517	0,228	22,7
	2	3,644	1,013	3,183	2,884	0,199	19,8
4	1	3,644	1,013	3,183	2,884	0,199	19,8
	2	2,765	0,819	2,572	1,202	0,161	16,0
5	1	2,765	0,819	2,572	1,202	0,161	16,0
	2	1,885	0,585	1,838	0,291	0,115	11,4
6	1	1,885	0,585	1,838	0,291	0,115	11,4
	2	1,005	0,324	1,017	0,000	0,064	6,2

Table 2: Calculation of the air separation and the size of the pieces

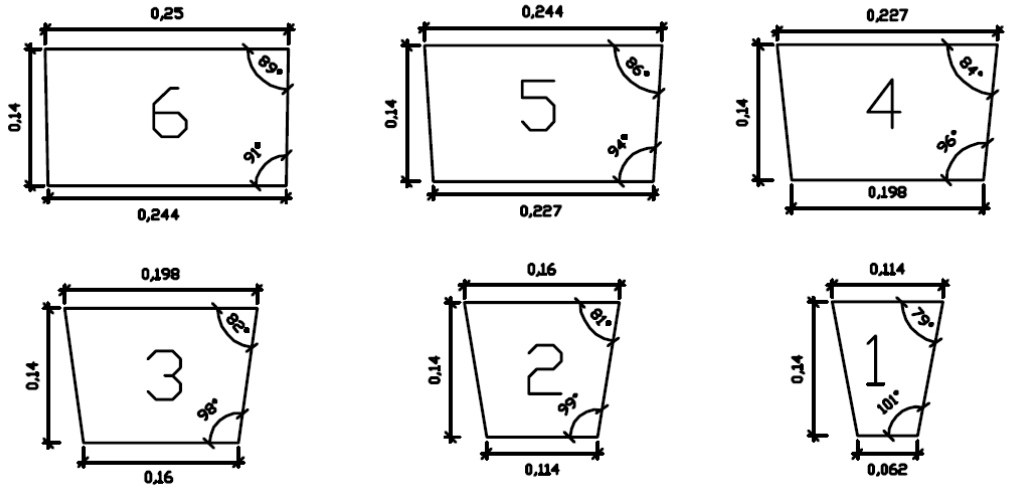

Figure 44: Dimensions of the different elements

In order to obtain a certain margin of movement and positioning between the elements, the edges of them which will form the transversal joints have been given a curved form.

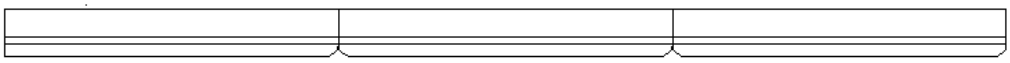

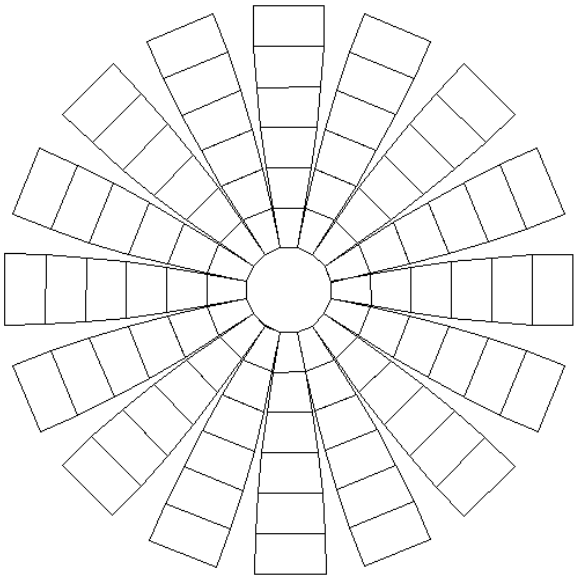

Figure 45: Flat structure formed by flat elements

1.4 Construction process

The first step in the construction of the model is the cutting of the 3 pieces which compose each of the 96 elements according to the previous geometry calculations.

At this point it is useful to remember that each element is formed by 3 layers (Figure 46). The mission of the middle layer is to generate the necessary spaces for the cables.

Figure 46: Sketch of the layers of each independent element

The images below show the 3 pieces which compose the element which has been numbered in the used sketch with number 4. The rest of the elements, except for element number 6 (the one placed on the base ring), have the same division. Also the pieces corresponding to element number 6 are shown due to the special cable distribution on them. With this geometry it is only required to anchor only the cables on the top part of each segment and not in both ends.

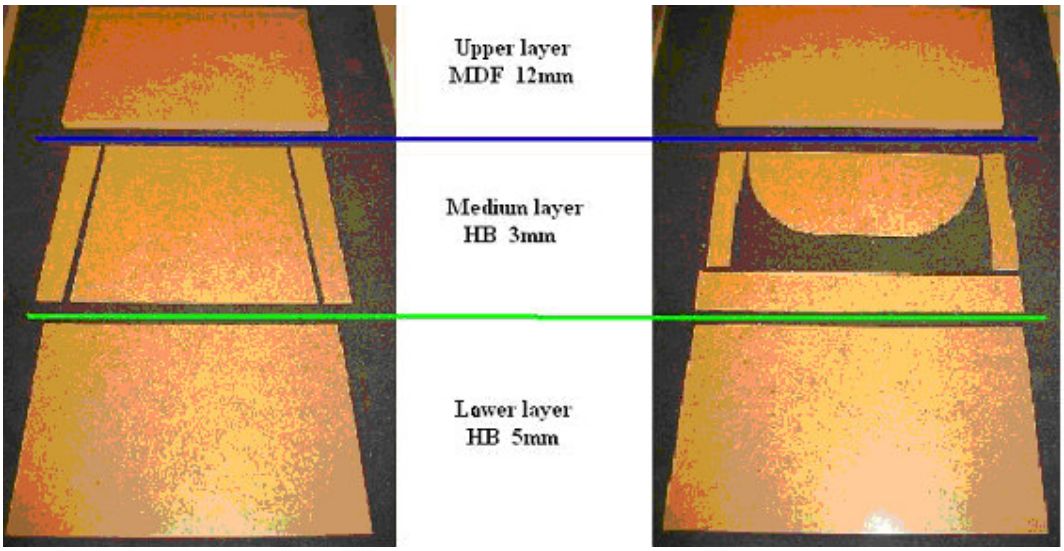

Figure 47: Pieces which form element number 4 (left) and element number 6 (right)

The following picture is useful to understand how the cables are distributed inside piece number 6.

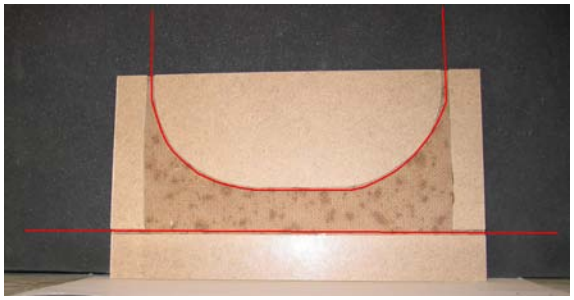

Figure 48: Cables distribution inside piece number 6

The longest edges of the lower layer pieces are sanded in order to achieve a curved edge to facilitate the connection and the relative movements between consecutive pieces.

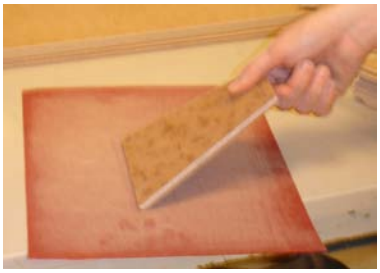

Fig. 49 and 50: Sanding of the piece edge

Next the different layers are glued with the special feature that it is necessary to put the wires inside piece number 6 before joining the last one, otherwise its placement would be difficult.

Fig. 51, 52 and 53: Gluing of the pieces

After gluing the upper and the middle layers it is posible to observe the channels which have been created in order to place the wires inside each element, as well as the special geometry of the element number 6. The divisions of the middle layer have been done taking into account that the distribution of the cables inside each longitudinal segment needs to be symmetric to have a good structural behaviour and that they need to be wide enough to place in them a 2 mm wire.

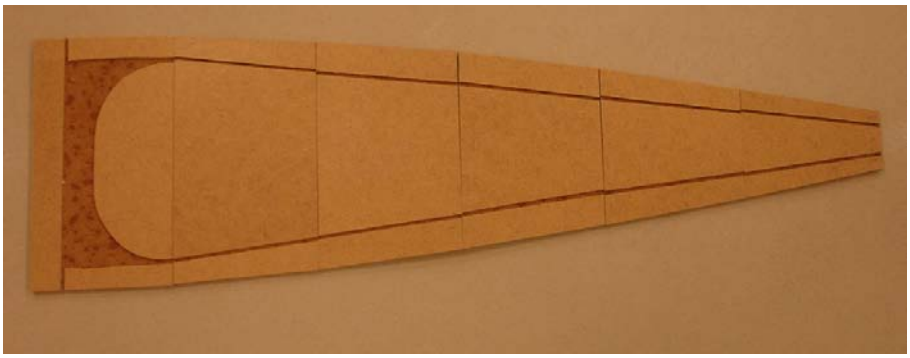

Figure 54: Section of a segment

The central piece is encased inside the U-profile which has been previously cut and holes have been done in it to let the cables fit through them. By using this rigid element we obtain a hard support for the edges of the cables which are localized in this area and it is possible to locate the cable which joins all the pieces in the central ring between this metallic piece and the wood element.

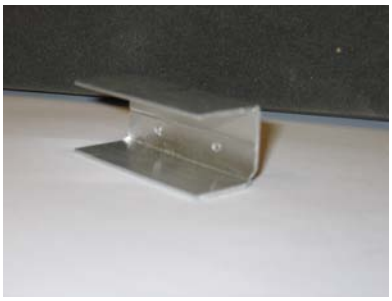

Figure 55: Cut and holed U-profile piece

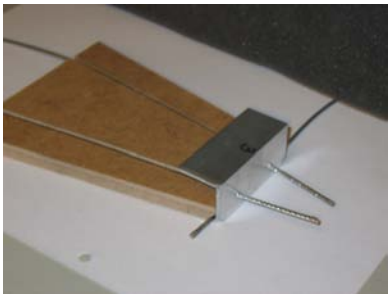

Figure 56: Piece nº1 with the cables system and the U-profile piece

When all parts are glued and all the cables are placed inside piece number 6 (they must be placed in it before gluing the last layer), the wires are introduced through each element in the corresponding order. The vertical cables system is shown in the following pictures.

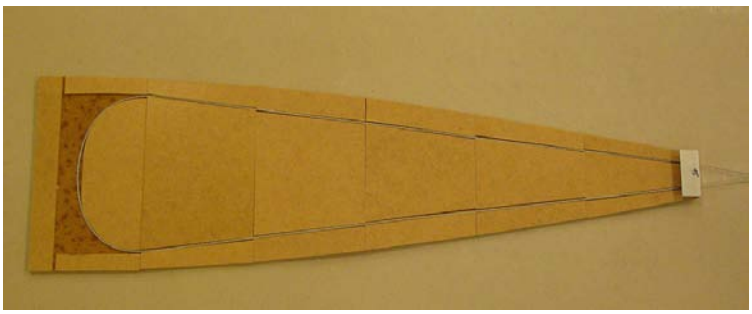

Figure 57: Meridional cables distribution inside a total segment

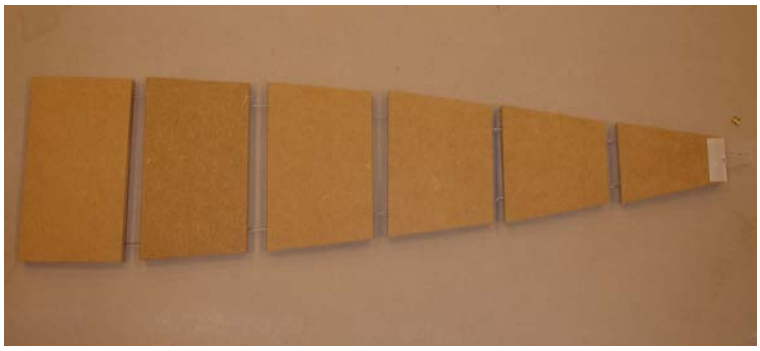

Figure 58: Different pieces joined by the meridional cables

The cables are fixed with the metallic part of the multiple screw terminal that has been separated before from the plastic part. They act like anchorages.

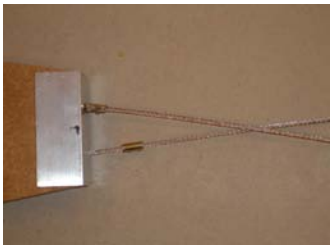

Figure 59: Anchorage system of the cables

There is also a cables system in the ring direction. Before the raising of the structure only the central one is placed and adjusted, due to the fact that the perimeter of this circle is going to be constant. The cables which join pieces number 6 are also put in each element, but it is not adjusted in this moment because the circle perimeter is going to change considerably.

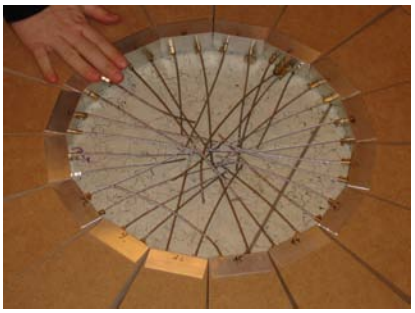

Figure 60 and 61: Central ring with the anchorage system of the meridian and the central ring cables

All the elements of each segments are now joined by the vertical cables and all the segments are joined by the transversal central cable. The structure is prepared to be lifted.

Figure 62: Final plate

1.5 Structure erection

The final aim of the research is to achieve a final semispherical shell from the constructed flat plate. The raising of the plate is performed by a pneumatic formwork placed underneath it and during this process the horizontal cables are gradually adjusted as the perimeter of each ring is reduced.

The structure erection has been decisive to detect which parts of it do not work properly. Several attempts have been carried out to fix the needed changes in order to achieve a suitable final model. Next each of this attempts and its later improvements are described.

First attempt

In the first raising attempt the previously described plate is used without any change.

Before the elevation process only the cables of the central ring and of the outer perimeter in piece number 6 are placed. The rest of them are going to be installed manually in the space between pieces when the structure has almost reached its final position.

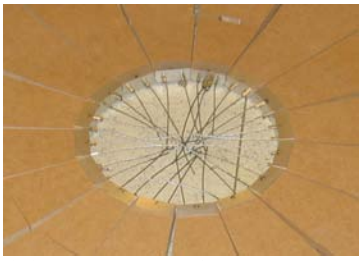

Figures 63 and 64: Cables of the central ring and outer perimeter

The air jack which raises the structure is the typical one which is usually used to lift the cars in order to facilitate its repair. The air pump is connected to the side part of the air jack by a rubber tubbing.

Figure 65: Air jack

Fig. 66: Placement of the air jack underneath the plate

The final shape after the raising process was not the expected one (Figure 67).

Figure 67: Final shape after the firt raising attempt

As the previous figure shows, there are some mistakes in the design or construction process:

- There are spaces between the pieces of the segments, which means that the vertical cables are not properly tighted.
- The final shape fits to the shape of the air jack.
- The segments are not heavy enough. They do not have displacement resistance during the lifting proces and some of them are floating on the air.

Second attempt

In this new attempt the previous mistakes have been tried to be corrected.

First, the lifting system has been changed. A new oval pneumatic formwork has been created by gluing two circular planes of polyethylene. In order to allow the air entrance a central rubber tubbing connection has been installed.

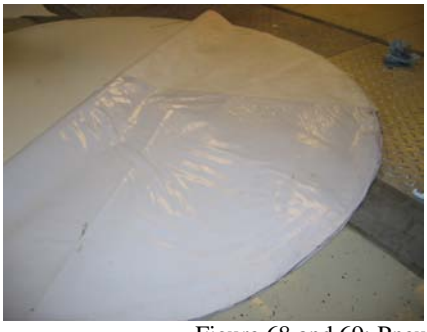

Figure 68 and 69: Pneumtic formwork construction

Moreover, some weights have been put on the extreme of each segement and the vertical cables has been correctly tightened.

Figure 70: Inflated pneumatic formwork

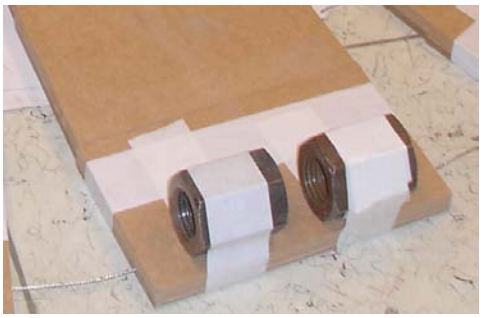

Figure 71: Weights on the segment extreme

The flat structure has been placed over the air supported formwork and it has been inflated through the rubber tubing connection. As the air goes inside the pneumatic formwork, the structure raises.

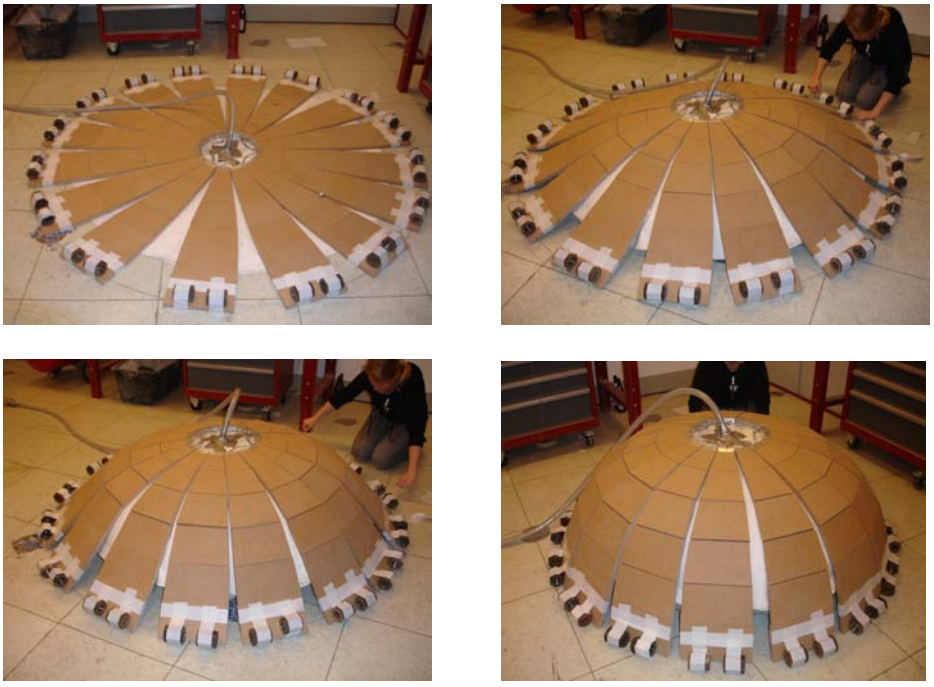

Figure 72: Steps of the raising process

Before placing the rest of the ring cables (only the central and the outer ones are already installed) the reached final shape is quite suitable. Once this cables are placed in the spaces between pieces and adjusted, the gap between each segment is still considerable. One of its causes is the short sliding of the cables between the pieces and its consequent difficulty of manual adjustment. Moreover there are some elements which are not in the right position.

Figure 73: Manual adjustment of the ring cables

Figure 74: Final shape

Figure 75 and 76: Obsevable mistakes

Third attempt

To avoid the mentioned problems closed hooks have been used on each piece to place the cables.

The situation of the hooks on each piece has been decided attending to the structural behaviour of a dome which has been already explained in a prevous section of this project. The horizontal cables contribute to the resistance of the anular stresses which appear as the consequence of the self-weight of the shell or after the application of a load.

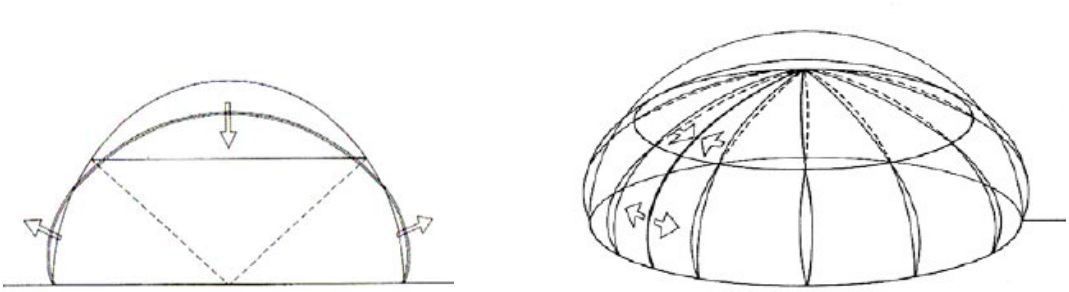

Figure 77: Deformation of the segments under the application of a distributed load. The upper part of the segments descends and they overlap when the curvature decreases. The lower part becomes deformed towards the exterior and it opens when the curvature increase.

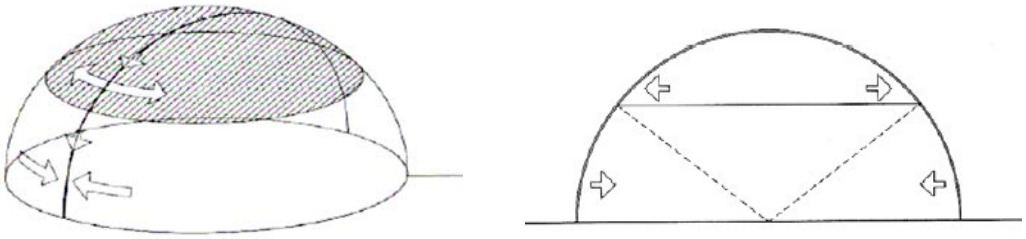

Figure 78: Anular shape effect. The horizontal rings are opposite to the deformations. The upper part behaves like a sequence of compressed rings and the lower part like a sequence of rings working in traction.

The main contribution of the cables takes place on the lower part, where the tension appears, since they avoid in this area the seperation of the pieces. The function of this cable is the horizontal joining of the different pieces, as well as the contribution to the structural strength. Due to the fact that this tension anular stresses grow from the point of the shell where the compression stresses are zero until the base of it, the cables are placed on the lower part of each piece where the biggest tension appears.

Figure 79: Placement of the ring cables

The obtained results with this placing system of the horizontal cables are considerably better than before. There are not spaces between pieces and the elements are in the right

position. The final suitable shape has been reached. The following step is testing the strength and the displacements of the structure with a specific applied load.

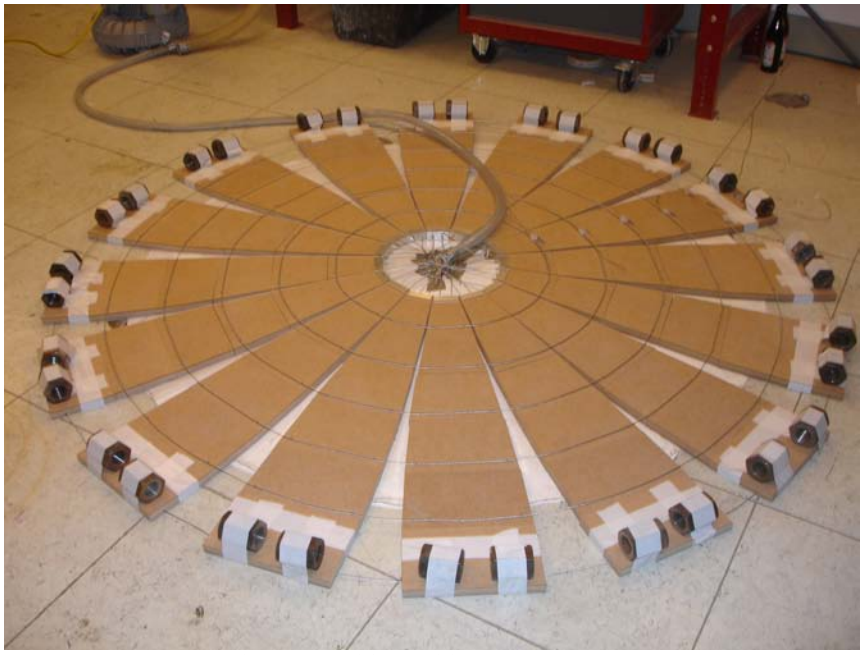

Figure 80: Initial position: plate structure

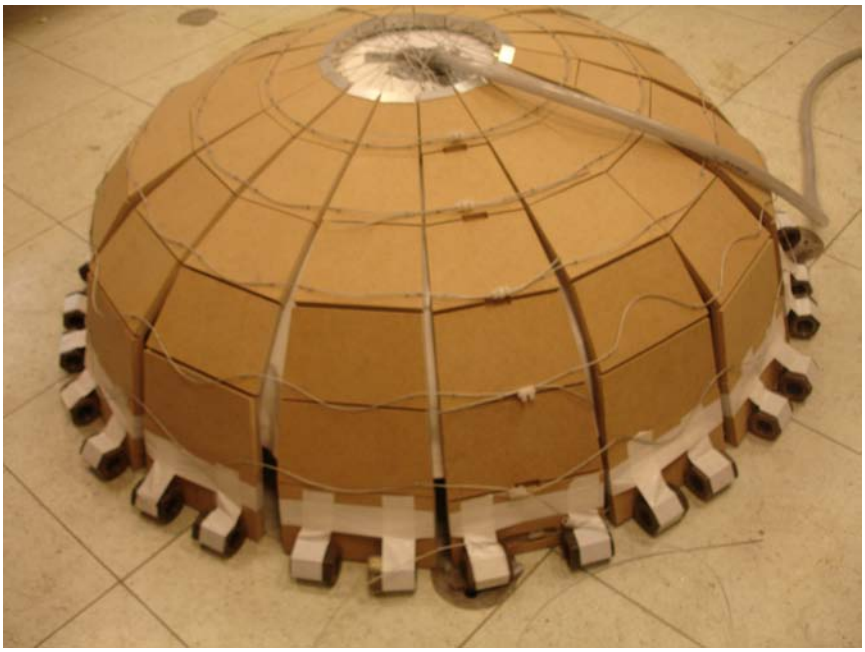

Figure 81: Intermediate step of the raising process

Figure 82: Final reached shape

1.6 Load test

Once a suitable final shape has been reached and all the elements have correctly fit, the strength and the behaviour of the structure must be tested. This experiment is also carried out in the laboratory of the Institute for Structural Engineering of the Vienna University of Technology.

Before the test, all the cables in the ring direction have been tightened with a force of approximately 300 N. Due to this fact, they will contribute more to the general strength of the structure and will decrease the separation of the pieces in the tensile lower part.

The aim of the test is not the obtaining of the breaking load, but the displacements in several points of the shell after a specific action. Attending to the dimensions of our model, no high forces are required. Therefore human force is enough to apply the desired load. The system which has been employed to carry out this load test is shown and explained in the following pictures.

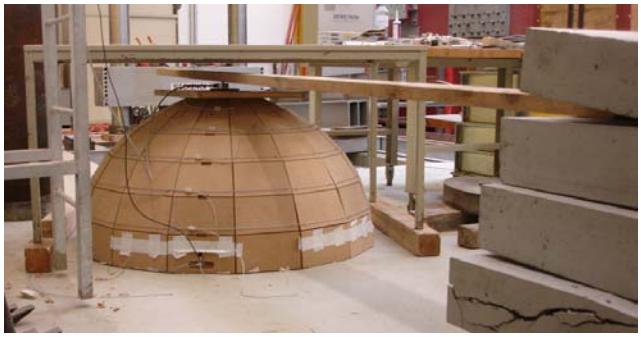

Figure 83: Assembly of the load system

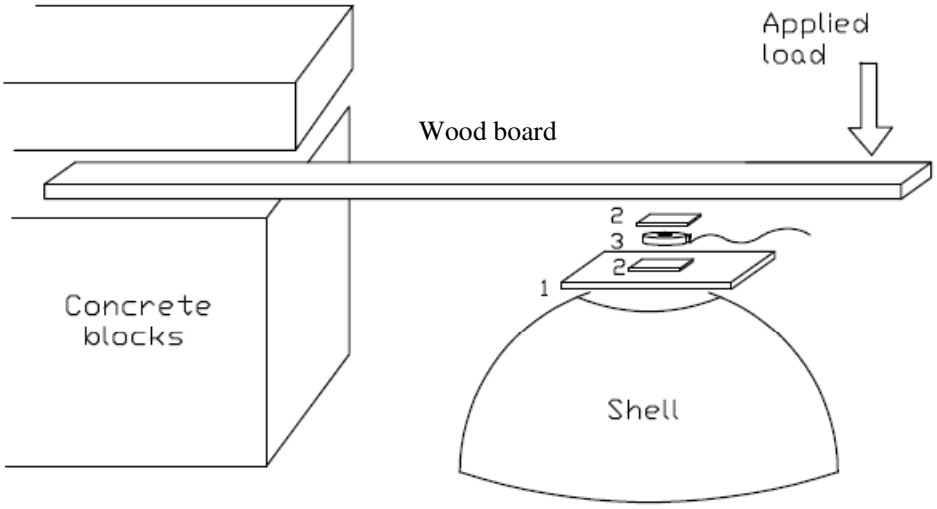

Figure 84: System sketch

This system consists on a wood board which is clamped in one end among concrete blocks and has a simple support in one point along its length. The force is applied at the free end.

Over the shell a smaller wood board (1) is placed to distribute the point charge along the central ring. In order to know the magnitude of the applied force a dynamometer (3) is set between the main wood board and this smaller one which transfers the load. Two iron plates are used to avoid the direct contact between the dynamometer and the irregular wood surfaces.

From an analytical point of view, this mechanism can be represented in the following way:

Figure 85: Structural sketch

The reaction R_2 is also the force which is transfered to the shell. Solving this statically indeterminate system is posible to declare that this reaction is bigger than the applied force F. The reaction R_1 has a negative value, which means that the drawn direction of the vector is not correct.

Four movement sensors are placed on different elements of the model to measure the horizontal displacements. Another sensor has been placed in the middle of the structure to measure the vertical ones.

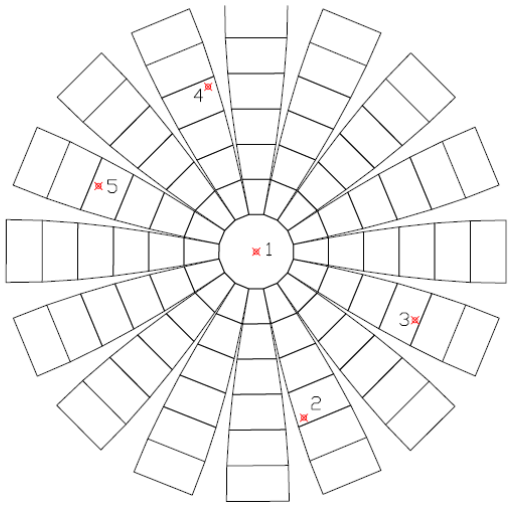

Figure 86: Placement of the movement sensors

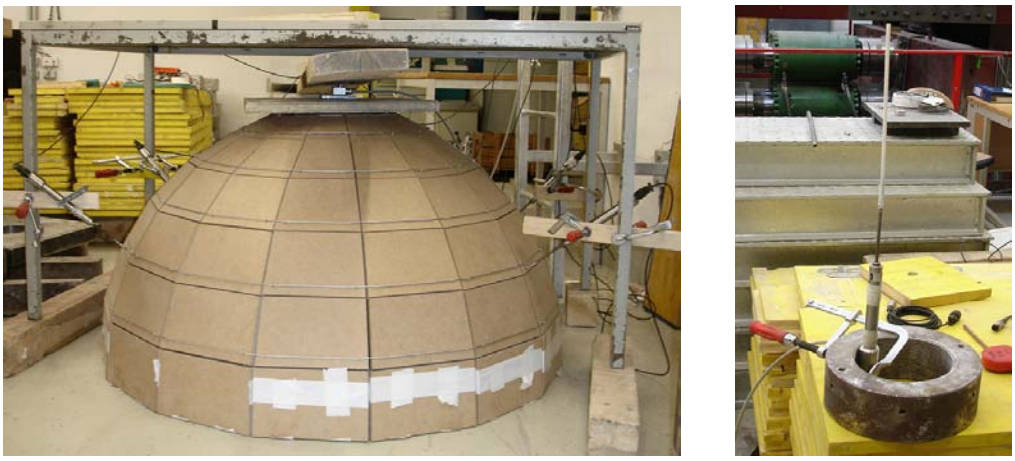

Figure 87: Lateral and central movement sensors

All the movement sensors, as well as the dyanamometer are connected to a computer where all the results are registered.

In order to guarantee the reliability of the obtained data two tests have been done. The coincidence in the magnitude order of the final values which have been obtained in both cases checks the validity of the test. The synthesis of the results are shown in the following graph and tables.

The following tables collect the corresponding data to the load stages where the biggest deformations are produced in both cases.

Dateikommentar:

Zeit DEVICE_1	Kraft	Weg 1	Weg 2	Weg 3	Weg 4	Weg 5
s	kN	mm	mm	mm	mm	mm
153,500007	-1,0368	3,132	0,018	0,09	-0,13	-0,106
154,000007	-1,0674	3,344	0,026	0,09	-0,132	-0,108
154,500007	-1,1106	3,714	0,046	0,094	-0,132	-0,118
155,000007	-1,1058	3,926	0,048	0,094	-0,126	-0,124
155,500007	-1,0812	3,972	0,048	0,094	-0,122	-0,126
156,000007	-1,0602	3,968	0,048	0,094	-0,12	-0,13
156,500007	-1,0578	3,972	0,048	0,094	-0,118	-0,132
157,000007	-1,0074	3,948	0,046	0,094	-0,112	-0,134
157,500007	-0,9318	3,898	0,04	0,094	-0,106	-0,132
158,000008	-0,8394	3,81	0,032	0,094	-0,098	-0,132

Table 3: Results Load Test 1

Dateikommentar:

Zeit DEVICE_1 s	Kraft kN	Weg 1 mm	Weg 2 mm	Weg 3 mm	Weg 4 mm	Weg 5 mm
55,0000026	-0,8784	1,99	0,106	0,062	-0,038	-0,072
55,5000026	-0,9216	2,106	0,114	0,066	-0,04	-0,072
56,0000027	-0,963	2,26	0,124	0,07	-0,04	-0,074
56,5000027	-0,9786	2,34	0,128	0,072	-0,04	-0,076
57,0000027	-1,0224	2,512	0,142	0,074	-0,04	-0,08
57,5000027	-1,0662	2,828	0,158	0,07	-0,04	-0,086
58,0000028	-1,0788	3,068	0,164	0,068	-0,038	-0,088
58,5000028	-1,0704	3,12	0,164	0,066	-0,034	-0,09
59,0000028	-1,0698	3,162	0,164	0,066	-0,032	-0,09
59,5000028	-1,0596	3,178	0,164	0,064	-0,03	-0,092
60,0000028	-1,0464	3,178	0,164	0,064	-0,03	-0,092
60,5000029	-1,0152	3,164	0,164	0,064	-0,026	-0,092
61,0000029	-0,9672	3,138	0,16	0,064	-0,022	-0,094
61,5000029	-0,8958	3,088	0,156	0,064	-0,016	-0,094
62,0000029	-0,8286	3,024	0,148	0,064	-0,01	-0,094
62,500003	-0,7788	2,964	0,142	0,064	-0,006	-0,092
63,000003	-0,7302	2,896	0,136	0,064	-0,002	-0,092

Table 4: Results Load Test 2

As it is shown, the load stages are not constant in magnitude and time due to the fact that the load is not applied by a machine, but by a person. The sign of the displacement depends only on the calibration of the sensor and in this test has not any meaning because it is previously known that in the ring where the measuring instuments are placed all the studied points move outwards. The sensors are in the tension area.

The highest displacements of each sensor are highlighted. All of them do not correspond with the maximum applied load. Even some of this biggest movements are produced at the beginning of the unloading process. Nevertheless, this fact can be easily understood taking into account that all this measures are taken in a really short period of time and that the structure is not a continuos solid, but a set of joined elements which are resetting and interacting along the experiment.

As far as the magnitude of the measurements, the biggest is the vertical one. Nevertheless this displacement is less than 4 mm. The maximun lateral displacement is 0.164 mm.

.

The global behaviour of the whole structure during the loading and the unloading process can be analyzed in the next graph.

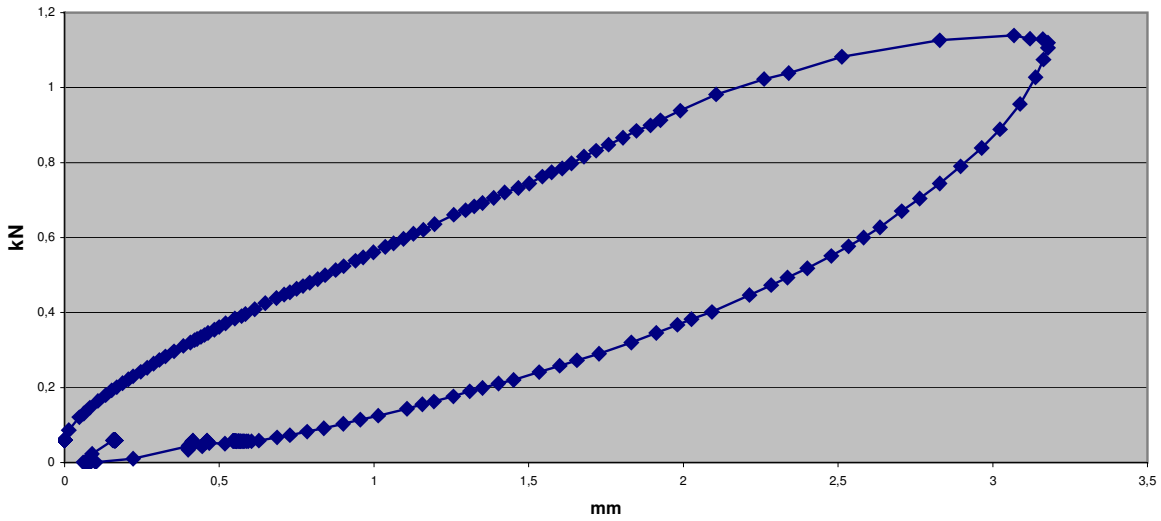

Figure 88: Relation between the applied load and the vertical displacement (sensor 1)

This graph shows the relation between the applied load and the vertical displacemts which are recorded by sensor 1. This instrument is placed in the center of the structure and it is in contact with the horizontal wood board placed on the top of the shell.

Each load stage is represented in the graph by a square. As the graph shows, the structure has almost a linear elastic behaviour. In light of these results it seems that the breaking load is far away from this reached value.

After the also gradual unloading process it does not appear any important permanent deformation and the whole structure recovers its initial height.

1.7 Feasibility and improvement proposals

In this conclusion section the procedure and results of the model construction and behaviour are analyzed. Furthermore, some improvement methods and aspects to take into account in the construction of a real shell are expounded.

This experiment is the first step in the research studies which are being devoloped in the construction of shell strucutures by joining different precast elements. Its main aim is to find out the means to achieve a suitable final shape, an effective wire system and a resistant structural behaviour.

All of this purposes have been reached in this model with a plan diameter of 2 m. The displacements under the action of a fixed load are acceptable. In a subsequent part of this project they are compared to the displacements given by analytical solutions and computer models.

With respect to the lifting system of the structure, the shape of the pneumatic formwork seems to be decisive to achieve a correct final shape of the shell. If some kind of little crane had been used to raise the plate pulling it upwards, the final shape would have been probably different. This is obvious because the air jack for cars with not concret shape has not worked to raise it. However, the air supported formwork may not be so important in bigger structures with cables with a thicker diameter and another lifting system may be used.

Nevertheless, other techniques to improve the behaviour of the structure have been conceived.

The first of them is filling the gaps between pieces with some kind of cement in order to increase the resistance of the shell. In this way, the structure would work like a continious solid and the tranfer of forces between elements would not occur only through the contact line or the cables which join them. Moreover, parts of the cables are in the open between the pieces. Therefore, in the construction of real thin shells with this technique, the filling of the gaps is necessary in order to protect them from some external actions like corrosion. The aesthetic aspect is also improve with this method.

Another way which may improve the joining of the elements is using thin cylindrical elements in the joinings. The edges of each element would be provided with the correct shape to place it. The element would be fixed to one of the pieces and just fit in the other one. This method would make easy the transfer of forces and would decrease the relative movements among pieces (Figure 89).

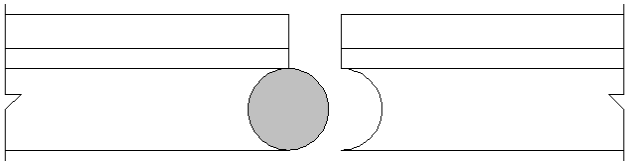

Figure 89: Connection between pieces

A cylindrical element would be placed along each edge of the piece. The radius of this element and of the necessary hole in the wood would be determinated taking into account the angle between the pieces in the final shape.

The small model which has been developed works correctly and this measures are not necessary. The pieces fit in a suitable way. However, this model is not too big and the applied load is not very high. Maybe, other models with the same number of pieces but with a bigger need to apply some of the previous methods. In order to analyze the influence of the size and the feasibility of this technique in bigger shells another dome is going to be built also using wood.

After this second experiment, enough information and results will be obtained about the feasibility of shells construction by joining different precast element with a system of vertical and horizontal cables. The following step is to use this technique in the construction of a thin concrete shell with a bigger size. The possibility of applying this technique in the construction of temporary ice shells is also considered. If the results with the previous models and experiments are favourable, ice shells are supposed to be also built.

2. CONSTRUCTION OF THE SECOND DOME (PLATE DIAMETER = 4 m)

2.1 Introduction

Following the same steps for the design, the construction and the erection a bigger shell have been carried out in the laboratory. Nevertheless, some measures have been taken in order to improve its structural behaviour and facilitate its construction procedure.

Despite the successful previous experiment, another model with a flat diameter of 4 m has been decided to be built. The aim of this work is to contrast the validity of this method, to determine if the dimension has a relevant influence and to study the application of some improvement purposes which were done in the previous section.

2.2 Materials and design of the model

The materials which are used for the creation of this dome are the same as in the other model. The only difference is that the order of the layers is reversed. The MDF piece is now the lower one and the HB of 5 mm is the upper one. The middle layer is the same - HB of 3 mm. The MDF has been perforated in order to place on it the rods which are going to be the connetion elements between pieces.

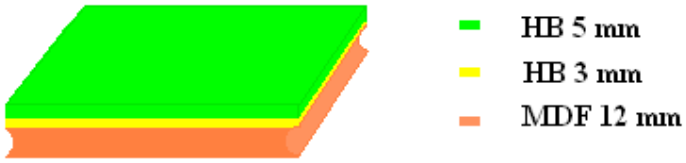

Figure 90: Sketch of the layers in an element

For the design the same calculation procedure has been used. Nevertheless the hinges between different pieces have been simulated with cylindrical rods. The height of the pieces and the radius of the central ring have been fixed to 28 cm. The diameter of the plate is 3.92 m without taking into account the increment which is caused by the placement of the cylinders between the pieces.

Dp: plane diameter
Ds: spatial diameter
Up: plane perimeter
Us: spatial diameter

Dp	Ds	Up	Us	Inc. U	Air	Piece length	Piece height
3,92	2,5000	12,3150	7,8540	4,4611	0,2788	0,49	0,28
3,36	2,4373	10,5558	7,6570	2,8987	0,1812	0,48	0,28
2,8	2,2523	8,7965	7,0758	1,7207	0,1075	0,44	0,28
2,24	1,9952	7,0372	6,2681	0,7691	0,0481	0,39	0,28
1,68	1,5591	5,2779	4,8981	0,3798	0,0237	0,31	0,28
1,12	1,0860	3,5186	3,4118	0,1068	0,0067	0,21	0,28
0,56	0,5576	1,7593	1,7518	0,0075	0,0005	0,11	0,28

Table 5: Calculation of the pieces dimensions

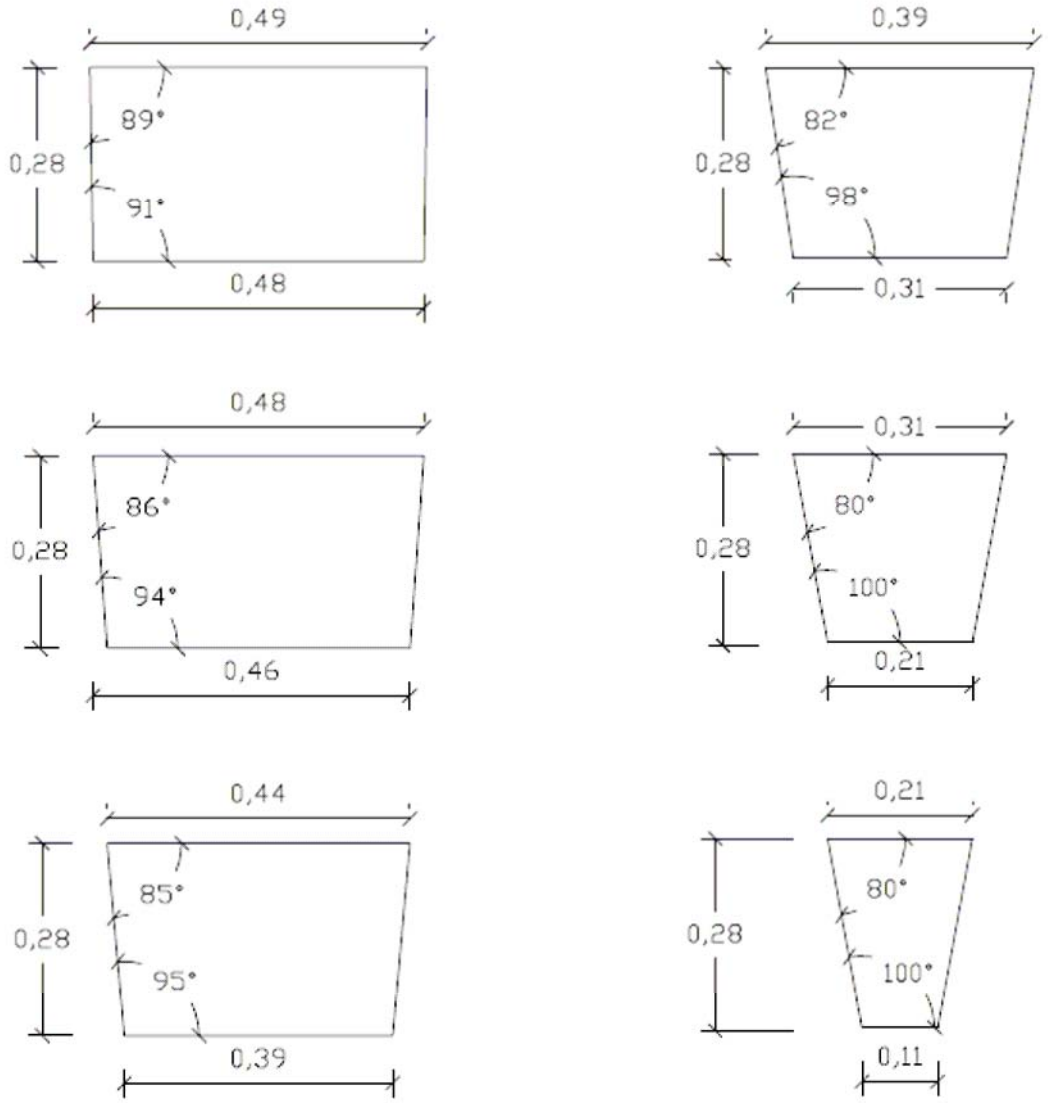

Figure 91: Dimensions of the pieces

The rods are fixed to one of the pieces and the other piece has a cylindrical hole on its edge to fit it. The rods are placed in the layer of MDF with 12 mm of thickness. The diameter of the rods is also 12 mm. The radius of the hole has been determined depending on the angle which is left between the flat elements after the raising of the structure. This diameter has a value of 4.5 mm (Figure 92).

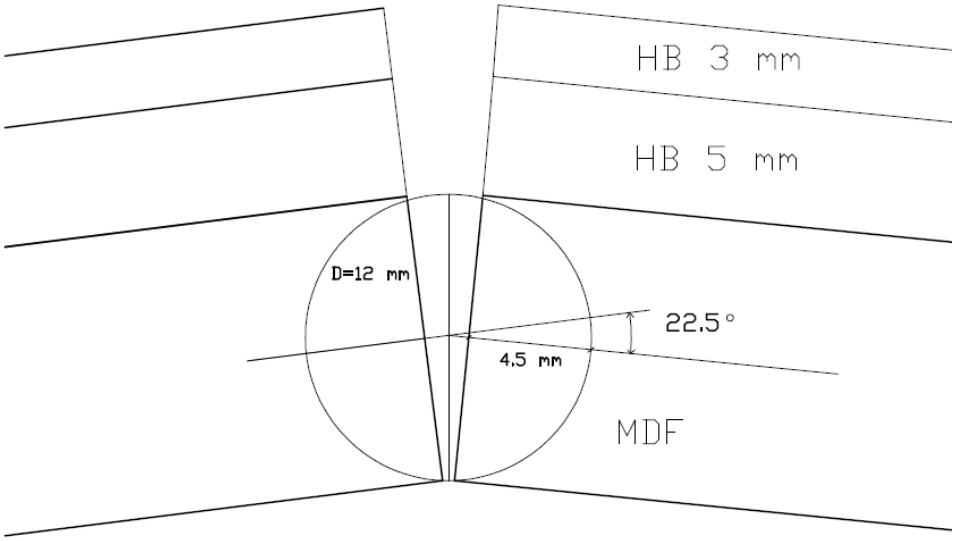

Figure 92: Sketch of the connection between pieces in the final position

2.3 Construction process

The steps of the construction process can be summed up in the following way:

1. Cutting and gluing of the pieces to fabricate the 96 independent elements which form the plate.
2. Sanding of the edges.
3. Cutting of the wooden and metallic rods and gluing of these to each element.
4. Construction of the pneumatic formwork.
5. Placement of all the pieces over the pneumatic formwork and installation of the cable system.
6. Tightening of the central ring cable.
7. Installation of the anchorage system and adjusment of the anchorage elements of the meridional cables.
8. Placement of weights at the base of each segment.

Following all the details corresponding to the previous steps are going to be shown.

The different pieces of each independent element are cut and glued together following the same steps as in the previous model.

The only difference in the construcion of this shell is also related to the use of the rods for the connections between pieces. Two different materials have been chosen for these rods. The ones which are placed in the meridional direction are made of wood. The rods which are placed in the ring direction are metallic and they are empty. Due to this fact it is possible to pass the ring cables through them. Nevertheless, the piece which is on the base of the structure, has the same internal conducts for both ring and meridional cables, that as in the previous case.

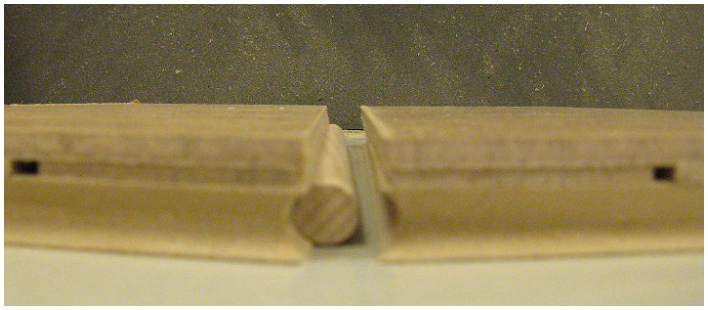

Figure 93: Connection between pieces in meridional direction

Figure 94: Connection between pieces in the deformed position

Figure 95: Wood and metallic rods placed on each element

Wooden rods are placed on the right side of each piece and metallic ones are placed on the upper edge of them (Figure 95). The pieces on the center of the plate do not have any metallic cylinder on the upper side. In the central ring the same U-profile which was used in the other model is going to be fixed and the merdional central cable is going to be placed in the left hole between it and the piece (Figure 100).

Once all the pieces are finished a new bigger pneumatic formwork is created in order to raise the plate. Also two circular planes of polyethylen have been cut and glued together. Before its use the air supported air formwork has been inflated to test it.

Figure 96, 97 and 98: Pneumatic formwork from the initial plane position to the inflated final one

Once the suitable operation of the pneumatic formwork has been verified, all the wooden elements are placed on it and the system of cables are installed.

The meridional cables are placed before the raising of the structure. During the transforming process the pieces are going to rotate over the rod and the angle between them is going to increase (Figure 99).

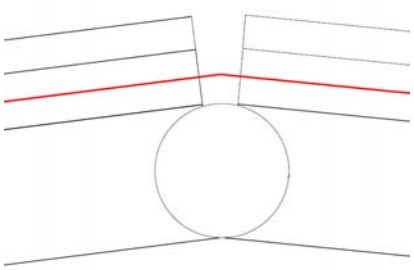

Figure 99: Increase of the angle between pieces in the final position

In order to allow the elongation of the cables caused by the increasement of the angle betwen pieces, springs are placed on the top of the central pieces between the wood element and the anchorages (Figure 100). If the cables need to increase their length to adopt the final semispherical shape, the springs will shorten. Moreover, a space of 5 mm has been left between the base of the springs and the U-profile in both extrems to guarantee that the segment can be curved and it can adopt the final shape. A piece of wood with a thickness of 5 mm has been put between both elements before the adjustment of the anchorages and then it has been put away to provide this space (Figure 101). At this moment the vertical cables are tightened and the anchorages are fixed.

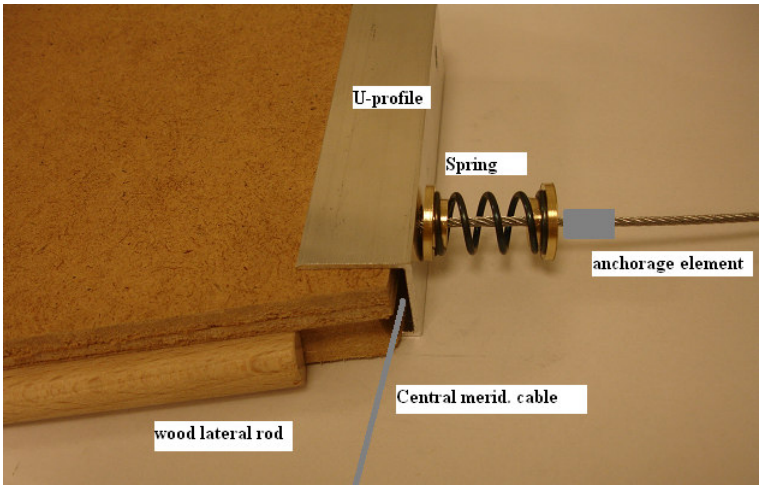

Figure 100: Anchorage system in central pieces

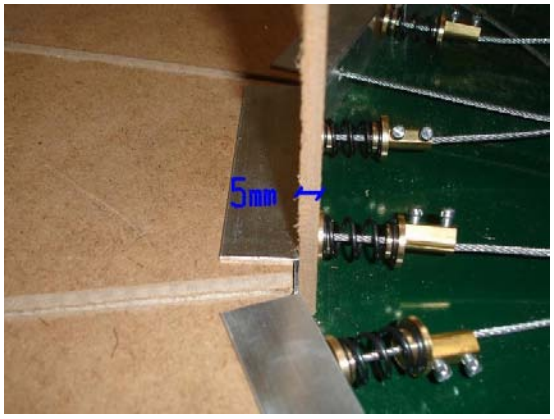

Figure 101: Space of 5 mm between the spring and the U-profile

The cables in the ring direction are passed through the metallic cylinders, but they are not pre-stressed. Thery are going to be tightened durind the raising process. Only the central ring cable is going to be tightened before. A hole have been made in all the metallic cylinders of one segment in order to install the anchorages and allow the exit of the cables.

Figure 102: Hole made in some of the metallic cylinders to allow
the exit of the cables placed in the ring direction

Some weights are fixed at the base of the outer elements in order to avoid the lifting of these pieces which must be in contact with the ground. In this way the rest of the elements are raised before and the semispherical shape is achieved.

Figure 103: Weights on the segement base

The following pictures show several views of the plate structure once everything is ready for the raising process.

Figure 104: Central ring with all the meridional anchorages

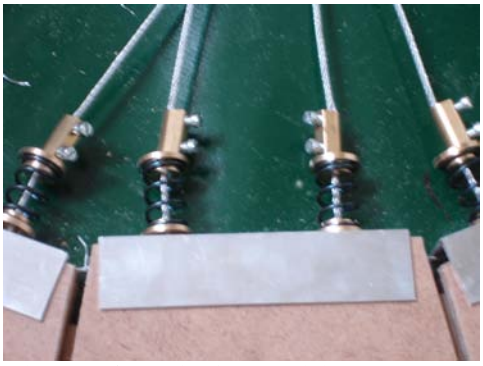

Figure 105: Detail of the meridional anchorages

Figure 106: Plate prepared for the raising process

2.4 Structure erection

The plate structure is raised by inflating the pneumatic framework. First the structure is slowly raised until the base elements lose the contact with the floor. Then some air is let out and the cables in the ring direction are adjusted. It is possible to observe the considerable gaps between pieces. Again the pneumatic framework is inflated, the air is let out and the cables are adjusted. By repeating this process the gaps reduce its size until the desired semispherical shape is reached.

Next are shown some pictures of the process.

Figure 107: Raising process of the shell

Figure 108: Detail of the ring cable anchorage system before being tightened

Figure 109: View of the final model

2.5 Conclusions

This model has a big difference with the previous one. The contact line between pieces which allowed to transfer the forces among two consecutive elements is in this new model a cylindric rod. This should mean an improvement in the structural behaviour of the shell, due to the fact that the forces will be transfered from element to element through a surface instead of through a line.

The reached final shape is the suitable semispherical one. Nevertheless there are some small gaps between pieces on the top part of the elements placed in the upper half of the shell (Figure 110).

Figure 110: Gaps between different elements

To decrease this gaps maybe the adjustment process must be repeated several times more. It can be also caused by an inaccurate cutting of the pieces which form each element. This problem could be solved with the application of some material to fill them.

This construction procedure seems to be useful to build big models and with the applied improvements its erection has been made easier.

Next experiments which will be carried out at Vienna University of Technology will study its validity with other materials like concrete or ice.

CHAPTER 3

ANALYSIS OF SEMISPHERICAL DOMES

Chapter content

In this chapter several models are developed in order to analyze and simulate the structural behaviour of a semispherical dome.

The first section of this chapter constitutes an overview about the dome theories and the existing analysis methods which have been developed during the years.

The second part of it includes the analysis of a semispherical concrete dome of radius 1 m. First, the analysis is carried out by using analytical formulas. Later, the same structure is designed by using FEM (finite element methods) computer based programs. Morever, the dome is approximated to a truss structure. In all of them the forces and stresses are evaluated. At the end these results are compared and conclusions are made.

The last part contains the analysis of the wood dome which has been built in the laboratory. The aim of this part is to compare the displacements which have been registered during the load test with the displacements which result from the previous analysis methods and models, in particular with the analytical solution and the FEM solution. No forces or streses are evaluated for this model.

1. Dome theories and analysis methods

In the mid-eighteenth century, Poleni was one of the first recorded to formally analyze domes when he used static analysis to assess meridional cracks in the dome of St. Peter´s in Rome. The line of thrust, or funicular polygon, is the path on which internal forces in a structure transport external loads to the support. Applying Robert Hooke´s discovery that a hanging chain model represents an inverted force line of a strucutre in compression, Poleni correctly concluded that the line of thrust for the dome´s load conditions remained within the effective thickness of the structure, rendering the dome as safe. However, this lower bound approach was conservative because the hanging chain represented forces in only two dimensions: hoop forces in the third dimension would have further assured the dome´s stability [20].

In 1866, Johann Schwedler [22] presented the membrane theory, which provided the basis for preliminary mathematical equations later published by other authors, including Rankine (1904) [29]. The membrane theory makes four primary assumptions:

1. Applied loads are resisted by internal forces within the surface, which has no stiffness against bending; therefore internal forces are either pure tension or pure compression.

2. On a symmetrically and uniformly loaded dome, internal forces act perpendicularly to each other in the meridional and latitudinal, or hoop, directions.

3. Internal forces are coplanar; that is, the membrane has zero thickness.

4. The membrane plane is located along the centerline of the dome´s effective thickness; thus the lines of thrust must also lie on this median surface.

The latter two assumptions, which constrain the location of the thrust line to the median radius and reduce the dome´s thickness to zero, limit hoop force values to those needed to equilibrate meridional forces; as a result, the membrane solutions tend to underestimate the dome´s ability to attain stability. In addition, the equations, limited in versatility, are difficult to apply to domes with unconventional geometries and conditions.

Around the turn of the twentieth century, engineers and architects used graphical analysis methods in conjunction with basic equilibrium equations to design and analyze domes. In 1877, Eddy [23] published a method of graphical analysis specifically for masonry domes based on the funicular polygon. Eddy identified that, for a hemispherical dome loaded axisymmetrically, the transition between compressive hoop forces near the crown and tensile hoop forces near the base occurs at 51º49` from the axis of rotation. Bellow the “point where the compression vanishes (and) we shall not

assume that the bond of the masonry is such that it can resist the hoop tensions which is developed," Eddy limited the thrust line to lie within the middle third in order for the "upper part of the dome to be then carried by the lower part as a series of masonry arches standing side by side".

The middle- third rule states that satisfactory design is obtained when the thrust line lies within the middle third of a structure´s effective thickness. Should the thrust line pass outside this region, the elastic bending theory assumes that the section will experience tensile forces that may separate the masonry voussoirs. Though it remains a built-in safety factor in masonry construction today, the rule presumes purely linear-elastic behaviour of the masonry. In actuality, the state of a structure constantly changes due to enviromental factors or settlement. Thus elastic analyses, including one posed by Navier in the mid-nineteenth century, are inaccurate in gauging masonry dome behaviour. For example, the membrane theory, a lower bound method within the framework of limit analysis, makes no assumptions about the elastic properties of the material.

Wolfe (1921) [24] published a graphical method similar to Schwedler´s graphical method which is based on the membrane theory that, like the membrane theory, is conservative due to its constraint of the thrust line to the dome´s median radius.

O´Dwyer (1999) [25] used linear programming and geometric constraints to model a masonry dome as a three-dimensional discrete network of forces applied at nodes. However, he limited his discussion to the analysis process, and less on new insights arising from his methodology or detailed analyses of specific dome case studies.

D´Ayala (2001) [26] explored the role of friction-induced tensile strength in masonry domes by investigating the minimum t/R for a hemispherical dome under self-weight. She assumed tensile resistance from friction due to internal forces developed between the faces of the masonry voussoirs. Though voussoirs likely develop some friction at their interfaces, the presence of masonry cracks limits the reliability of this resistance.

The current prevalent method to design and analyze thin-shell domes and structures is numerical finite element modeling (FEM) computer software. Though several recent studies have attempted to analyze historic masonry structures through FEM, these computer programs tell little more than what the basic membrane and bending theories reveal.

In addition, the input process for these programs, which may assume nonlinear behaviour with either plastic or elastic behaviour, is typically laborious, particularly for nonlinear models. Meanwhile the solution is limited in its demonstration of structural behaviour, and often includes tensile internal forces, which are inapplicable to masonry construction. Linear elastic results say nothing about potential collapse states. The results can be difficult to interpret correctly while remaining mindful of the associated risks and downfalls of the analysis methods. Too often a solution produced from FEM is quickly accepted as the singular solution when the stresses predicted by linear elastic FEM do not occur in reality. In this thesis, the obtained results using FEM software are contrasted with analytical results in order to avoid wrong assumptions.

Methods for finding the upper bound limits of masonry domes remain largely unproven. Through analytical and computational means, several authors have attempted to estimate upper bound limits of domes by conducting an equilibrium analysis of a structure at incipient collapse. Hodge and Lakshmikantham (1963) [27] assumed limit analysis theorems and the applicability of virtual work to predict the theorical yield-point load of rigid, perfectly plastic, axisymmetrical shallow shells; however, their work assumed ductile material behaviour that yields in a plastic manner, which is not representative of masonry behaviour. Livesley (1992) [28] also used linear programming to model the collapse mode of three-dimensional masonry structures by examining the sliding, twisting and hinging mechanisms of discrete blocks due to foundation movement, but did not examine the limits of applied loads on the dome surface itself.

2. Analytical and numerical analysis of a concrete semispherical dome

2.1 Characteristics of the dome and load cases

In this section of the project the structural behaviour of a concrete dome with 1 m of radius under the action of some fixed loads is going to be studied by using several methods:

- Analytical formulas
- Finite elements method
- Design of a truss model

The properties of the material which has been used in this analysis are following shown.

CONCRETE	
E (N/mm2)	24821,126
G (N/mm2)	10342,136
μ	0,2
γ (KN/m3)	23,56

Two load cases are taken into account in the analytical and numerical analysis. These are the self-weight of the structure and a distributed load over the shell crown. The last one simulates the kind of load which has been applied during the load test in the laboratory. It will be useful to create models to compare the obtained displacement results during the load test on a later part of this chapter.

In order to study the behaviour of the shell with the distributed load a value of 10 KN/m has been chosen for the concrete model.

A semispherical dome with constant thickness is a revolution structure. Due to its axis-symmetry it is only necessary to study the points which belong to one meridian. All the points situated in the same shell ring will have the same properties, forces, stresses and displacements. The points where the resultant forces and the stresses are calculated are defined in the following arch sketch.

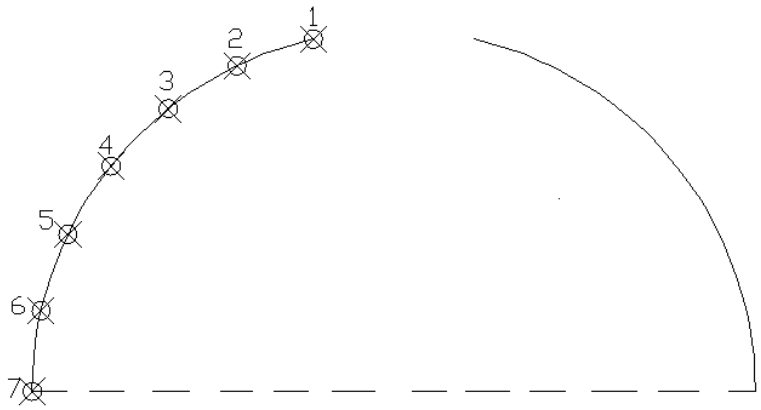

Figure 111: Position of the analyzed points

At the base of the shell the displacements in the horizontal plane are free. Nevertheless the vertical displacements are not allowed. Only vertical reactions will be obtained.

2.2 Analytical analysis

In order to carry out the analytical analysis some formulas which provide the solution to several kinds of shells based on the shells theory, in particular for semispherical domes, have been used [31].

The analytical results have been very useful to compare to the numerical models. Nevertheless, the comparison has shown several limitations and differences due to the fact that it provides valid solutions for a continuous shell. It is important to outline that the built model is formed by independent flat elements joined by a cable system. The created model is not a continuous solid.

Following, the parameters of the formulas, the used symbols and the formulas themselves are shown and explained.

Dimensional parameters

θ	Meridional angle
φ	Perimetrical angle
r	Radius
s	Ordinate length of the meridians
t	Shell thickness

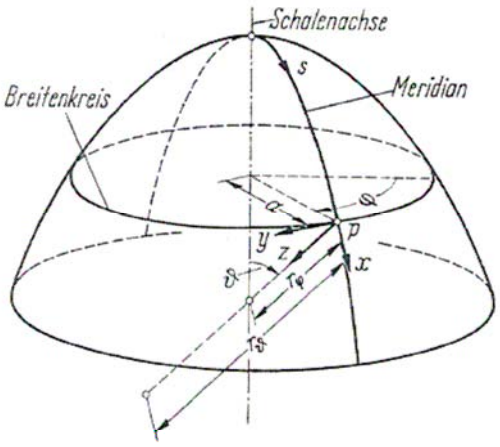

Figure 112: Dimensional parameters [31]

Deformations

u	Translational displacement in x-direction
w	Translational displacement in z-direction
$\overline{w}$	Translational displacement perpendicular to shell axis
χ	Elongation of the meridian tangent
E	Modulus of elasticity
μ	Poisson´s ratio
$x = \sqrt[4]{3(1-\mu^2)\frac{r^2}{t^2}}$	Dimensionless shell parameter

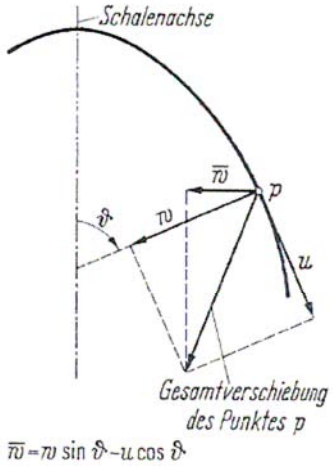

Figure 113: Deformations [31]

Load types, load components and stresses resultants

p_E [k/L^2]	Self-weight of the shell per unit of middle surface
p_x [k/L^2] p_y [k/L^2] p_z [k/L^2]	Surface load components
N_θ [k/L] N_φ [k/L]	Normal forces
T [k/L]	Tangential force
M_θ [kL/L] M_φ [kL/L]	Moments
Q [k/L]	Shear force

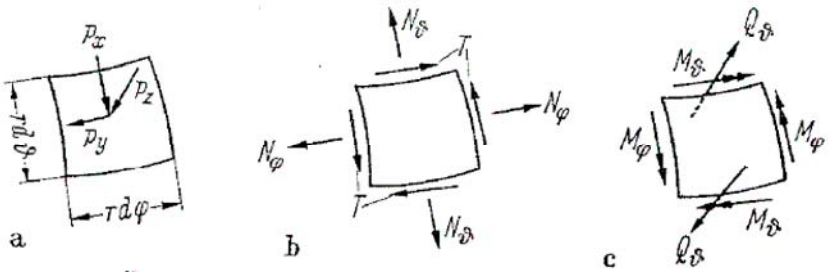

Figure 114: Load components and resultant forces [31]

The formulas which have been used to calculate the resultant forces in the two studied load cases are:

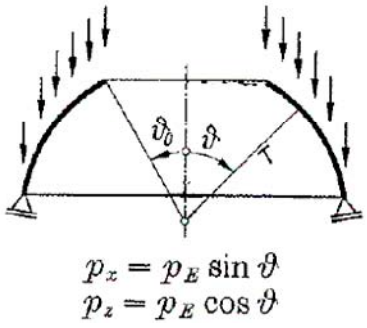

$$p_x = p_E \sin\vartheta$$
$$p_z = p_E \cos\vartheta$$

$$N_\vartheta = -\,p_E\, r\, \frac{\cos\vartheta_0 - \cos\vartheta}{\sin^2\vartheta}$$

$$N_\varphi = p_E\, r \left[\frac{\cos\vartheta_0 - \cos\vartheta}{\sin^2\vartheta} - \cos\vartheta\right]$$

$$T = 0$$

Figure 115: Forces caused by self-weight load [31]

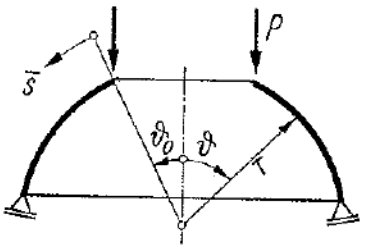

$$M_\vartheta = -\,P\cos\vartheta_0\,\frac{r}{\varkappa}\,e^{-\varkappa\frac{\bar{s}}{r}}\sin\varkappa\,\frac{\bar{s}}{r}$$

$$M_\varphi = -\,\frac{P\cos\vartheta_0\cos\vartheta}{2\sin\vartheta}\,\frac{r}{\varkappa^2}\,e^{-\varkappa\frac{\bar{s}}{r}}\times$$
$$\times\left[\cos\varkappa\,\frac{\bar{s}}{r} + \sin\varkappa\,\frac{\bar{s}}{r}\right] - \mu\, M_\vartheta$$

$$Q_\vartheta = -\,P\cos\vartheta_0\,e^{-\varkappa\frac{\bar{s}}{r}}\left[\cos\varkappa\,\frac{\bar{s}}{r} - \sin\varkappa\,\frac{\bar{s}}{r}\right]$$

$$N_\vartheta = -\,P\,\frac{\sin\vartheta_0}{\sin^2\vartheta} - Q_\vartheta\cot\vartheta \qquad T = 0$$

$$N_\varphi = -\,2P\cos\vartheta_0\,\varkappa\,e^{-\varkappa\frac{\bar{s}}{r}}\cos\varkappa\,\frac{\bar{s}}{r} + P\,\frac{\sin\vartheta_0}{\sin^2\vartheta}$$

Figure 116: Forces caused by a distributed load over the crown [31]

Stresses

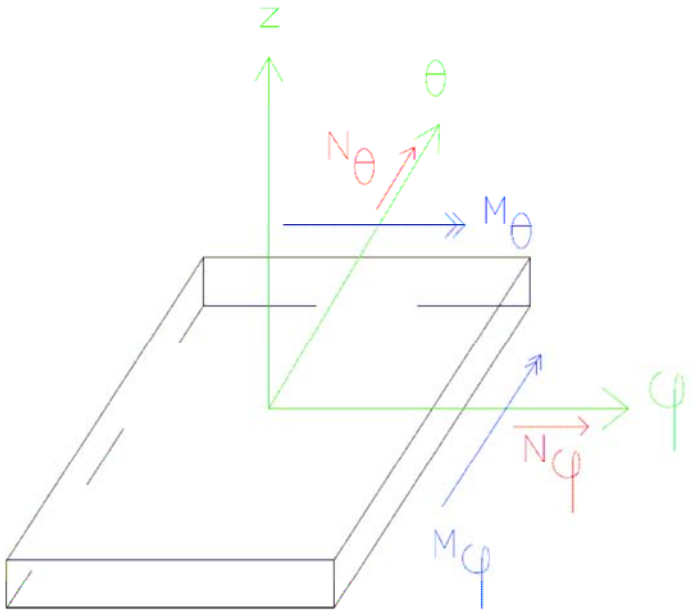

Figure 117: Shell element with local axis

$$\sigma_{\varphi} = \frac{N_{\varphi}}{A} + \frac{M_{\varphi} z}{I_{\theta}}$$

$$\sigma_{\theta} = \frac{N_{\theta}}{A} - \frac{M_{\theta} z}{I_{\varphi}}$$

Results

CONCRETE DOME **R = 1 m** **LOAD CASE: SELF-WEIGHT**

Parameters

r (m)		1
Self-Weight	(KN/m3)	23,56
Pe	(KN/m)	0,4712
t	(m)	0,02
vo	(rad)	0,2244
w	(m2)	6,66667E-05

	Analytical Solution					
	GEOMETRICAL PAR.		FORCES (KN/m)		STRESSES (N/mm2)	
Point	**s (m)**	**v (rad)**	**Nθ**	**Nφ**	**σθ**	**σφ**
1	0,000	0,224	0,0000	-0,4594	0,0000	-0,0230
2	0,224	0,449	-0,1851	-0,2394	-0,0093	-0,0120
3	0,449	0,673	-0,2341	-0,1343	-0,0117	-0,0067
4	0,673	0,898	-0,2709	-0,0229	-0,0135	-0,0011
5	0,898	1,122	-0,3141	0,1096	-0,0157	0,0055
6	1,122	1,346	-0,3730	0,2682	-0,0187	0,0134
7	1,346	1,571	-0,4594	0,4594	-0,0230	0,0230

Forces representation

Nθ (meridional forces) Nφ (ring forces)

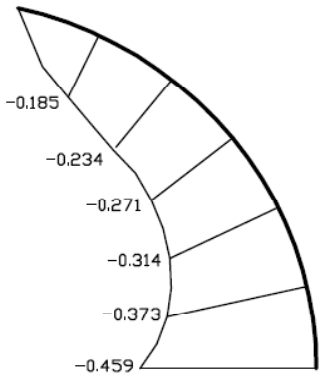

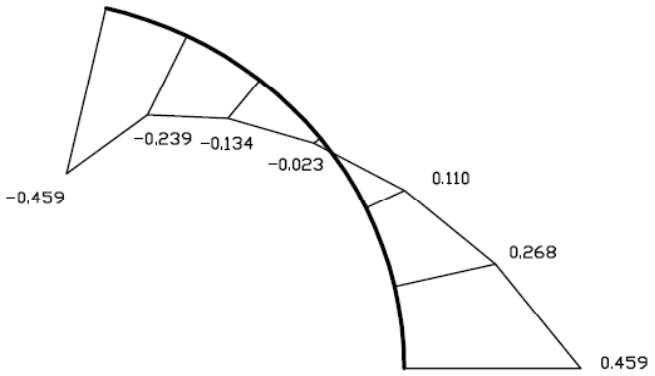

CONCRETE DOME **R = 1 m** **LOAD CASE: 10 KN/m**

Parameters

vo (rad)	0,2244
r (m)	1
x	9,2116
μ	0,2
t (m)	0,02
w (m2)	6,6667E-05
P (KN/m)	10

Geometrical parameters of the studied points

Point	s (m)	v (rad)
1	0,000	0,224
2	0,224	0,449
3	0,449	0,673
4	0,673	0,898
5	0,898	1,122
6	1,122	1,346
7	1,346	1,571

	Analytical Solution					
	FORCES (KN,m)				STRESSES (N/mm2)	
Point	Nθ	Nφ	Mφ	Mθ	σθ	σφ
1	-2,2257	-134,6803	-0,25164	0	-0,111285	-10,508615
2	-15,2929	22,6438	0,01747	-0,11778	1,002055	1,39424
3	-5,6678	7,297	-0,00124	0,0142	-0,49639	0,34625
4	-3,6239	3,2781	-0,00012	0,00018	-0,183895	0,162105
5	-2,7433	2,7603	4,61E-05	-0,0002485	-0,1334375	0,13870605
6	-2,3416	2,3452	-4,83E-06	2,71E-05	-0,1174871	0,11718755
7	-2,2257	2,225	-1,42E-07	7,10E-07	-0,11129564	0,11124787

Forces representation

Nθ (meridional forces)

Nφ (ring forces)

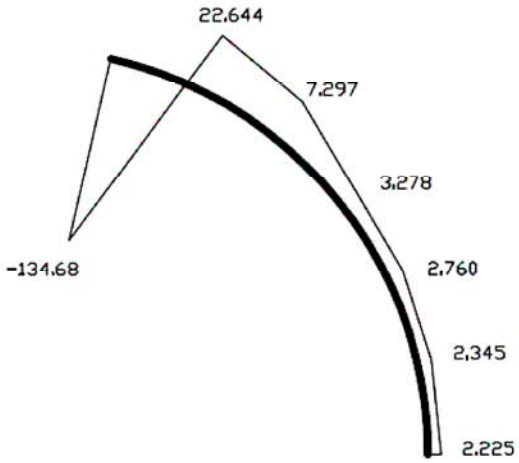

Mφ (moment of meridian direction axis)

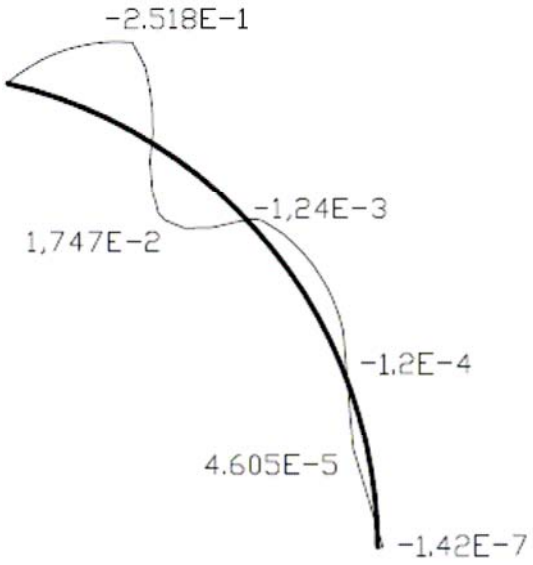

Mθ (moment of ring direction axis)

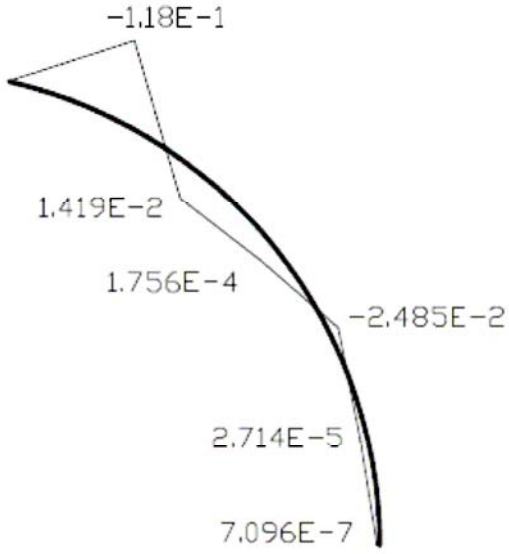

2.3 FEM Analysis

The finite element method (FEM) is used for finding approximate solutions of partial differential equations (PDE) as well as integral equations. The solution approach is based either on eliminating the differential equation completely (steady state problems), or rendering the PDE into an approximating system of ordinary differential equations, which are then solved using standard techniques such as Euler´s method, Runge-Kutta, etc.

In solving partial differential equations, the primary challenge is to create an equation that approximates the equation to be studied, but is numerically stable, meaning that errors in the input data and intermediate calculations do not accumulate and cause the resulting output to be meaningless

The method consists on dividing the body, structure or domain (continious medium) – which has defined over it several integral equations which define the physical behaviour of the problem – in a group of subdomains which do not intersect which are called finite elements. In each element representative points called “joints” are distingished.

The calculations are done over a mesh or discretization created in the domain with special programs called mesh generators, in a previous stage. In connection with this adjacent or connetion relations the value of a group of unknown variables called degrees of freedom is defined. The set of relations of a concrete variable among joints can be writen like a linear equations system. The matrix of this system is the matrix of stiffness. The number of equations is proportional to the number of degrees of freedom.

Typically the FEM is programed to calculate the displacements field. Later the deformations and stresses are obtained by using kinematics and constituent relations when it is a problem of solids mechanics.

An important property of the method is the convergence. If finite elements partitions sucessively thinner are considered, the numerical calculated solution converges quickly to the exact solution of the equations system.

In this part of this chapter FEM programs have been used to calculate the forces and stresses caused in the concrete shell by the two already known load cases. These programs are SAP 2000 and ABAQUS. Both of them give a suitable solution for the meridional and ring forces. Nevertheless, the solution for the moments in the model created with SAP 2000 is not accurate. The solution given by ABAQUS approximates more to the analytical one but it is still significantly different. Due to this fact the solution for the moments is not shown in both analysis. The difference between the different distribution can be caused by the fact that the models which are generated in these programs are not continuous solids. However, the analytical formulas are related to a continuous semispherical dome.

2.3.1 Analysis with SAP 2000

SAP2000 is a program for structures computation which uses finite elements for the static and dynamic analysis and also for linear and non-linear anlaysis.

With this program it is possible to work in 2D and 3D. All kind of structures can be analyzed and each element can be designed in an accurate way with the more used regulations (ACI in EU, RCDF in Mexico, EUROCODES in Europa, etc.)

Using SAP2000 it is possible to model complex geometries, to define several load cases, to generate self-weights automatically, to assign sections, materials, as well as to calculate concrete and steel structures based on the current regulations.

Design of the model

The geometrical dimensions of this model are the same which has been used in the analytical analysis. Also the properties of the concrete do not have differences with it.

In order to create the model with SAP 2000 shell elements have been used. A shell element is a three- or four-node formulation that combines separate membrane and plate-bending behaviour [30].

The membrane behaviour uses an isoparametric formulation that includes translational in-plane stiffness components and a rotational stiffness component in the direction normal to the plane of the element.

The plate bending behaviour includes two-way, out-of plane, plate rotational stiffness components and a translational stiffness component in the direction normal to the plane of the element. The plate bending behaviour does not include any effects of shear deformation.

The shell element always activates all six degrees of freedom at each of its connected joints.

An eight-point numerical integration formulation is used for the shell stiffness. Stresses and internal forces and moments are evaluated at the 2-by-2 Gauss integration points and extrapolated to the joints of the element.

The thickness of all the shells is 20 mm.

The restrains at the base of the dome are defined in order to allow the deformation of the shell in the horizontal plane. The vertical displacements of this joints are impeded.

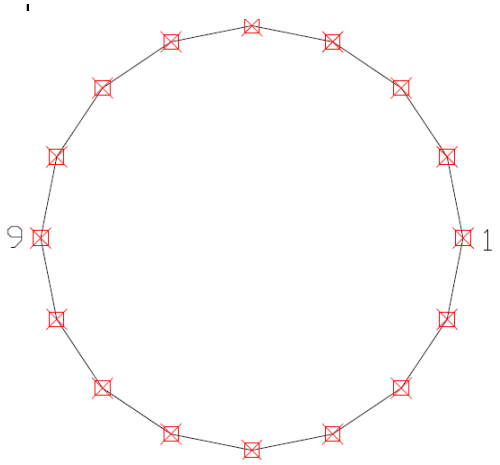

Figure 118: Supports initial position

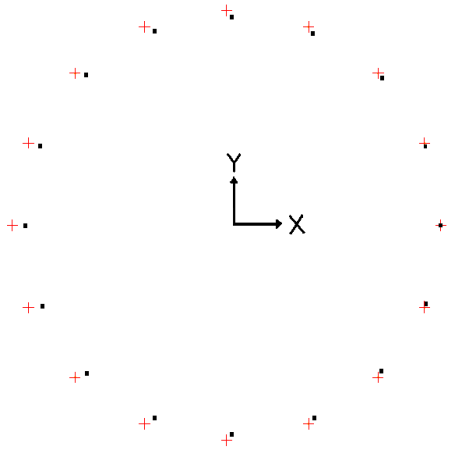

Fig. 119: Supports displacement under the load action

The used axis in the following explanation are the global ones used in the picture of the deformed shape. The z-axis is perpendicular to the paper plan. All the restrains allow the rotation in all directions. The restraint number 1 restricts the displacement in all directions. The restraint number 9 restricts the displacement in z-direction and in y-direction. The rest of restraints avoid only the the displacement in z-direction. The only reaction which will appear at the supports of the structure will be vertical, in the z-direction.

Views of the model

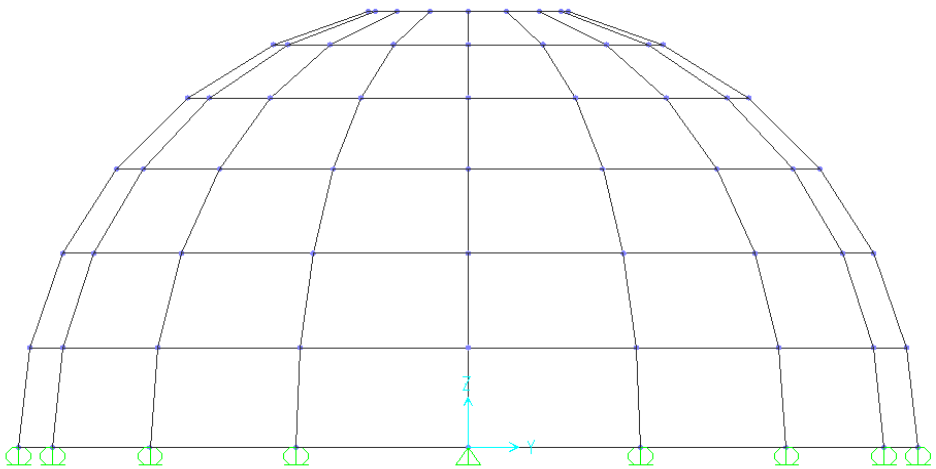

Figure 120: SAP2000 model elevation

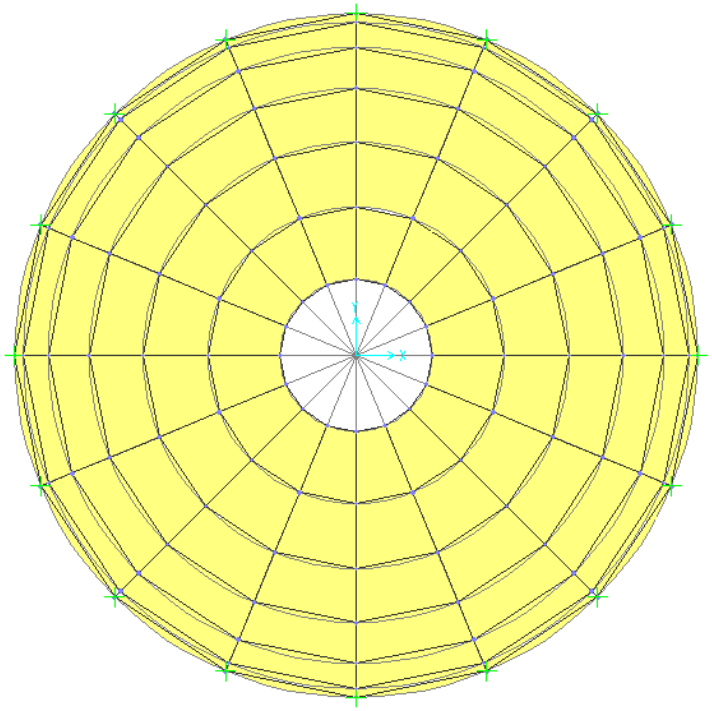

Figure 121: SAP2000 model plan view

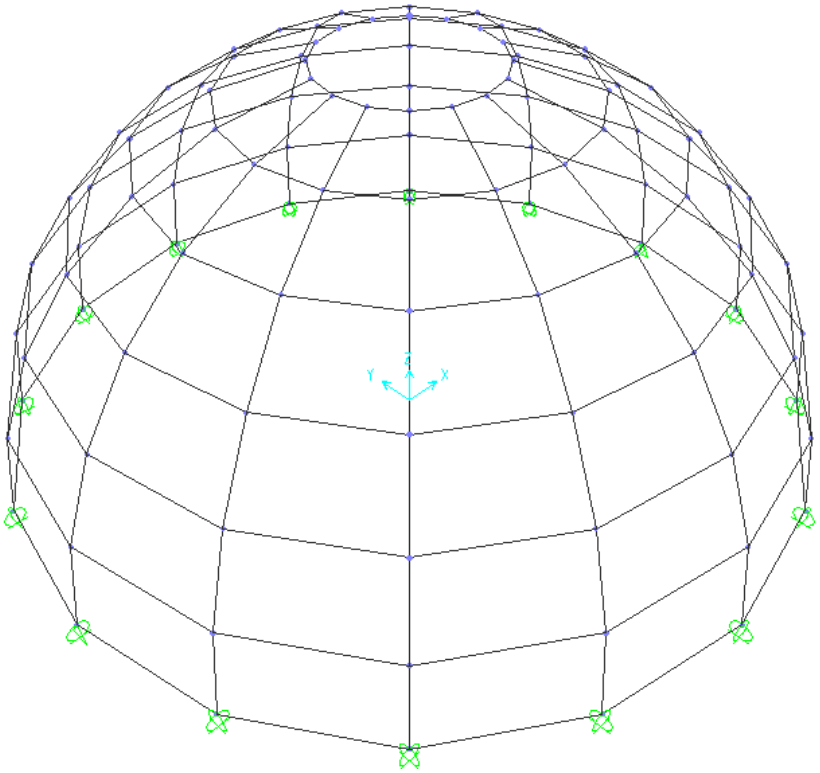

Figure 122: 3D SAP2000 model

Results

The results which have been obtained by using the program SAP2000 provide just an approximate solution for the ring and meridian forces. Therefore, the moments which are generated with the load case of 10 KN/m are not shown.

The influence of the number of considered finite elements has been evaluated by the creation of two different models. The first of them has the same number of elements as the dome which has been built in the laboratory (6 ring segments x 16 circumferencial elements). The second one has been divided into more elements in order to obtained a more accurate solution (36 ring segments x 96 circumferencial elements).

The results are calculated in the local axis system which is used by the program for each shell element . The local axis 1 is tangent to the ring direction at each point of the shell. Local axis 2 is tangent to the meridian direction. Local axis 3 is perpendicular to both of them and it is positive outwards the shell. The following picture complements the previous explanation.

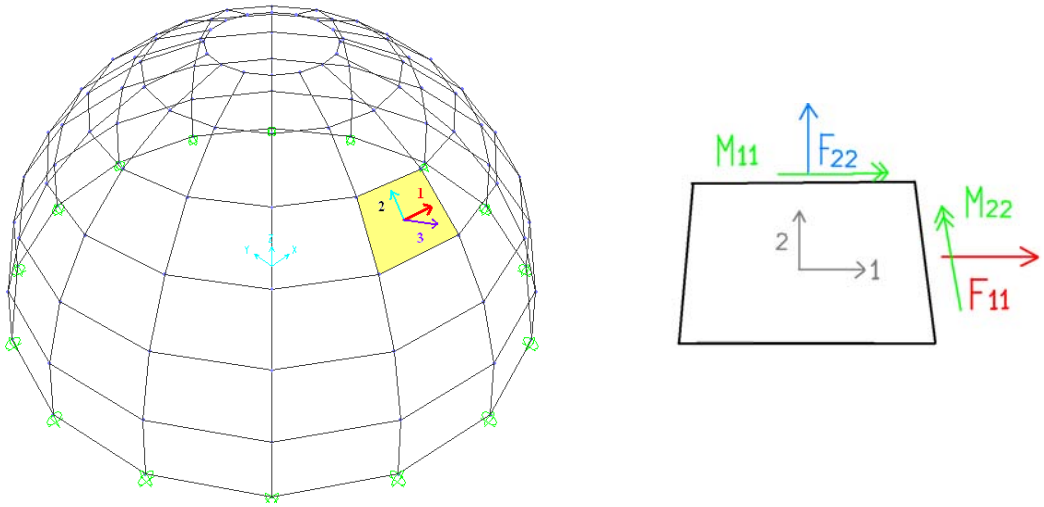

Figure 123: Local axis of the shell elements

In this section, some brief conclusions and comparisons to the analytical solution are going to be done. Nevertheless, more details will be given and the solutions will be compared all together in the corresponding part at the end of this section after the presentation of all the used methods.

LOAD CASE: SELF-WEIGHT

1. SAP MODEL: 6x16

	SAP Solution 6/16			
	FORCES (KN/m)		STRESSES (N/mm2)	
P	F22	F11	σ22	σ11
1	-0,1821	-0,5373	-9,105E-03	-2,687E-02
2	-0,2208	-0,2169	-1,104E-02	-1,085E-02
3	-0,2604	-0,1396	-1,302E-02	-6,980E-03
4	-0,3016	-0,0361	-1,508E-02	-1,805E-03
5	-0,355	0,08802	-1,775E-02	4,401E-03
6	-0,4321	0,2346	-2,161E-02	1,173E-02
7	-0,3864	0,4634	-1,932E-02	2,317E-02

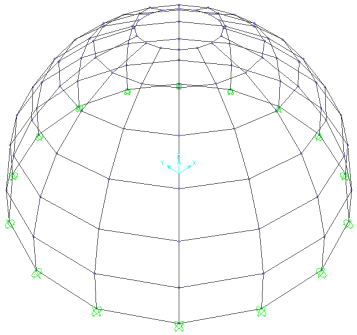

Figure 124: 6x16 SAP model

2. SAP MODEL: 36x96

	SAP Solution 36x96			
	FORCES (KN/m)		STRESSES (N/mm2)	
P	F22	F11	σ22	σ11
1	-0,04494	-0,4749	-2,247E-03	-2,375E-02
2	-0,1768	-0,2364	-8,840E-03	-1,182E-02
3	-0,2288	-0,1333	-1,144E-02	-6,665E-03
4	-0,2654	-0,02196	-1,327E-02	-1,098E-03
5	-0,3073	0,1106	-1,537E-02	5,530E-03
6	-0,3822	0,2658	-1,911E-02	1,329E-02
7	-0,4467	0,4611	-2,234E-02	2,306E-02

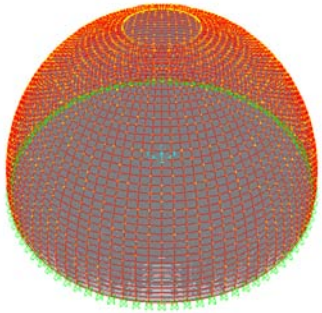

Figure 125: 36x96 SAP model

The main difference with the previously obtained analytical values is that the force in the meridional direction in the point number 1 which is place at the crown of the shell must be zero. The second model where more finite elements are taken provides a better solution for this point. If more finite elements are taken, the solution approximates to the real one. The rest of the obtained values are valid and quite similar to the analytical solution.

The following sketches represents only the forces for the second model, due to the fact that this provides a better solution.

Forces representation (solution 36x96)

F22 (KN/m) - forces in meridional direction

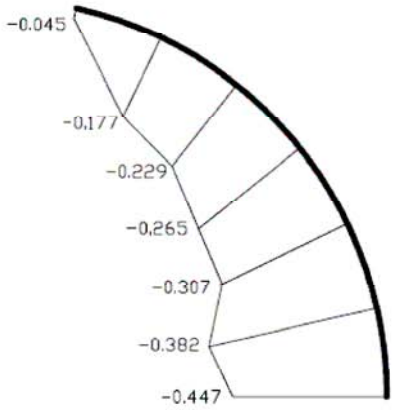

f22 sap2000 self-weight 36x96

F11 (KN/m) - forces in ring direction)

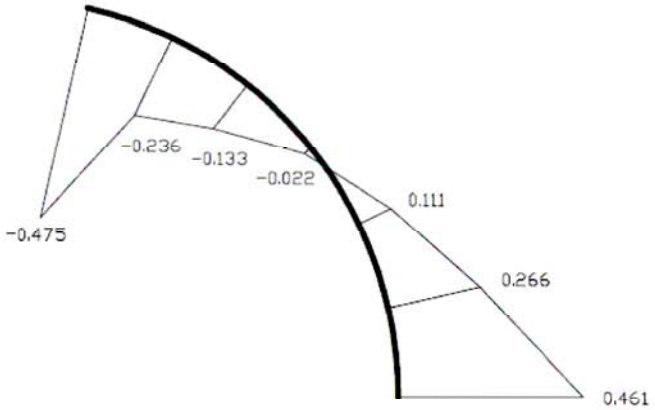

f11 sap2000 self-weight 36x96

LOAD CASE: 10 KN/m

1. SAP MODEL: 6x16

	SAP Solution 6/16			
	FORCES (KN/m)		STRESSES (N/mm2)	
P	**F22**	**F11**	**σ22**	**σ11**
1	-36,850	-117,400	-1,843E+00	-5,870E+00
2	-7,850	27,960	-3,925E-01	1,398E+00
3	-3,640	7,810	-1,820E-01	3,905E-01
4	-3,190	2,040	-1,595E-01	1,020E-01
5	-2,430	2,960	-1,215E-01	1,480E-01
6	-2,240	2,270	-1,120E-01	1,135E-01
7	-2,000	2,050	-1,000E-01	1,025E-01

2. SAP MODEL: 36x96

	SAP Solution 36x96			
	FORCES (KN/m)		STRESSES (N/mm2)	
P	**F22**	**F11**	**σ22**	**σ11**
1	-19,13	-148,63	-9,565E-01	-7,432E+00
2	-12,79	19,52	-6,395E-01	9,760E-01
3	-5,43	6,88	-2,715E-01	3,440E-01
4	-3,87	3,52	-1,935E-01	1,760E-01
5	-2,76	2,84	-1,380E-01	1,420E-01
6	-2,39	2,42	-1,195E-01	1,210E-01
7	-2,3	2,28	-1,150E-01	1,140E-01

The solution improves also if more finite elements are considered. Following is shown the graphical representation for the model 6x16.

Forces representation (solution 6x16)

F22 (KN/m) - forces in meridional direction

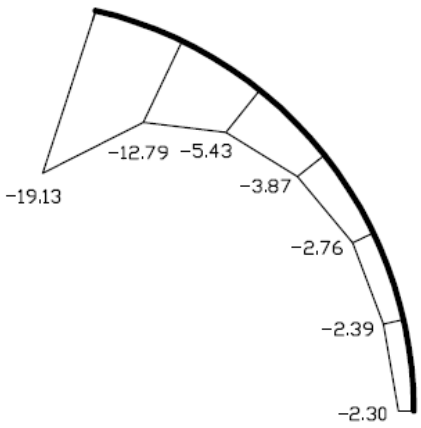

f22 sap2000 10 KN/m 36x96

F11 (KN/m) - forces in ring direction)

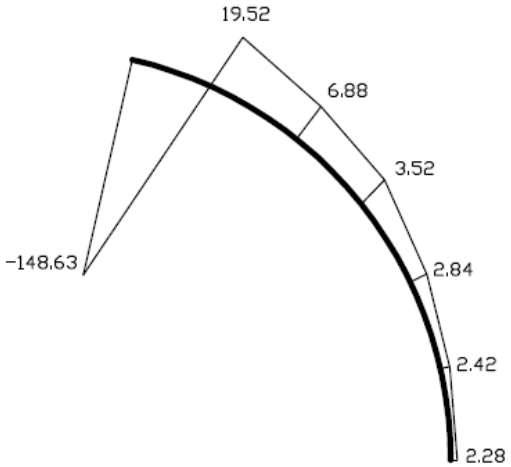

f11 sap2000 10 KN/m 36x96

2.3.2 Analysis with ABAQUS

Abaqus is a highly sophisticated, general purpose finite element program, designed primarily to model the behaviour of solids and structures under externally applied loading. It includes capabilities for both static and dynamic problems and the ability to model very large shape changes in solids, in both two and three dimensions.

Design of the model

The geometrical dimensions and the boundary conditions of this model are the same which has been used in the previous cases.

Two different models have been created and compared with this program. The first of them simulates a continuous solid which constitutes a perfect semispherical dome. The second of them has been made by the rotation of the segment which is shown in the following picture.

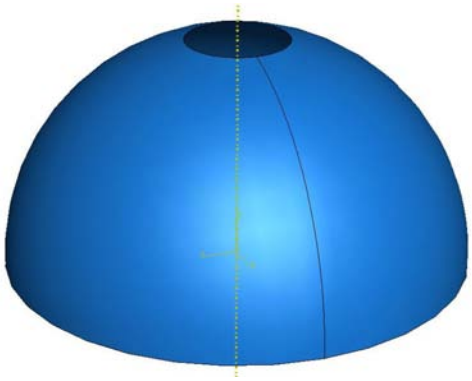

Figure 126: Model 1. Continuous semispherical dome

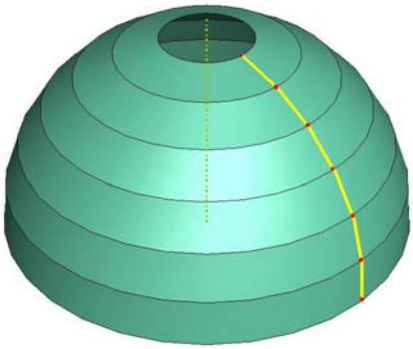

Figure 127: Model 2

The same concrete properties and thickness of 20 mm has been used in both models.

The following sketch shows the direction of the local axis and the forces in order to facilitate the interpretation of the results.

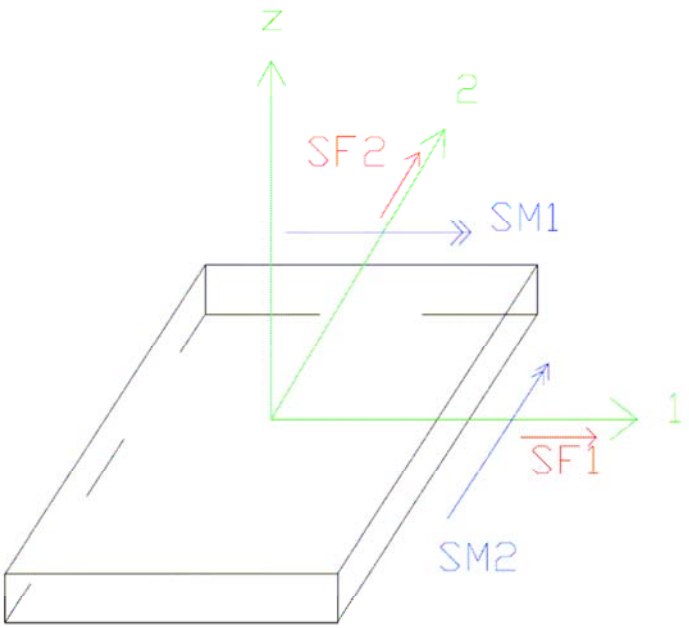

Figure 128: Local axis and forces direction used by ABAQUS

Results

MODEL 1

LOAD: SELF-WEIGHT

Point	SF1 (KN/m)	SF2 (KN/m)
1	-0,4403	-0,0237
2	-0,2423	-0,1824
3	-0,1409	-0,2316
4	-0,0318	-0,2687
5	0,1023	-0,3118
6	0,2641	-0,3713
7	0,4449	-0,4524

LOAD: 10 KN/m

Point	SF1 (KN/m)	SF2 (KN/m)	SM1 (KN/m)	SM2 (KN/m)
1	-6,3442	-122,1670	4,9458E-02	-5,4763E-02
2	-13,6275	17,6430	1,1683E-01	1,6708E-02
3	-5,6751	7,1920	1,0351E-02	2,7240E-03
4	-3,5960	3,7624	1,0296E-02	1,9910E-03
5	-2,7131	2,9663	8,2844E-03	1,6423E-03
6	-2,3211	2,2635	6,2962E-03	1,2629E-03
7	-2,2038	3,6526	-2,3191E-03	-5,6660E-04

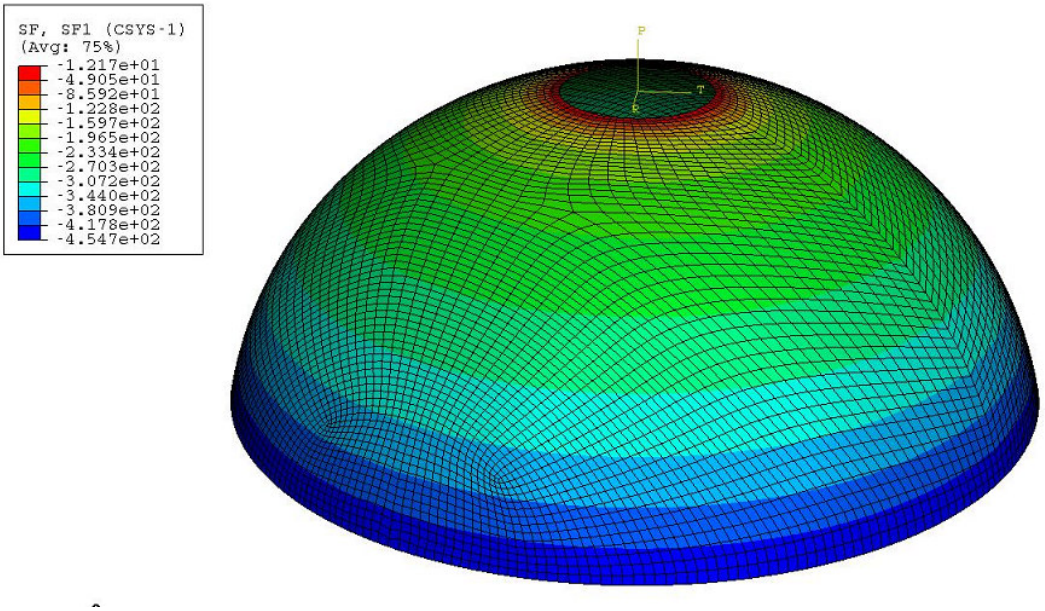

Figure 129: Model 1. Forces representation in the meridional direction

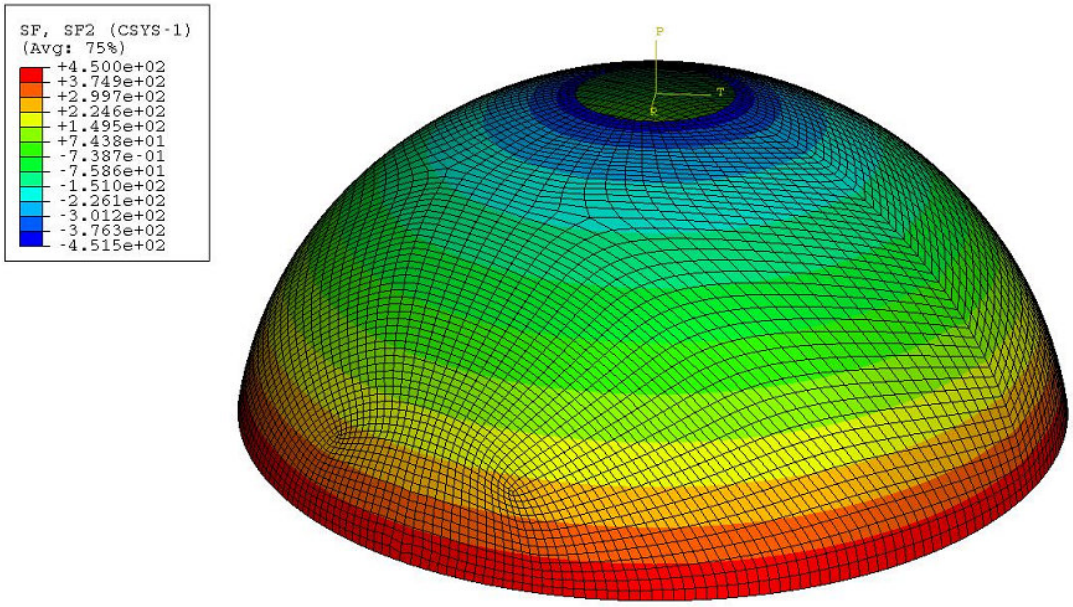

Figure 130: Model 1. Forces representation in the ring direction

MODEL 2

LOAD: SELF-WEIGHT

Point	SF1 (KN/m)	SF2 (KN/m)
1	-0,0213 €	-0,4276 €
2	-0,1826 €	-0,2236 €
3	-0,2314 €	-0,1154 €
4	-0,2679 €	-0,0003 €
5	-0,3105 €	0,1361 €
6	-0,3699 €	0,2436 €
7	-0,4497 €	0,7371 €

LOAD: 10 KN/m

Point	SF1 (KN/m)	SF2 (KN/m)	SM1 (KN/m)	SM2 (KN/m)
1	-5,2342	-121,0830	4,0342E-02	1,2453E-01
2	-14,4277	17,7470	9,0558E-02	1,1330E-02
3	-5,8836	7,1824	-6,9649E-03	-2,5963E-04
4	-3,6699	3,5231	-4,2900E-04	1,3810E-05
5	-2,7401	2,7632	1,6540E-04	1,3610E-04
6	-2,3263	2,3366	2,7700E-06	4,8600E-05
7	2,3366	2,2016	1,8590E-06	1,4300E-05

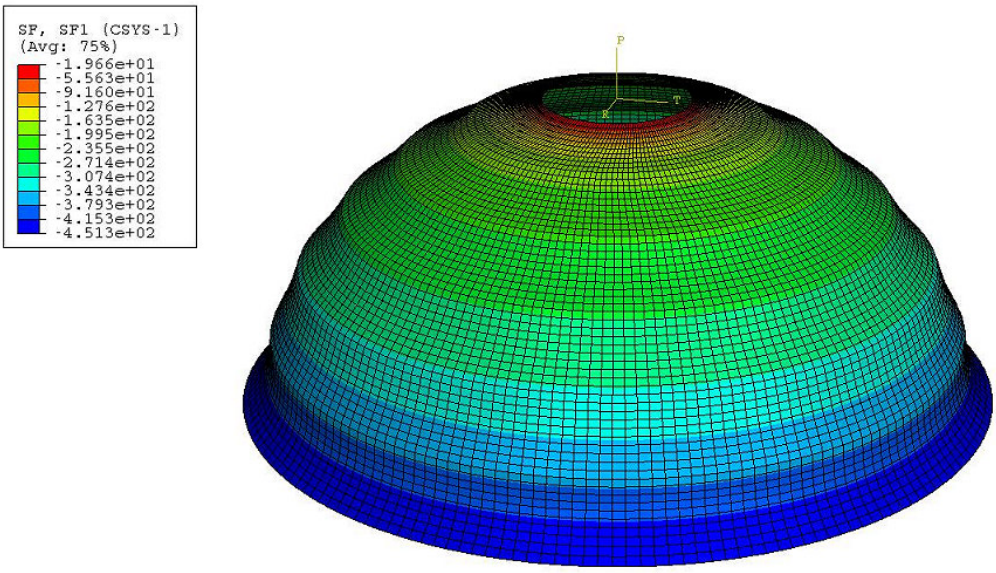

Figure 131: Model 2. Forces representation in the meridional direction

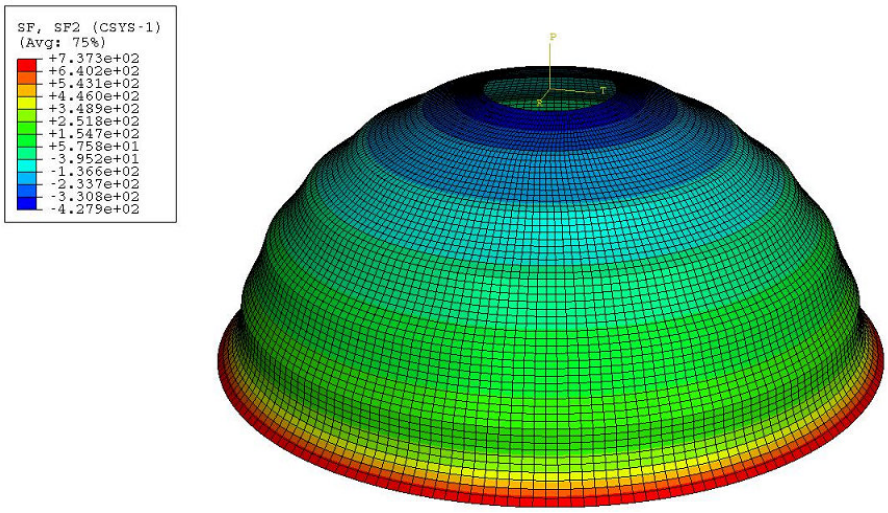

Figure 132: Model 2. Forces representation in the ring direction

Due to the fact that not a really distributed load is applied over the crown, points which belong to the same ring have different meridional force values in the nearest area to the central ring. It is important to remember that in our simulation the distributed load has been simplified into 16 joint loads of the same total value. The following pictures shows this forces distribution.

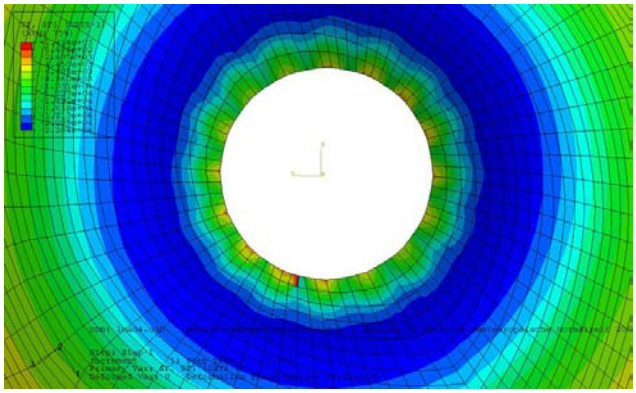

Figure 133: Distribution of the meridional forces on the crown of the shell

The obtained results are quite similar to the analytical ones. The moment distribution is the most suitable which has been obtained. There are some obvious differences between the results of the two models due to the fact that one of them is continious and the other one is not.

The distribution of the forces will be represented in the section related to the results comparison.

2.4 Truss model analysis

The semispherical built dome can be also modelled like a truss structure. To carry out this purpose, the program which has been chosen is RSTAB v 5.15, a 3D structural program that includes various integrated modules.

The axial symmetry of the structure and the absence of shear force makes possible to simulate each independent element with horizontal, diagonal and vertical trusses. This bars will work only to compression or tension. The horizontal trusses will transmit the ring forces of the original model. The vertical trusses will do the same with the forces in the meridional direction. The diagonal bars will not contribute significally to the force transmission, but they are indispensable to obtain a stable system which can be calculated by the used programm.

In order to verify the validity of the approximation only the concrete dome of 1 m of radius has been designed. The two load cases have been evaluated.

Design of the model

Horizontal and vertical bars

The cross section, the length and the properties of the bars have been carefully assigned. To facilitate the design the pieces have been approximated to rectangles with the same height (14 cm) of the real pieces but with the middle width of each of them. The considered cross sections of the vertical and horizontal bars are rectangles whose dimensions are explained in the following picture:

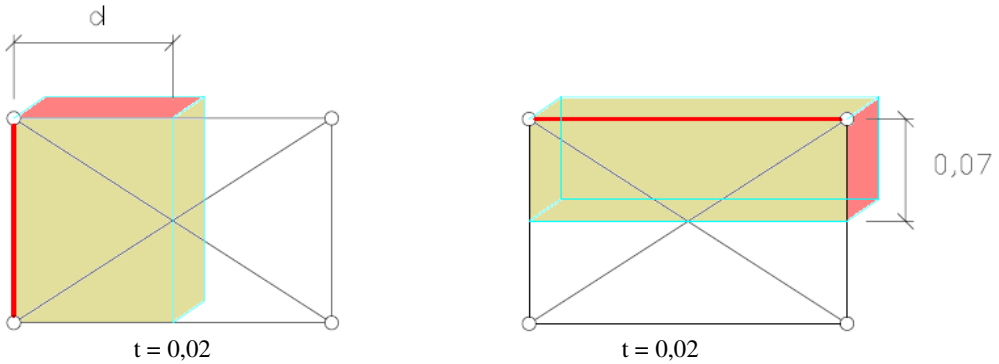

Figure 134: Cross section of the vertical and the horizontal bars

The used cross section for each element is represented in red. The figure on the left side shows the dimensions of the vertical bars. The length of the vertical bars is the height of the pieces – 14 cm. The cross section is a rectangle of $d \times t$. The dimension d represents the half of the middle width of each element. Its values for all of them are gathered in table 6 where the upper vertical bar is numbered with 1 and the bar placed on the base of the shell with number 6. The dimension t is the thickness of the element which is 20 mm.

Vertical element	d (cm)
1	4,4
2	6,85
3	8,95
4	10,625
5	11,775
6	12,35

Table 6: d values for each vertical bar

The figure on the right side shows the cross section which is used for the horizontal bars. The dimensions of the rectangle are the same for all the bars – 20×70 mm. The length of these bars is the one corresponding to the upper and lower edges of each element.

All of the bars have hinges in both ends which allow the free relative rotation between bars.

The chosen material for this elements is concrete. The properties of it are the same that were defined at the beginning of the chapter. Due to the fact that the section is being considered twice with the chosen cross sections, the used weigth per unit of volume is the half of the real one. In this way, a value of 11,78 KN/m^3 has been assigned to the concrete. Therefore it has been possible to reach a good approximation for the self-weight load case.

Diagonals

As it has been said before, the diagonals do not contributed significantly to the transfer of forces and the strenght of the structure. They have been used to generate a model suitable for its analysis with the used program.

The characteristics of the cross section are following shown.

Type	circle
Area (mm2)	20
I-1 torsion (cm4)	2,00E-10
I-2 bending (cm4)	2,00E-10
I-3 bending (cm4)	2,00E-10
Material	steel

Also the diagonals are connected to the rest of elements by hinges.

Supports of the shell

The same supports that have been employed in the created model with SAP2000 have been used in this case. In all the restraints the rotation in all directions is allowed and the vertical displacements are restricted. The restraint number 1 avoids the displaments in any direction. The restraint number 9 only permits the displament in the x-direction. The rest of restraints allow the displacement in the x-y plane.

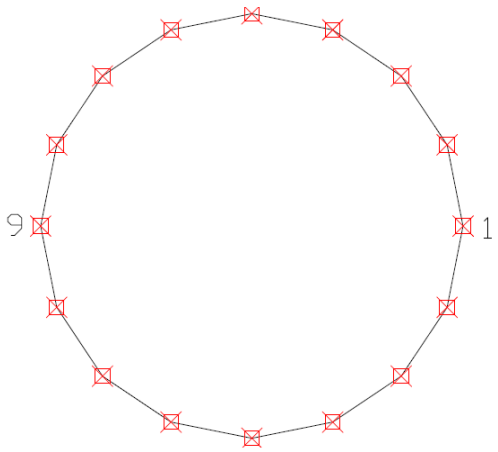

Figure 135: Supports initial position

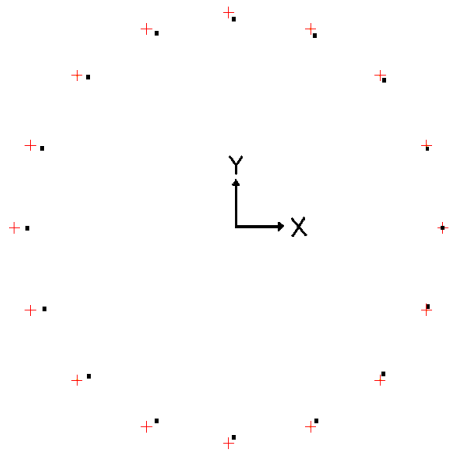

Figure 136: Supports displacement under the load action

Views of the model and loads

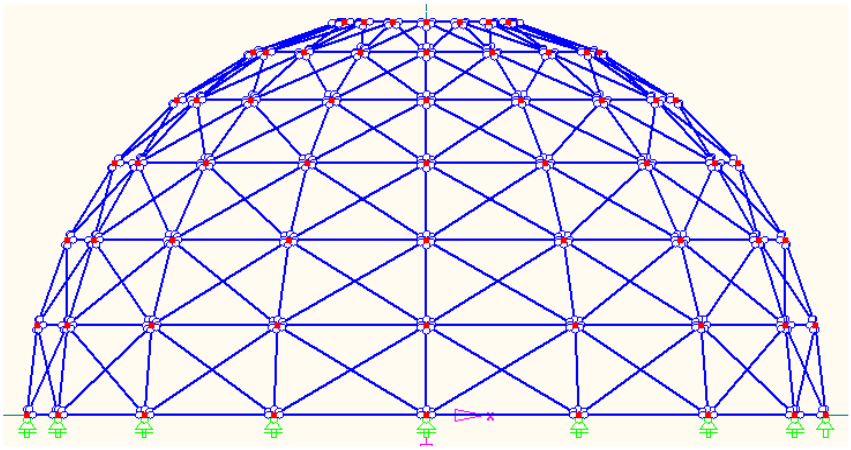

Figure 137: Elevation of the truss model

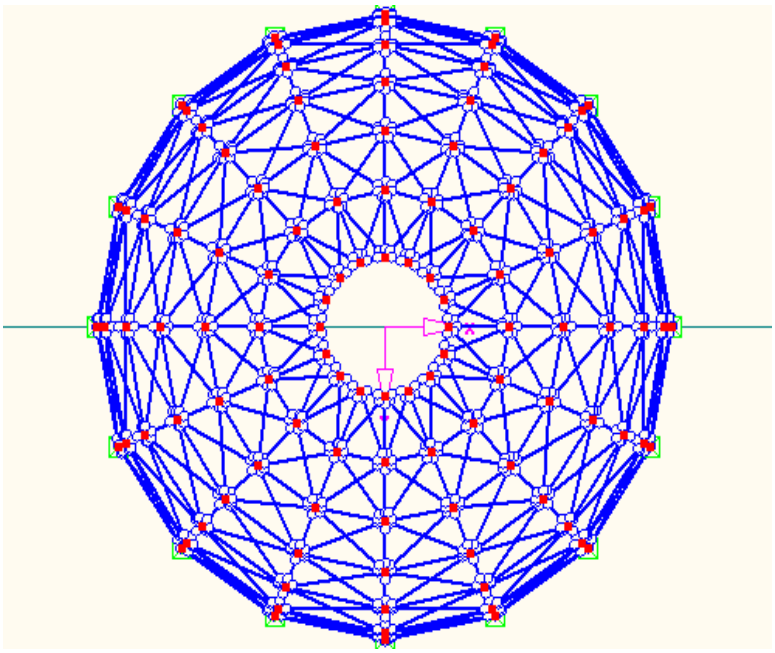

Figure 138: Plan view of the turss model

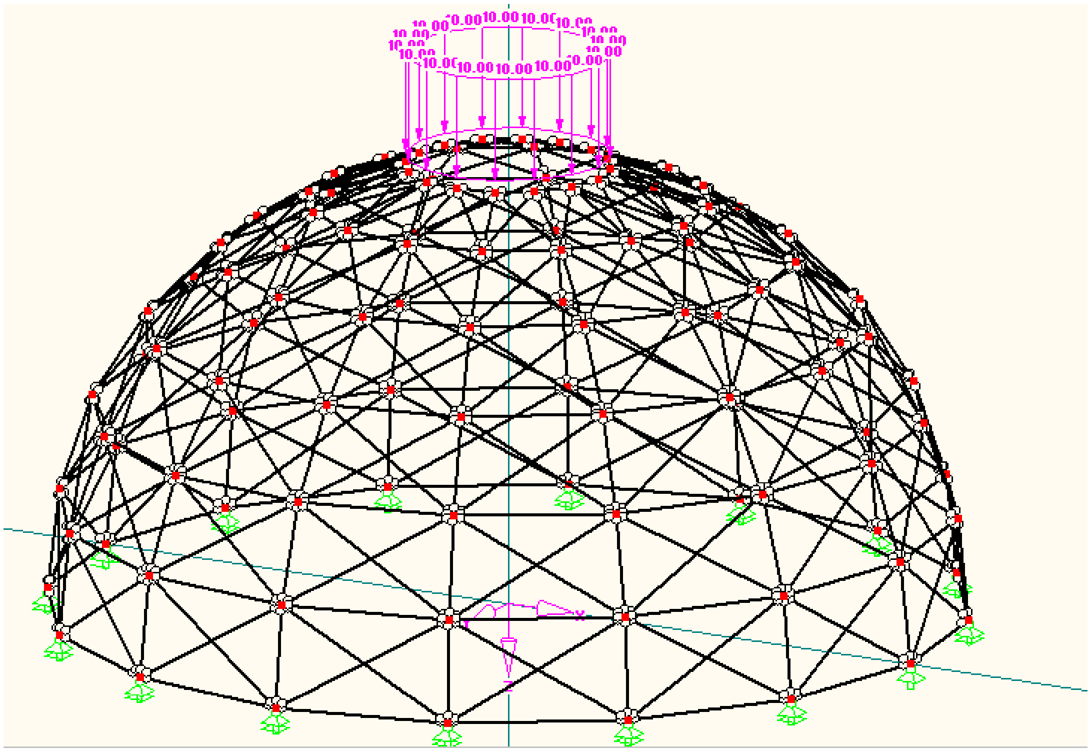

Figure 134: 3D model with load of 10 kN/m over the crown

Results

LOAD CASE: SELF-WEIGHT

VERTICAL BARS

N (KN)	N/d (KN/m)	σ (N/mm2)
-1,4170E-03	-1,6102E-02	-8,0511E-04
-2,8410E-02	-2,0737E-01	-1,0369E-02
-4,6870E-02	-2,6184E-01	-1,3092E-02
-6,5790E-02	-3,0960E-01	-1,5480E-02
-8,6030E-02	-3,6531E-01	-1,8265E-02
-1,0200E-01	-4,1296E-01	-2,0648E-02

HORIZONTAL BARS

N (KN)	N/b (KN/m)	σ (N/mm2)
-2,7530E-02	-3,9329E-01	-1,9664E-02
-2,3630E-02	-1,6879E-01	-1,6879E-02
-6,7600E-03	-4,8286E-02	-4,8286E-03
3,0400E-03	2,1714E-02	2,1714E-03
1,2370E-02	8,8357E-02	8,8357E-03
3,0550E-02	2,1821E-01	2,1821E-02
2,7670E-02	3,9529E-01	1,9764E-02

N force representation

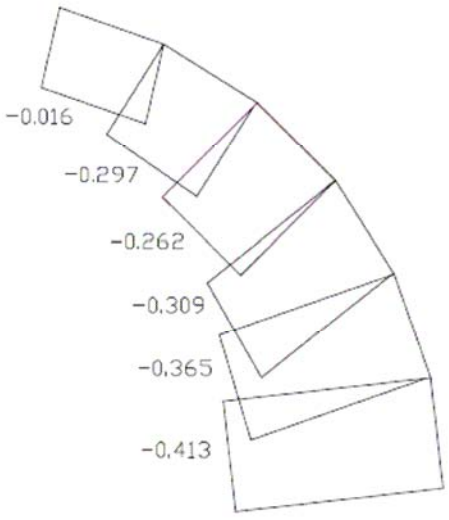

vertical forces
truss model
self-weight

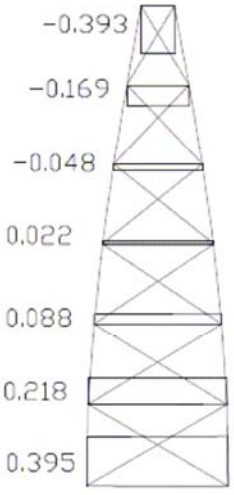

horizontal forces
truss model
self-weight

LOAD CASE: 10 KN/m over the crown

VERTICAL BARS

N (KN)	N/d (KN/m)	σ (N/mm2)
-2,23997	-25,45420455	-1,272710227
-1,5643	-11,41824818	-0,570912409
-1,21909	-6,810558659	-0,340527933
-1,02906	-4,842635294	-0,242131765
-0,93497	-3,97014862	-0,198507431
-0,88763	-3,593643725	-0,179682186

HORIZONTAL BARS

N (KN)	N/b (KN/m)	σ (N/mm2)
-6,2123	-88,74714286	-4,437357143
2,92996	20,92828571	1,046414286
1,34776	9,626857143	0,481342857
0,8289	5,920714286	0,296035714
0,60419	4,315642857	0,215782143
0,50391	3,599357143	0,179967857
0,2389	3,412857143	0,170642857

N force representation

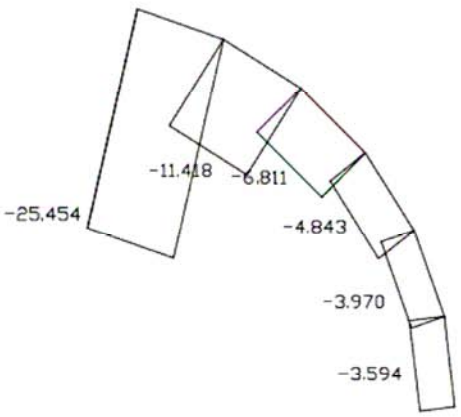

vertical forces truss model
10 KN/m

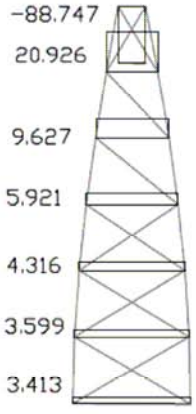

horizontal forces truss model
10 KN/m

It is important to outline that with this model it is only possible to analyze and compare the ring and the meridian forces. In the bars which form the structure no bending moments appear due to the fact that there are hinges at the ends of each one. Only axial forces are developed.

The axial forces on the diagonal elements are not shown because they are comparatively much lower than the others. This was the aim of the design in order to transfer the forces mainly through the vertical and horizontal elements.

2. 5 Comparison of results

In the last part of this section a comparison between the results which has been obtained by using the different previous methods are going to be shown in order to understand how a semispherical dome really works and the limitations of each one in the structural study.

First, the forces and stresses related to the load case self-weight are going to be analyzed. A graphical comparison will also be established. Later, the same study will be done with the load of 10 KN/m over the crown.

The local axis of each element has been named in each method using the given formulation by the simulation software or the analytical formulas. In order to estabilsh an understandable comparison the one which has been globally used is following shown.

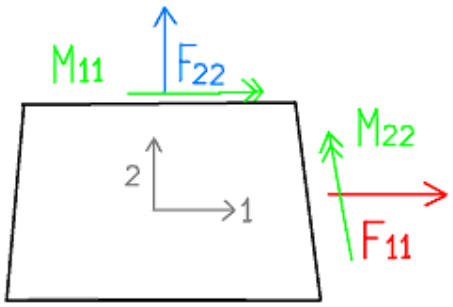

F11: force in the ring direction
F22: force in the meridian direction
M11: moment of tangent axis to the ring direction
M22: moment of tangent axis to the meridian direction
σ11: total stress in the ring direction
σ22: total stress in the meridan direction

The following table shows the results which has been obtained for the load case *self weight* using all the previous methods all together. In all of them except in the truss model point number one is placed on the crown and point number 7 at the base of the dome. In the truss model the forces are related to the bars. There are 6 vertical bars and 7 horizontal bars. The bar number 1 is in both cases related to the one placed on the upper part and the last one to the one placed at the base.

SELF-WEIGHT

	Analytical Solution			
	FORCES (KN/m)		STRESSES (N/mm2)	
Point	**F22**	**F11**	**σ22**	**σ11**
1	0	-0,4594	0,00E+00	-2,30E-02
2	-0,1851	-0,2394	-9,30E-03	-1,20E-02
3	-0,2341	-0,1343	-1,17E-02	-6,70E-03
4	-0,2709	-0,0229	-1,35E-02	-1,10E-03
5	-0,3141	0,1096	-1,57E-02	5,50E-03
6	-0,373	0,2682	-1,87E-02	1,34E-02
7	-0,4594	0,4594	-2,30E-02	2,30E-02
	SAP Solution 36x96			
Point	**F22**	**F11**	**σ22**	**σ11**
1	-0,0449	-0,4749	-2,25E-03	-2,38E-02
2	-0,1768	-0,2364	-8,84E-03	-1,18E-02
3	-0,2288	-0,1333	-1,14E-02	-6,67E-03
4	-0,2654	-0,0220	-1,33E-02	-1,10E-03
5	-0,3073	0,1106	-1,54E-02	5,53E-03
6	-0,3822	0,2658	-1,91E-02	1,33E-02
7	-0,4467	0,4611	-2,23E-02	2,31E-02
	ABAQUS model 1 continious			
Point	**F22**	**F11**	**σ22**	**σ11**
1	-0,0237	-0,4403	-1,19E-03	-2,20E-02
2	-0,1824	-0,2423	-9,12E-03	-1,21E-02
3	-0,2316	-0,1409	-1,16E-02	-7,05E-03
4	-0,2687	-0,0318	-1,34E-02	-1,59E-03
5	-0,3118	0,1023	-1,56E-02	5,11E-03
6	-0,3713	0,2641	-1,86E-02	1,32E-02
7	-0,4524	0,4449	-2,26E-02	2,22E-02
	ABAQUS model 2 different rings segments			
Point	**F22**	**F11**	**σ22**	**σ11**
1	-0,0213	-0,4276	-1,06E-03	-2,14E-02
2	-0,1826	-0,2236	-9,13E-03	-1,12E-02
3	-0,2314	-0,1154	-1,16E-02	-5,77E-03
4	-0,2679	-0,0003	-1,34E-02	-1,44E-05
5	-0,3105	0,1361	-1,55E-02	6,81E-03
6	-0,3699	0,2436	-1,85E-02	1,22E-02
7	-0,4497	0,7371	-2,25E-02	3,69E-02
	TRUSS MODEL			
Bar	**F22**	**F11**	**σ22**	**σ11**
1	-0,0161	-0,3933	-8,05E-04	-1,97E-02
2	-0,2074	-0,1688	-1,04E-02	-1,69E-02
3	-0,2618	-0,0483	-1,31E-02	-4,83E-03
4	-0,3096	0,0217	-1,55E-02	2,17E-03
5	-0,3653	0,0884	-1,83E-02	8,84E-03
6	-0,4130	0,2182	-2,06E-02	2,18E-02
7		0,3953		1,98E-02

Table 7: Resultant forces and stresses for load case self weight

Following these results are graphically shown. In both graphs the seven analyzed points are reprensented at x-axis. As it has been said before, point 1 is placed on the top of the dome and point 7 at the base. The resultant forces are represented at y-axis. These forces are expressed in kN/m. The first graph shows the forces in the ring direction and the second graph in the meridional one, both for the load case of *self weight*.

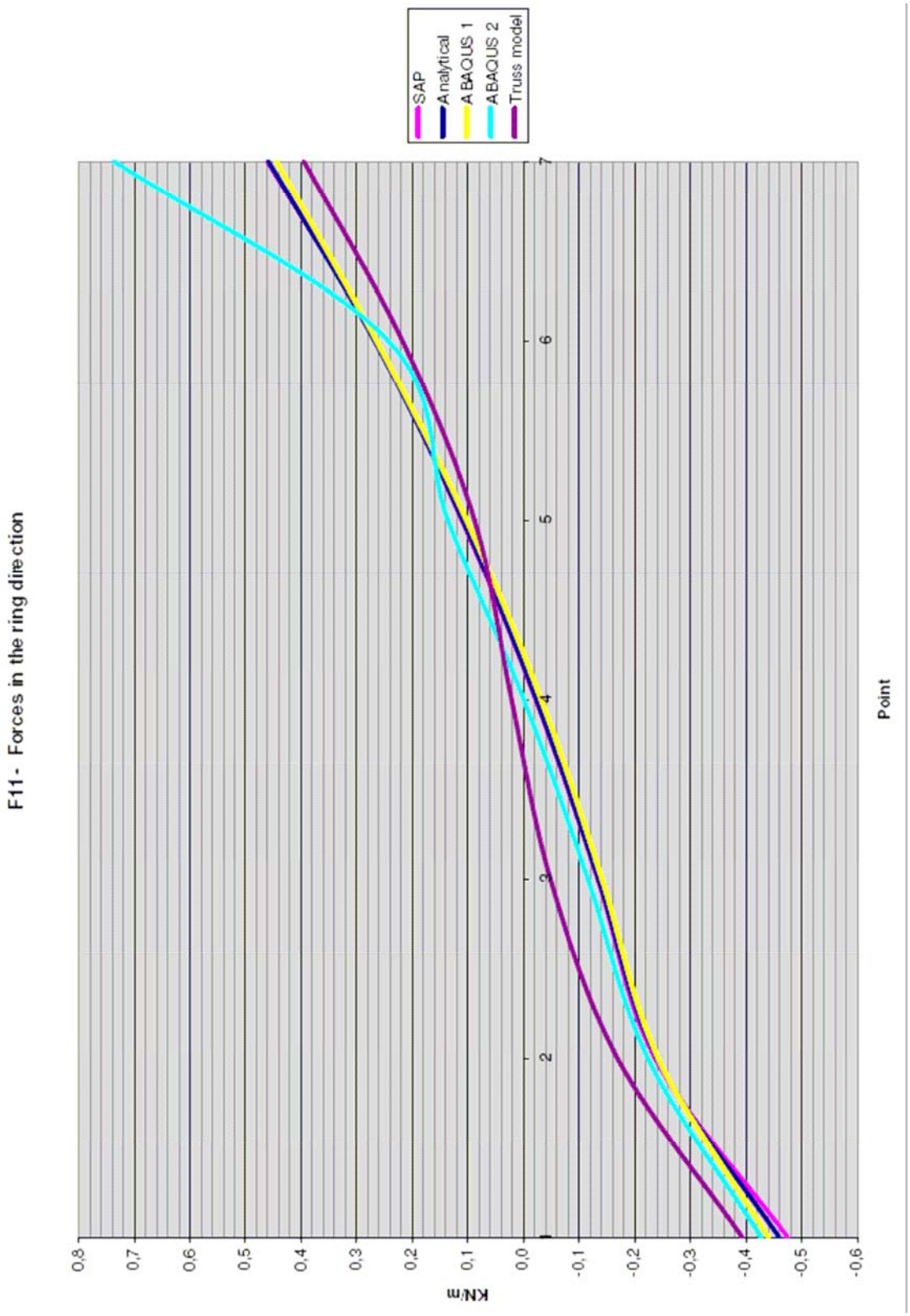
SAP
Analytical
ABAQUS 1
ABAQUS 2
Truss model
F11 - Forces in the ring direction
KN/m
Point
0,8
0,7
0,6
0,5
0,4
0,3
0,2
0,1
0,0
-0,1
-0,2
-0,3
-0,4
-0,5
-0,6
1
2
3
4
5
6
7

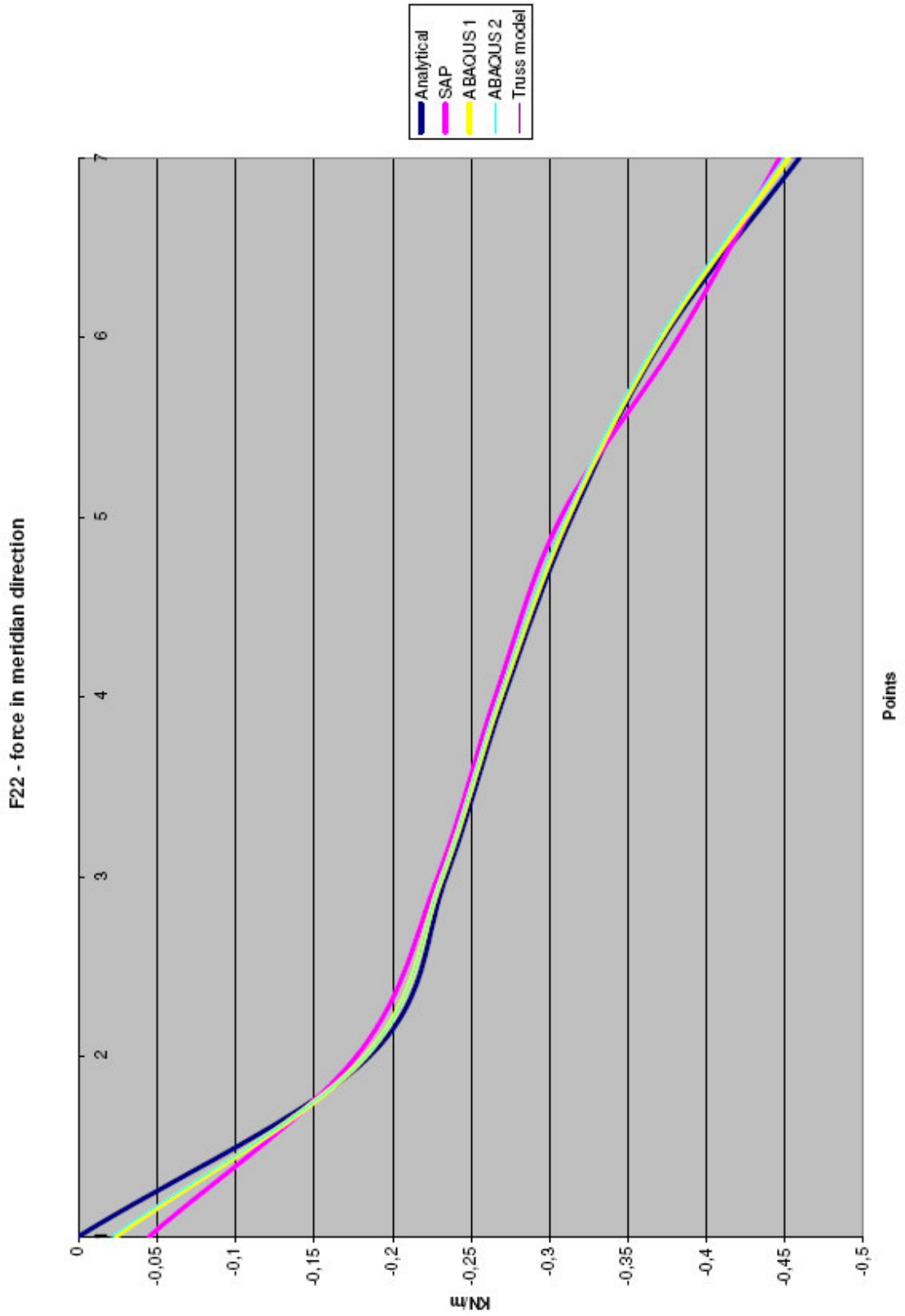
Analytical
SAP
ABAQUS 1
ABAQUS 2
Truss model
F22 - force in meridian direction
kN/m
Points
0
-0,05
-0,1
-0,15
-0,2
-0,25
-0,3
-0,35
-0,4
-0,45
-0,5
1
2
3
4
5
6
7

The analytical solution and the solution of ABAQUS in model 2 are related to a continuous semispherical dome. Therefore, they show some difference with the other obtained results. They are two different models.

The distribution of forces in the meridional direction is very similar in all models, as the previous graph shows. All the meridians work to compression.

The meridian force in point 1 (top of the shell) should be zero. Only the analytical solution provides this result. The other models have small values at this point. In the numerical models of FEM, the solution approximates to that value if more finite elements are considered in the definition of the structure. In the truss model it is important to outline that the forces and stresses which have been registered after the analysis are constant in all the bars. This stresses are related to the force of the whole bar. Due to this fact, the superior bar can not show a value of zero.

The distribution of forces in the ring direction is even more similar. The values which have been obtained do not present significant differences. The higher parts of the shell have compression forces. However, the lower parts have tension forces. This structural behaviour was the expected one.

There is only one important difference in the model 2 of ABAQUS. The total force up and down of a shell segment must be approximately the same, but with different sign. In this model the ring force at the base of the dome is much bigger. No one explanation has been found.

In the next table the results which have been obtained when a distributed load of *10 kN/m* acts over the crown are going to be shown all together in order to compare them easily.

Then, the data which are contained in this table are graphically compared in two different graphs. The first of them corresponds to the ring forces which appear on the dome in the load case *10 kN/m over the shell crown*. The second one represents the meridional forces which are generated.

The axis of both graphs represent the analyzed points of the shell and the values of the corresponding forces as in the graphs which have been used for the load case self weight.

The only distribution of moments which is accpeted is the one which has been obtained with the analytical analysis. The rest of them have significant differences even for similar models analyzed with different application software. The graph corresponding to this calculated moments are shown in the previous section where the analytical analysis is carried out.

LOAD CASE: 10 KN/m

	Analytical Solution					
	FORCES (KN,m)				STRESSES (N/mm2)	
Point	**F22**	**F11**	**M22**	**M11**	**σ22**	**σ11**
1	-2,2257	-134,6803	-2,5164E-01	0,0000E+00	-0,111285	-1,0509E+01
2	-15,2929	22,6438	1,7470E-02	-1,1778E-01	2,531345	1,3942E+00
3	-5,6678	7,2970	-1,2400E-03	1,4200E-02	-0,49639	3,4621E-01
4	-3,6239	3,2781	-1,2000E-04	1,8000E-04	-0,183895	1,6210E-01
5	-2,7433	2,7603	4,6100E-05	-2,4850E-04	-0,1334375	1,3871E-01
6	-2,3416	2,3452	-4,8300E-06	2,7100E-05	-0,1174871	1,1719E-01
7	-2,2257	2,2250	-1,4200E-07	7,1000E-07	-0,11129564	1,1125E-01
	SAP Solution 36x96					
Point	**F22**	**F11**	**M22**	**M11**	**σ22**	**σ11**
1	-19,1300	-148,6300	-	-	-9,5650E-01	-7,4320E+00
2	-12,7900	19,5200	-	-	-6,3950E-01	9,7600E-01
3	-5,4300	6,8800	-	-	-2,7150E-01	3,4400E-01
4	-3,8700	3,5200	-	-	-1,9350E-01	1,7600E-01
5	-2,7600	2,8400	-	-	-1,3800E-01	1,4200E-01
6	-2,3900	2,4200	-	-	-1,1950E-01	1,2100E-01
7	-2,3000	2,2800	-	-	-1,1500E-01	1,1400E-01
	ABAQUS MODEL 1 continious					
Point	**F22**	**F11**	**M22**	**M11**	**σ22**	**σ11**
1	-6,3442	-122,1670	-	-	-3,1721E-01	-6,1084E+00
2	-13,6275	17,6430	-	-	-6,8138E-01	8,8215E-01
3	-5,6751	7,1920	-	-	-2,8376E-01	3,5960E-01
4	-3,5960	3,7624	-	-	-1,7980E-01	1,8812E-01
5	-2,7131	2,9663	-	-	-1,3566E-01	1,4832E-01
6	-2,3211	2,2635	-	-	-1,1606E-01	1,1318E-01
7	-2,2038	3,6526	-	-	-1,1019E-01	1,8263E-01
	ABAQUS MODEL 2 continious					
Point	**F22**	**F11**	**M22**	**M11**	**σ22**	**σ11**
1	-5,2342	-121,0830	-	-	-2,6171E-01	-6,0542E+00
2	-14,4277	17,7470	-	-	-7,2139E-01	8,8735E-01
3	-5,8836	7,1824	-	-	-2,9418E-01	3,5912E-01
4	-3,6699	3,5231	-	-	-1,8349E-01	1,7616E-01
5	-2,7401	2,7632	-	-	-1,3700E-01	1,3816E-01
6	-2,3263	2,3366	-	-	-1,1631E-01	1,1683E-01
7	2,3366	2,2016	-	-	1,1683E-01	1,1008E-01
	Truss model					
Point	**F22**	**F11**	**M22**	**M11**	**σ22**	**σ11**
1	-25,4542	-88,7471	-	-	-1,2727E+00	-4,4374E+00
2	-11,4182	20,9283	-	-	-5,7091E-01	1,0464E+00
3	-6,8106	9,6269	-	-	-3,4053E-01	4,8134E-01
4	-4,8426	5,9207	-	-	-2,4213E-01	2,9604E-01
5	-3,9701	4,3156	-	-	-1,9851E-01	2,1578E-01
6	-3,5936	3,5994	-	-	-1,7968E-01	1,7997E-01
7		3,4129	-	-	0,0000E+00	1,7064E-01

Table 8: Resultant forces and stresses for load case 10 kN/m over the crown

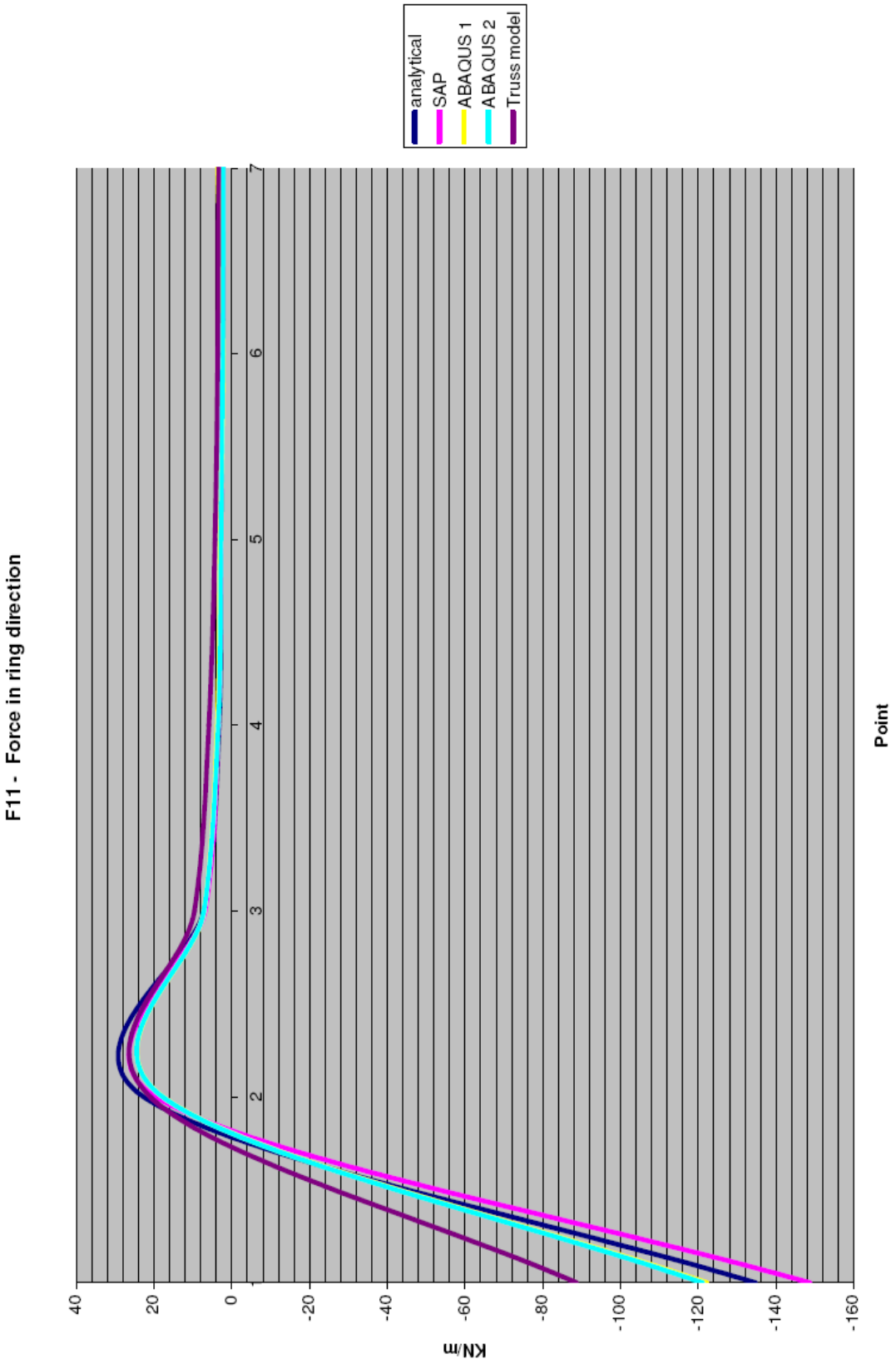
analytical
SAP
ABAQUS 1
ABAQUS 2
Truss model
F11 - Force in ring direction
KN/m
Point
40
20
0
-20
-40
-60
-80
-100
-120
-140
-160
1
2
3
4
5
6
7

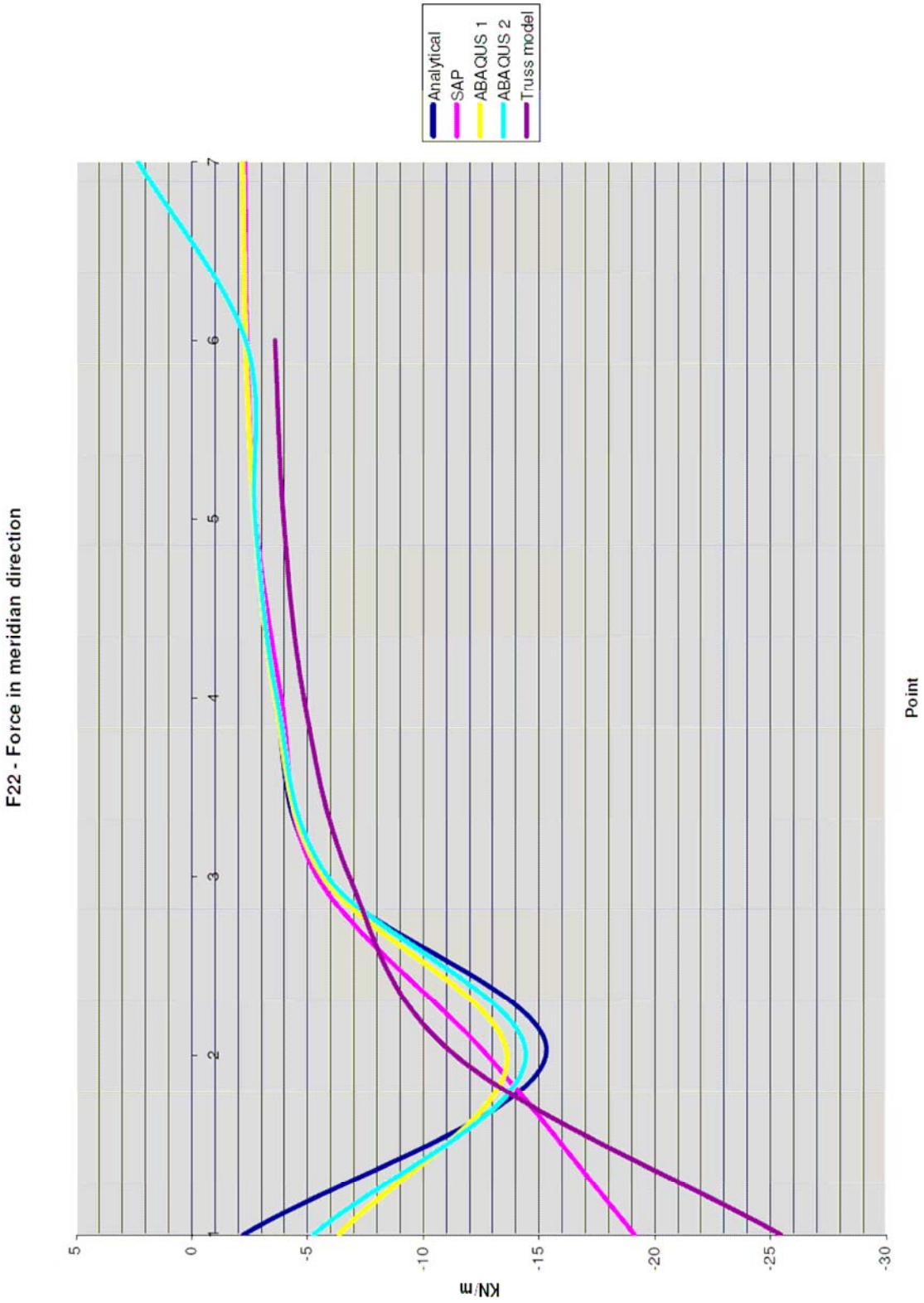
Analytical
SAP
ABAQUS 1
ABAQUS 2
Truss model
F22 - Force in meridian direction
KN/m
Point
5
0
-5
-10
-15
-20
-25
-30
1
2
3
4
5
6
7

Under the action of a distributed load over the crown of the shell normal forces and bending moments are produced on the shell.

The forces in the meridional direction show the same problems as in the self-weight load case. The value of this forces is smaller than the one which has been obtained in the analytical analysis, specially in the SAP2000 and the truss models.

The two ABAQUS models and the analytical solution provide similar forces distributions in the meridional direction. An explanation for this similarity can be found in the fact that the simulated shell in Abaqus is continuous in model 1 and continuous in the ring direction in model 2. The analytical solution is valid for a continuos shell. The other two methods are not as accurate at the top of the structure, but it approximates at the lower part. In this methods the structure is modelled as a set of connected elements.

The forces in the ring direction are quite similar. Only the truss model gives a smaller value at the upper part of the structure. All the used methods provide better solutions for the hoop forces than for the meridional ones.

The only solution which is going to be taken into account for the bending moments which appear on the shell are the results of the analytical analysis. Due to the differences in the meridional forces, the moments are quite different between each model. The only valid solution which has been obtained is the analytical one. It is not going to be compared with the other solutions. It is also understable this difference due to the fact that several models – continuous and not continuous – have been used in the analytical and numerical methods.

3. Analysis of the constructed wooden dome

3.1 Characteristics of the dome and load cases

The aim of this section is to use the previous analysis methods to obtain the theoretical diplacements in the same points of the shell where the displacements where measured in the load test.

The semispherical dome which has been constructed has a radius of 0.64 m.

Each of the pieces which forms the dome is made of 3 different layers, as it has been explained in the corresponding design section of this project. The used materials and the thickness of these layers are:

- Superior layer: MDF (medium density fiberboard); t = 12 mm
- Intermediate layer: HB (hardboard); t = 3 mm
- Lower layer: HB; t = 5 mm

The global thickness which has been considered in the analysis is 20 mm.

In the models which has been created to analyzed the shell the material which has been used is wood. Its properties are shown in the following table.

WOOD	
E (N/mm2)	1000
G (N/mm2)	400
μ	0,25
γ (KN/m3)	8,83

The applied load in the laboratory was a distributed load over the crown of the shell. The maximal total force which was registered by the dynamometer was 1,1106 KN. Taking into account that the perimeter of the crown is:

$$P_{crown} = 2 \cdot \pi \cdot r = 2 \cdot \pi \cdot 0{,}15 = 0{,}942 \text{ m}$$

the applied force per lenght unit is:

$$P = \frac{F_T}{P_{crown}} = 1{,}1784 KN/m$$

Besides the applied load in the laboratory the self-weight of the structure is acting. It is necessary to consider the action of the two loads simultaneously.

3.2 Obtaining of the displacements

The lateral points which are being analyzed are situated in a distance of 0,56 m of the crown of the shell.

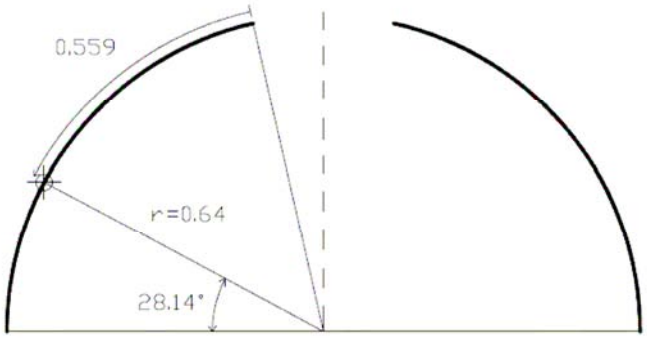

Figure 140: Situation of the studied lateral points

The vertical displacement of the crown points are also analyzed.

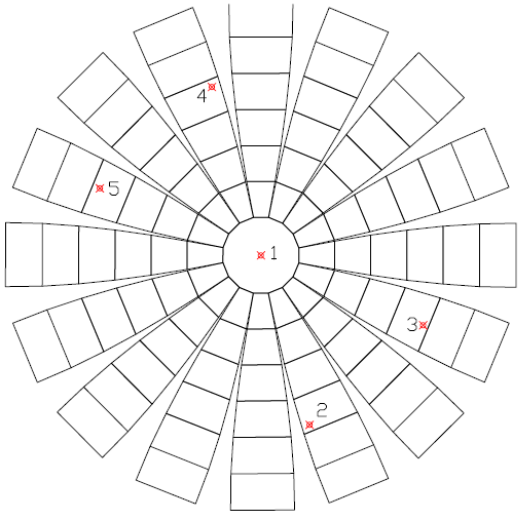

Figure 141: Placement of the movement sensors

3.2.1 Load test results

The results of the load test are the base of the comparison. With them it is possible to determine if the built model has a similar structure behaviour to the analyzed ones.

The first thing to take into account is that all the displacements of the lateral points should be the same, because of the axis symmetry. Nevertheless there are some differences between the measured displacements. These differences may have appeared because the built shell is not perfectly symmetric and the displacement sensors are not placed exactly in the radial position and with the same inclination angle.

The following tables collect the corresponding data to the load stages where the biggest deformations (lateral and vertical displacements in the crown) are produced in both carried out tests. The sensors 1 measures the vertical displacement. The other four sensors belong to the lateral one.

Zeit DEVICE_1 s	Kraft kN	Weg 1 mm	Weg 2 mm	Weg 3 mm	Weg 4 mm	Weg 5 mm
154,000007	-1,0674	3,344	0,026	0,09	-0,132	-0,108
154,500007	-1,1106	3,714	0,046	0,094	-0,132	-0,118
155,000007	-1,1058	3,926	0,048	0,094	-0,126	-0,124
155,500007	-1,0812	3,972	0,048	0,094	-0,122	-0,126
156,000007	-1,0602	3,968	0,048	0,094	-0,12	-0,13
156,500007	-1,0578	3,972	0,048	0,094	-0,118	-0,132
157,000007	-1,0074	3,948	0,046	0,094	-0,112	-0,134
157,500007	-0,9318	3,898	0,04	0,094	-0,106	-0,132
158,000008	-0,8394	3,81	0,032	0,094	-0,098	-0,132

Table 9: Results Load Test 1

Zeit DEVICE_1 s	Kraft kN	Weg 1 mm	Weg 2 mm	Weg 3 mm	Weg 4 mm	Weg 5 mm
56,0000027	-0,963	2,26	0,124	0,07	-0,04	-0,074
56,5000027	-0,9786	2,34	0,128	0,072	-0,04	-0,076
57,0000027	-1,0224	2,512	0,142	0,074	-0,04	-0,08
57,5000027	-1,0662	2,828	0,158	0,07	-0,04	-0,086
58,0000028	-1,0788	3,068	0,164	0,068	-0,038	-0,088
58,5000028	-1,0704	3,12	0,164	0,066	-0,034	-0,09
59,0000028	-1,0698	3,162	0,164	0,066	-0,032	-0,09
59,5000028	-1,0596	3,178	0,164	0,064	-0,03	-0,092
60,0000028	-1,0464	3,178	0,164	0,064	-0,03	-0,092
60,5000029	-1,0152	3,164	0,164	0,064	-0,026	-0,092
61,0000029	-0,9672	3,138	0,16	0,064	-0,022	-0,094
61,5000029	-0,8958	3,088	0,156	0,064	-0,016	-0,094

Table 10: Results Load Test 2

The sign of the displacement depends only on the calibration of the sensor and in this test has not any meaning because it is previously known that in the ring where the measuring instruments are placed all the studied points move outwards. The sensors are in the tension area.

Maximal displacements are going to establish the comparison range. For the vertical displacement the average of the maximal values of each test has been taken. For the lateral displacements the extreme values has been ruled out and the maximal and minimal displacements indicate the results range. This results are expressed in mm.

Vertical (point 1)		3,575
Lateral (points 2, 3, 4, 5)	max	0,132
	min	0,048

Table 11: Maximal displacements during the load test

In order to establish a comparison with the results of the different model analysis, this displacements are going to be transformed taking into account the inclination of the movement sensor.

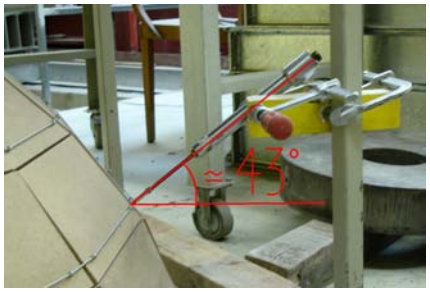

Figure 142: Inclination of the displacement sensors

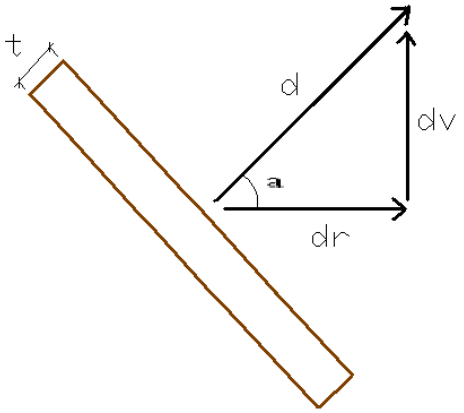

dr: radial displacement
dv: vertical displacement
d: sensor displacement
a: sensor inclination

dr = d cos a
dv = d sen a

Figure 143: Displacements descomposition

Point		dr (mm)	dv (mm)
1		unkown	3,575
2, 3, 4, 5	min	0,035	0,033
	max	0,097	0,090

Table 12: Maximal displacements during the load test expressed in global axis

3.2.2 Analytical results

The previous expounded formulas are now use to get the displacements.

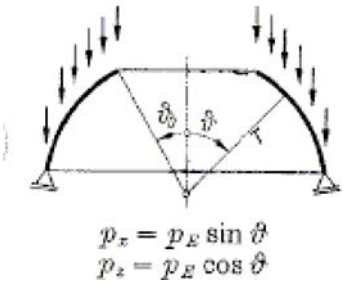

$$\overline{w} = -\frac{p_E r^2}{Et}\left[(1+\mu)\frac{\cos\vartheta_0 - \cos\vartheta}{\sin^2\vartheta} - \cos\vartheta\right]\sin\vartheta$$

$$\chi = -\frac{p_E r}{Et}(2+\mu)\sin\vartheta$$

Figure 144: Displacement formulas for load case self-weight

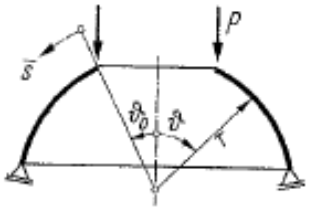

$$\overline{w} = -\frac{Pr}{Et}\left[(1+\mu)\frac{\sin\vartheta_0}{\sin\vartheta} - 2\sin\vartheta_0\cos\vartheta_0\,\varkappa\, e^{-\varkappa\frac{\bar{s}}{r}}\cos\varkappa\frac{\bar{s}}{r}\right]$$

$$\chi = -\frac{2P\cos\vartheta_0}{Et}\varkappa^2 \times e^{-\varkappa\frac{\bar{s}}{r}}\left[\cos\varkappa\frac{\bar{s}}{r} + \sin\varkappa\frac{\bar{s}}{r}\right]$$

Figure 145: Displacement formulas for load case load 10 kN/m

The displacement $\overline{w}$ is perpendicular to the shell axis and it is contained in the xy plane. χ is the rotation of the meridian tangent. With this formulas it is possible to

obtain the $\overline{w}$ displacements directly. Therefore only the displacement of the lateral points will be considered.

In order to obtain the displacement which is caused by the load combination (self-weight and the applied load) it is going to be supposed that the deformation as a result of the self-weight action occurs first and it is not as relevant in the shell shape to change it and avoid the use of the second set of formulas in order to get the displacements caused by the application of the load.

Parameters

r (m)	0,64
x	7,3257
vo (rad)	0,2244
μ	0,25
t (m)	0,02
E (KN/m2)	1000000
Self-Weight (KN/m3)	8,8290
Pe (KN/m)	0,1766
P (KN/m)	1,1784

Horizontal displacement lateral points 2, 3, 4, 5

LOAD CASE	dr (mm)
self-weight	-1,2047E-03
applied load	1,1696E-02
combination	1,0492E-02

3.2.3 SAP2000 results

The values of the displacement are directly obtained from the deformed shape in the studied points under the action of the two known loads combination. The applied load in the laboratory has been simulated like joint loads applied in the joints of the crown with a value of 0,07 kN. This simplification is done due to the difficulty of modelling the applied distributed load over the crown.

The results are collected in the following table.

Point	dr (mm)	dv (mm)
1	-1,015	-3,28
2, 3, 4, 5	0,026	-0,021

Table 13: Obtained displacements with SAP200

3.3 Comparison of results

VERTICAL DISPLACEMENT (mm) POINT 1 SITUATED IN THE CROWN OF THE SHELL

LOAD TEST	-3,575
ANALYTICAL SOLUTION	-
SAP2000 MODEL	-3,28

DISPLACEMENTS (mm) OF THE LATERAL POINTS 2, 3, 4, 5

		dr	dv
LOAD TEST	(min-max)	0,035 - 0,097	0,033 - 0,09
ANALYTICAL SOLUTION		0,0105	-
SAP2000 MODEL		0,026	-0,021

The comparison of these results has several limitations.

General properties of wood have been used for the calculations. The properties of the built model are just approximated. Actually the constructed shell is formed by 2 different materials – MDF and HB. Moreover, each element is composed of 3 layers.

The real model have tendoms in both directions which contribute to the structural strenght. Furthermore, the cables in the ring direction have been tightened with a force of 30 kg. These tendoms are not simulated with the simulation software. In the analytical model the shell has been considered as a continuous solid. In the SAP2000 model the shell is formed by different elements which are connected by hinges on their corners. But the connection between the different elements of the laboratory model with its cable system should be simulated with springs which ligthly hampers the rotation between different pieces.

After this explanation a vast comparison can be established.

The provided results by the analytical formulas for the lateral displacement are lower than the real and the SAP2000 model ones. These results were expected because of the shell continuity in the analytical analysis.

The results obtained with SAP2000 are also smaller than the ones of the real model. This difference was also expected due to the fact that in the laboratory model the

elements are joint by cables and in the FEM software these joints are simulated by using hinges.

Despite the existing differences between the shown values it is also important to outline that all the displacements have the same order of magnintude. This fact evidences that all the models have the same general behaviour of a dome with some differences due to the modelling characteristics.

List of figures

List of tables

References

[1] David P. Billington: *Thin shell concrete structures*. McGraw-Hill Book Company; United States of America; 1965.

[2] University of Colorado; *Shell Structures: basic concepts*. www.colorado.edu.

[3] Reinhard Harte: *Schalenstatik im Wandel der Zeit*; Manfred Weck: *Entwicklungstrends im Werkzeugmaschinenbau*; Nordrhein Westfäliche Akademie der Wissenschaften Vertrage nº454. Verlag Ferdinand Schöningh; Düsseldorf; 2001.

[4] B. Fletcher: A history of Architecture. 18th ed. London; Athelone Press; 1975

[5] *Domes*; http://litestraboen.blogspot.com/2007/01/domes.html

[6] R.Mark and P. Hutchinson: On the structure of the Pantheon. Art Bulletin; March; 1986

[7] G. Dehio and G. von Bezold: *Kirchliche Baukunst des Abendlandes*. Verlag der Cotta'schen Buchhandlung; Stuttgart; 1887-1901.

[8] Building the Roman Pantheon; http://www.angelfire.com/super/tyvernon/

[9] Department of Architecture, College of Enviromental Design, King Fahd University of Petrolum and Minerals; *Module 8: Early Christian and Byzantine Architecture*; www.ocw.kfupm.edu.sa

[10] Building Big: *Domes Basics*; www.pbs.org/wgbh/buildingbig/dome/basics.html

[11] E.Heinle and J.Schlaich; Kuppeln aller Zeiten – aller Kulturen; Deutsche Verlags - Anstalt; Stuttgart; 1996

[14] DI S. Dallinger: Thin shell concrete structures; Thesis proposal

[15] Ekkehard Ramm and Eberhard Schunck, editors. Heinz Isler: Schalen. vdf Hochschulverlag AG an der ETH Zürich, 2002.

[16] Monolithic Dome institute: www.static.monolithic.com

[17] Johann Kollegger. Construction method for free-formed reinforced concrete shells. In F. del Pozo and A. de las Casas, editor, *10 years of progress in shell and spatial structures – 30 anniversary of IASS*. Madrid, 1989.

[18] Stefan Krispel and Johann Kollegger. *Bau einer Stahlbeton ohne Schalung*. Beton-Zement, 2:24-29, 2006.

[19] Johann Kollegger, Clemens Preisinger and Michael Kaulfus.*Ice shells for temporary event architecture.* Structural Engineering International, 14:274-276, 2004.

[20] Wanda W. Lau. *Equilibrium analysis of masonry domes*. Thesis; B.S., Civil Engineering; Michigan State University; 2002.

[21] I. Requena Ruiz. *Análisis de tipologías estructurales: bóveda, lámina, cúpula y paraboloide.*

[22] J.W Schwedler: *Theorie der Brückenbalkensysteme*. In Zeitschrift für Bauwesen, 1, pp. 114-123,162-173, 265-278; 1851.

[23] H. T. Eddy: *New constructions in graphical statics*. D. Van Nostrand; New York:; 1877.

[24] W. S. Wolfe: *Graphical analysis: a text book on graphic statics*. McGraw-Hill Book Co.; New York; 1921

[25] D. O´Dwyer: *Funicular analysis of masonry vaults*. Computers & Strcutres, 73; 1999.

[26] D. D´Ayala: *Limit state analysis of hemispherical domes with finite friction*. P.B: and P. Roca (Eds.); Historical Constructions: Proceedings of the 3rd International Seminar; Guimarães, Portugal; University of Minho; 2001.

[27] Jr. Hodge and C. Lakshmikantham: *Limit analyisis of shallow shells of revolution*. J. Applied Mechanics; 1963.

[28] R.K. Livsley: *A computational model for the limit analysis of three-dimensional masonry structures*. Meccanica, 27, 161-172; 1992.

[29] W.J.M. Rankine: A manual of applied mechanics. C.Griffin and Co.; 17th edition; London; 1904.

[30] SAP2000 Integrated Finite element analysis and design of structures: Basic analysis reference; Tutorial.

[31] Alf Plüger: *Elementare Schalenstatik*. Springer-Verlag; 5th edition; Germany ; 1981

[32] H. W. Cowan: *The Maters Builders*. John Wiley and Son; New York; 1977.

Appendices

Appendix A

Related to chapter 2; section *1.3 Design of the model*

Technical drawings of the designed and built wooden dome with a final radius of 0.64 m. The plate diameter of this model is approximately 2 m.

Section A-A

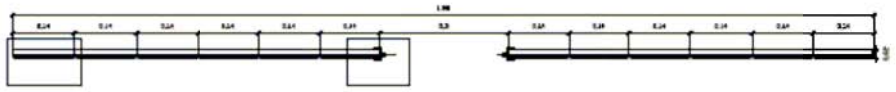

Detail B

Detail C

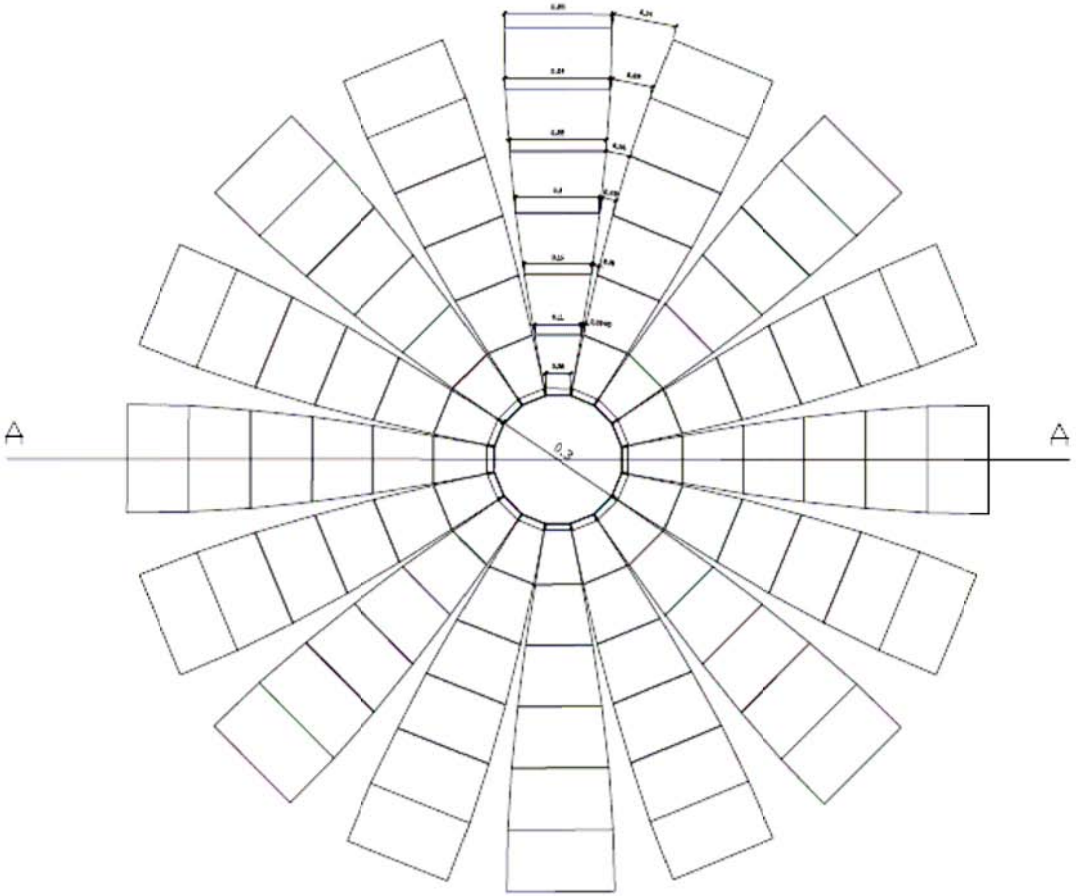

Plate structure

Plan view
Section A-A
Detail B, C
Pieces dimensions

FERNANDEZ Patricia

Detail C

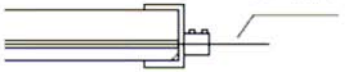

Detail B

Pieces Dimensions

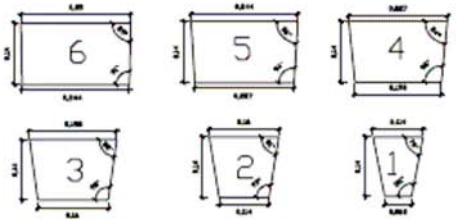

Dome section in the final position